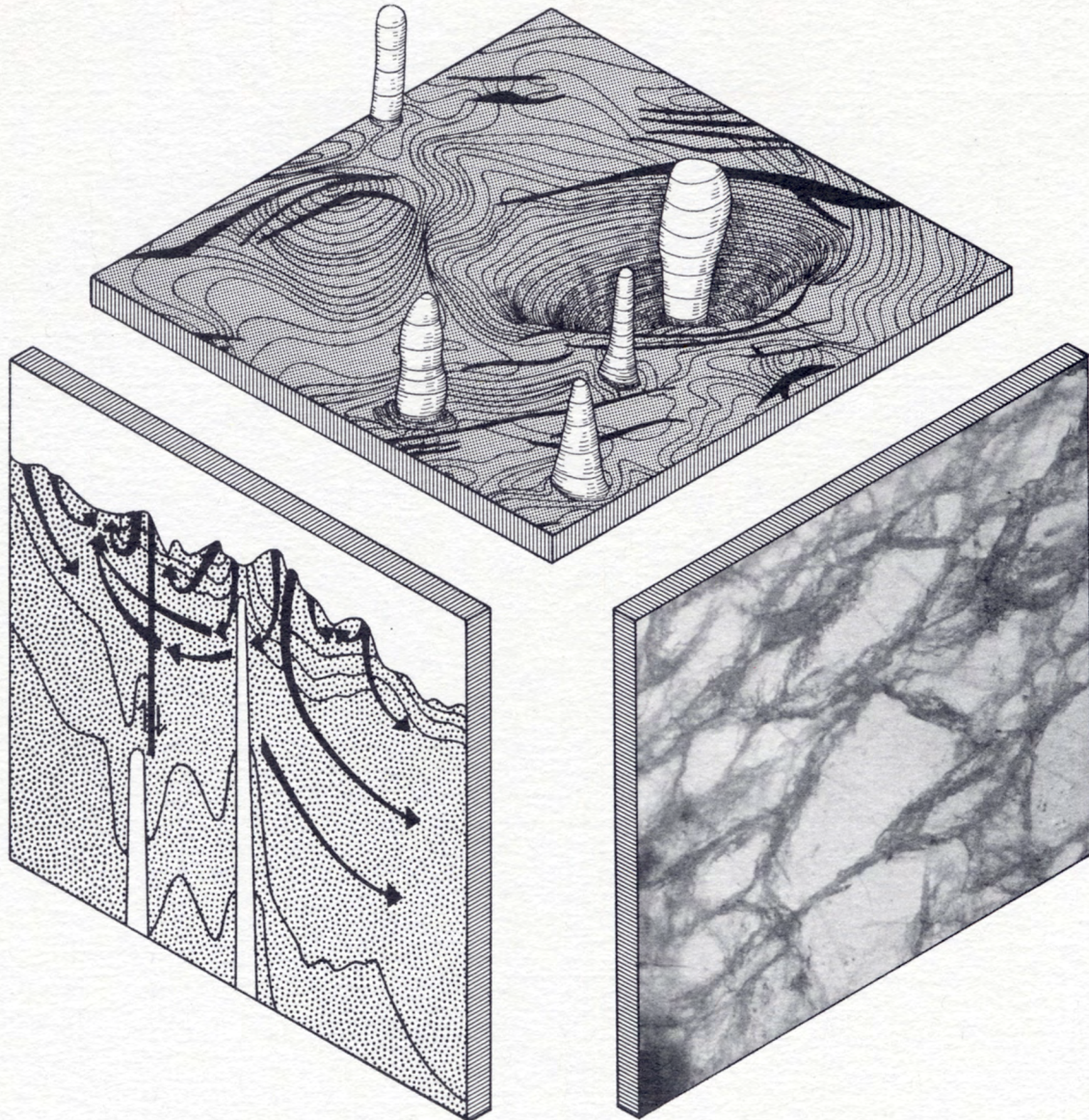


# Suitability of Salt Domes in the East Texas Basin for Nuclear Waste Isolation: Final Summary of Geologic and Hydrogeologic Research (1978 to 1983)

M.P.A. Jackson and Steven J. Seni



1984

**Bureau of Economic Geology**

W. L. Fisher, Director

The University of Texas at Austin

Austin, Texas 78713



QAe4837

Geological Circular 84-1

SUITABILITY OF SALT DOMES  
IN THE EAST TEXAS BASIN  
FOR NUCLEAR WASTE ISOLATION:  
FINAL SUMMARY OF  
GEOLOGIC AND HYDROGEOLOGIC RESEARCH  
(1978 to 1983)

M.P.A. Jackson and Steven J. Seni

Funded by the U.S. Department of Energy  
under Contract No. DE-AC97-80ET46617  
(formerly DE-AC97-79ET44605 and EW-78-S-05-5681)

Bureau of Economic Geology  
W. L. Fisher, Director  
The University of Texas at Austin  
University Station, P. O. Box X  
Austin, Texas 78713

1984



# CONTENTS

	<u>Page</u>
<b>Summary</b> . . . . .	1
<b>Evaluation</b> . . . . .	3
<b>Introduction to the East Texas Basin</b> . . . . .	7
The East Texas Waste Isolation program . . . . .	7
Tectonic evolution . . . . .	13
Structural framework . . . . .	15
Stratigraphic framework . . . . .	17
Regional hydrogeology . . . . .	21
Inventory of East Texas salt domes . . . . .	23
<b>Regional geologic studies</b> . . . . .	27
Present distribution and geometry of salt structures . . . . .	27
Mechanisms initiating salt flow . . . . .	31
Initiation of salt flow . . . . .	33
Diapirism . . . . .	35
Effects of dome growth on depositional facies of enclosing strata . . . . .	39
Effects of dome growth on structure of enclosing strata . . . . .	45
Effects of dome growth on surface processes . . . . .	47
Rates of dome growth . . . . .	51
Fault tectonics . . . . .	53
Seismicity . . . . .	57
Petroleum potential of domes . . . . .	61
<b>Regional hydrogeologic studies.</b> . . . .	65
Ground-water hydraulics . . . . .	65
Ground-water chemistry . . . . .	69
Subsurface salinity near salt domes . . . . .	71
Age of ground water . . . . .	75
Surface saline discharge . . . . .	79
Saline aquifers . . . . .	83
<b>Core studies of Oakwood Dome, East Texas</b> . . . . .	87
Lithology of salt . . . . .	87
Structure of salt . . . . .	91
Strain in salt . . . . .	95
Cap-rock - rock-salt interface . . . . .	97
Cap rock . . . . .	101
<b>Hydrogeologic studies of Oakwood Dome and vicinity</b> . . . . .	105
Hydrogeologic monitoring and testing . . . . .	105
Ground-water modeling: Wilcox multiple-aquifer system . . . . .	109
Ground-water modeling: flow rates and travel times . . . . .	113
<b>Acknowledgments</b> . . . . .	115
<b>References</b> . . . . .	116
<b>Appendix --</b> Lithologic descriptions, correlation notes, and selected references, East Texas Basin. . . . .	125

## Figures

1. Schematic cross sections showing evolutionary stages in formation of East Texas Basin and adjoining Gulf of Mexico . . . . .	14
2. Regional structural framework of the East Texas Basin. . . . .	16
3. Structural cross section across East Texas Basin. . . . .	16
4. Stratigraphic column, East Texas Basin . . . . .	18
5. Typical geophysical and lithic log, Rains County, Texas . . . . .	19
6. Ground-water flow lines for Wilcox-Carrizo system, East Texas Basin . . . . .	22
7. Salt domes of the East Texas Basin . . . . .	24
8. Major-axis orientation and proportional axial ratios of salt diapirs . . . . .	25
9. Major-axis orientation of turtle structures, salt pillows, and salt diapirs . . . . .	26
10. Axial ratio versus percentage overhang for 15 East Texas diapirs . . . . .	26
11. Isometric block diagram of salt structures in the East Texas Basin . . . . .	28
12. Salt provinces and salt-structure contours, East Texas Basin . . . . .	29
13. Salt-flow directions in dipping source layer and uniform, onlapping overburden . . . . .	32
14. Fluid gradient in salt pillow below denser cover . . . . .	32
15. Fluid gradient in tabular salt, induced by differential loading by dense, sand-rich delta . . . . .	32
16. Models of Late Jurassic - Early Cretaceous salt mobilization . . . . .	34
17. Diapir groups in the East Texas Basin . . . . .	36
18. Depositional facies during Washita - Glen Rose and Wilcox time . . . . .	37
19. Stages of dome growth . . . . .	40
20. Depositional facies during Wilcox time . . . . .	41
21. Net-sandstone map, Paluxy Formation, showing decrease in sandstone thickness over crests of pillows . . . . .	42
22. Cross section through Wilcox Group around Bethel Dome . . . . .	43
23. Isometric block diagram of salt diapirs and structure contours on top of Woodbine Group . . . . .	46
24. Significant correlation between depth to dome and index of preferred orientation. . . . .	49
25. Cross section of Quaternary floodplain deposits above Oakwood Dome . . . . .	50
26. Comparison of long-term rates of dome growth for East Texas, North Louisiana, and West German salt domes . . . . .	52
27. Fault traces on base of Austin Chalk and their relation to salt diapirs, salt pillows, and turtle structures . . . . .	54
28. Time-to-depth-converted seismic section showing symmetric buried graben over crest of Van-Ash salt pillow . . . . .	55

29.	Jacksonville main shock and aftershock from Mount Enterprise fault zone. . . . .	58
30.	Composite focal mechanism for located earthquakes and probable aftershocks . . . . .	59
31.	Time-to-depth-converted seismic section across Mount Enterprise fault . . . . .	60
32.	Salt-related structures and petroleum fields in central part of East Texas Basin. . . . .	62
33.	Production statistics for central part of East Texas Basin . . . . .	63-64
34.	Regional potentiometric surface of Wilcox-Carrizo aquifer in East Texas . . . . .	66
35.	Elevations of Wilcox-Carrizo water levels and major stream beds. . . . .	67
36.	Fluid pressure versus depth in fresh-water Wilcox-Carrizo aquifers . . . . .	68
37.	Piper diagram of Wilcox-Carrizo water chemistry . . . . .	70
38.	Relationship of percentage thickness of fresh water in Wilcox aquifer to trends of high sand percentage . . . . .	73
39.	Location of possible saline plume associated with Oakwood Dome. . . . .	74
40.	Ground-water <sup>14</sup> C ages in Wilcox-Carrizo aquifer near Oakwood Dome . . . . .	76
41.	Depths to top of East Texas Basin domes . . . . .	80
42.	Duggey's Lake overlying possible dissolution-induced collapse over Palestine Dome . . . . .	81
43.	Fluid pressure versus depth for saline aquifers in East Texas Basin . . . . .	84
44.	Calcium concentration versus total dissolved solids in saline aquifers in East Texas Basin . . . . .	85
45.	Values of dD (o/oo) and δ <sup>18</sup> O in East Texas ground water and meteoric water line. . . . .	86
46.	Oakwood Dome cross section showing location of TOG-1 well . . . . .	88
47.	Vertical profile of TOG-1 rock-salt core . . . . .	89
48.	Brine inclusions within halite in R-3 zone. . . . .	90
49.	Schistosity and anhydrite-rich layers in TOG-1 rock-salt core . . . . .	92
50.	Vertical section along TOG-1 rock-salt core . . . . .	93
51.	Inferred flow patterns within a laterally spreading, rising diapir fed by multiple emplacement of salt tongues as overthrust folds . . . . .	94
52.	Flinn diagram showing mean strains in Oakwood Dome rock salt . . . . .	95
53.	Statistically significant upward decrease in percentage shortening with decreasing depth . . . . .	96
54.	Tight contact between salt and overlying cap rock . . . . .	98
55.	Processes at cap-rock - rock-salt interface . . . . .	99
56.	Stylolitic laminae in anhydrite cap rock from TOG-1 . . . . .	102
57.	Potentiometric surface of Carrizo aquifer over Oakwood Dome . . . . .	106

58. Electric log resistivity values in the Wilcox Group compared with lab-derived K values . . . . .	107
59. Upper surface (top of Wilcox-Carrizo aquifer) of finite-difference model of ground-water flow, Oakwood Dome area . . . . .	110
60. Regional ground-water flow lines in Wilcox-Carrizo aquifer near Oakwood Dome. . . . .	111
61. Ground-water velocity vectors computed in model simulation A . . . . .	114

**Tables**

1. Evaluation of Oakwood salt dome as a potential repository. . . . .	4
2. Data base for the East Texas Waste Isolation program . . . . .	8
3. Studies in the East Texas Waste Isolation program . . . . .	9
4. Ground-water <sup>14</sup> C ages in Wilcox-Carrizo aquifer near Oakwood Dome . . . . .	77
5. Inferred processes at Oakwood Dome that are favorable for storage of nuclear wastes . . . . .	100
6. Inferred processes at Oakwood Dome that are unfavorable for storage of nuclear wastes . . . . .	100
7. Comparison of porosities and permeabilities of cap rock from Oakwood and Gyp Hill salt domes . . . . .	103
8. Test data from monitoring wells around Oakwood Dome . . . . .	108

## SUMMARY

This report summarizes results of the East Texas Waste Isolation (ETWI) program from January 1, 1978, to March 30, 1983. Having an extensive data base, the study comprised 33 different lines of research by 67 scientists and research assistants. The program included both basinwide and site-specific (mainly around Oakwood Dome) studies that used surface and subsurface data.

Mesozoic opening of the Gulf of Mexico accompanied thermal processes that controlled sedimentation during filling of the East Texas Basin. The basin contains as much as 7,000 m (23,000 ft) of shallow-marine and continental sediments overlying the Louann Salt. Deformation in the basin resulted from subsidence of its floor and gravitational flow of salt and from salt loss in the subsurface and at the surface. Regional studies have defined the present-day distribution of salt structures and the growth history of domes. The East Texas Basin is divided into four provinces on the basis of the shape of salt structures. Five forces that make salt flow operated from near surface to the deepest parts of the basin to form these structures. Salt flow began in pre-Gilmer (Late Jurassic) time with the growth of salt pillows. Three groups of diapirs can be differentiated on the basis of age and distribution. The growing salt structures affected topography, thereby influencing depositional facies and resulting in deposition of low-permeability facies around the salt stocks.

Rates of dome growth declined exponentially with time to rates of less than  $0.6 \text{ m}/10^4 \text{ yr}$ . Geomorphic evidence does not preclude Quaternary uplift over Oakwood Dome, but its southern flank may have subsided. All regional fault systems in the basin appear to be related to slow gravitational creep of salt downward toward the basin center or upward into salt pillows and diapirs. Nevertheless, at least eight probable earthquakes were recorded near the southern margin of the basin in 1981 and 1982, and their probable focus, the Mount Enterprise fault, is poorly understood.

The following conclusions were drawn from geologic study of a core drilled from Oakwood Dome: Salt core from the dome is more than 98 percent pure halite (anhydrite is the only other mineral present). The rock salt displays evidence of two distinct periods of recrystallization. Geometric analysis and strain analysis suggest that the crest of the dome was truncated, probably by ground-water dissolution, during the formation of anhydrite cap rock. Diapiric rise of salt formed a tight contact between salt and cap rock. The cap rock formed in a deep saline environment and appears to be a low-permeability barrier to dome dissolution.

**Keywords:** cap rock, diapirs, East Texas Basin, faults, hydrochemistry, hydrogeology, hydraulic modeling, lineaments, nuclear waste repositories, petroleum, salt domes, salt tectonics, seismicity, stable isotopes, strain analysis



Two major aquifer systems lie above and below the hypothetical repository level in the dome: the Wilcox-Carrizo fresh-brackish aquifer system above and the Woodbine saline aquifer below. Only the five shallowest domes have saline springs and are thus poor sites for potential repositories. The geochemistry of false cap rock over two of these domes suggests that this alteration may be due to upward discharge of deep-basin brines.

Of the domes that penetrate the Wilcox-Carrizo aquifer system, only Oakwood Dome has a slightly brackish plume, possibly caused by salt dissolution. None of the salt domes shows evidence of extensive exposure to circulating ground water. The salt domes are isolated at least partly by low-permeability cap rock and mud-rich facies.

Regional circulation in the Wilcox-Carrizo aquifer system correlates closely with topography and geologic structure. A potential for downward flow prevails except beneath the Trinity and Sabine River drainage systems. Potential for downward flow between the Wilcox-Carrizo and the Woodbine aquifers is due to marked basinwide pressure declines in the Woodbine caused by oil and gas production.

As Wilcox-Carrizo ground water moves from recharge to artesian sections, it evolves from an acidic, oxidizing, Ca-Mg-HCO<sub>3</sub>-SO<sub>4</sub> water to a basic, reduced, Na-HCO<sub>3</sub> water. Dating of the ground water by <sup>14</sup>C methods indicates ages of 10<sup>3</sup> yr in recharge areas to 1.5 x 10<sup>4</sup> yr in the artesian section.

Three-dimensional modeling of ground-water flow in the Wilcox-Carrizo aquifer near Oakwood Dome shows that the stratified sand-mud fabric causes poor vertical connection of sand bodies and very low (~ 10<sup>-3</sup> to 10<sup>-4</sup>) ratios of vertical to horizontal hydraulic conductivity. Rates of vertical ground-water flow are only 11 m/10<sup>4</sup> yr. Ground-water travel times from Oakwood Dome to potential discharge areas are approximately 10<sup>4</sup> yr in well-connected channel-fill sand bodies and 10<sup>5</sup> to 10<sup>6</sup> yr in poorly connected interchannel facies. These interchannel facies constitute large potential aquitards. Realistic modeling of flow rates in the Wilcox or in similar aquifers requires incorporation of data on sand-body geometry and interconnection.

The Woodbine aquifer is the shallower of the two deep saline aquifer systems surrounding salt domes immediately below the hypothetical repository level. Mixing of deep saline waters with the overlying fresh-water system is limited.

## EVALUATION

*According to proposed guidelines from the Nuclear Waste Policy Act of 1982, Oakwood salt dome has 23 favorable characteristics, 15 potentially adverse characteristics, and 3 disqualifying characteristics. We find no characteristic that is generic to salt domes that precludes their use as a repository for nuclear waste.*

The East Texas Waste Isolation project is one of three subprograms studying interior salt basins in the Gulf Coast area. These subprograms constitute part of the National Waste Terminal Storage program, which is designed to assess the suitability of dome salt, bedded salt, basalt, tuff, and crystalline rock as host media for deep underground containment of high-level nuclear waste. As with other projects, the goal of the East Texas project was a progressive screening in which the best site (in this case, a salt stock in the core of a salt dome) was selected by eliminating less favorable sites.

All 15 shallow salt domes in the East Texas Basin were examined, and 3 were chosen: Keechi, Oakwood, and Palestine. By 1980, Palestine Dome had been eliminated because of ongoing subsidence of strata above the dome induced by earlier brining operations. By 1981, further screening had eliminated Keechi Dome because it was too small and too shallow (Office of Nuclear Waste Isolation, 1981). Therefore, from this point, research in the ETWI program was directed to (1) a better understanding of Oakwood Dome and vicinity and (2) supplying information generic to all salt domes, which could be applied to the other three candidate domes in the North Louisiana and Mississippi interior salt basins.

In accordance with the requirements of the Nuclear Waste Policy Act of 1982, the Department of Energy has circulated "Proposed General Guidelines for Recommendation of Sites for Nuclear Waste Repositories," which appear in the Federal Register, Part II, of February 7, 1983. On the basis of these guidelines, which are still being discussed by the Department of Energy and interested parties, the Oakwood Dome area is evaluated in table 1. Regarding its suitability as a repository for high-level nuclear waste, Oakwood Dome has 23 favorable characteristics, 15 potentially adverse characteristics, and 3 disqualifying characteristics. These three disqualifying characteristics are related to petroleum exploration and are specific to Oakwood Dome. According to our survey of the East Texas Basin, we find no characteristic generic to salt domes that precludes their use as a repository for nuclear waste.

Table 1. Evaluation of Oakwood Dome as a potential repository in terms of proposed guidelines set by Nuclear Waste Policy Act of 1982.

	Favorable	Potentially adverse	Disqualifying
<u>SITE GEOMETRY (Oakwood Dome)</u>			
Potential repository depth >300 m	*		
Erosional denudation in $10^4$ yr = 1 to 2 m	*		
Thickness and lateral extent	*		
<u>HYDROGEOLOGY (Oakwood Dome and Regional)</u>			
Predominantly downward vertical hydraulic gradient basinwide	*		
Local recharge over Oakwood Dome to shallow (Carrizo) aquifer	*		
No evidence of interaction between saline and fresh aquifers around Oakwood Dome	*		
Upward discharge of deep-basin fluids at Butler Dome		*	
Saline plume at Oakwood Dome		*	
Travel time of ground water to discharge areas: Modeling: connected Wilcox sands = $10^3$ to $10^4$ yr disconnected Wilcox sands = $10^5$ to $10^6$ yr	*	*	
Carbon-14 dating: Wilcox = $1.6 \times 10^4$ yr	*		
Oakwood Dome area modeled with reasonable accuracy	*		
Low-permeability Wilcox facies around dome	*		
Low-permeability cap rock above and partly flanking dome	*		
Tight seal in core between rock salt and cap rock	*		
Vertical extension fractures in anhydrite cap rock		*	
Possible subsidence over southern part of Oakwood salt stock		*	
Inferred escape of brines from former dissolution cavity below cap rock (inferred to be >3 Ma [millions of years] ago)		*	
Structural evidence of truncation of dome crest (mainly during the Cretaceous)		*	
62 boreholes through salt overhang probably connect shallow fresh-water aquifer and deep saline aquifer, possibly allowing rapid salt dissolution by fresh water			*
<u>ROCK CHARACTERISTICS (Oakwood Dome)</u>			
Evidence of self sealing in anhydrite cap rock during strain	*		
Rock-salt mineral assemblage unchanged during thermal loading	*		

Table 1 (cont.)

	Favorable	Potentially adverse	Disqualifying
Recrystallization of uppermost 2 m (6 ft) of rock salt probably caused by entry of water from cap-rock base (inferred to be >3 Ma ago)		*	
In-place concentration of intracrystalline fluid in foliated (R-1) rock salt at level of hypothetical repository is unknown because of artificial introduction of water into core		*	
Preferred migration paths of intercrystalline fluids are partly predictable from strain analysis and geometric analysis of rock salt	*		
Structure of rock salt where intersected by borehole reasonably well understood	*		
<u>TECTONIC ENVIRONMENT (Mainly Regional)</u>			
Fastest uplift rates over domes is <0.6 m/10 <sup>4</sup> yr, estimated by extrapolation of growth rates from 112 to 48 Ma ago	*		
Geomorphic evidence does not preclude current differential uplift over most of Oakwood Dome		*	
Geomorphic evidence suggests subsidence of the southern part of Oakwood Dome		*	
No evidence of rapid regional uplift or subsidence	*		
Most regional fault systems are reasonably well understood and apparently aseismic	*		
No regional faults within 10 km (6 mi) of dome	*		
Small Quaternary faults at surface 18 km (10.8 mi) from Oakwood Dome		*	
Vertical extent of small post-Queen City surface faults over Oakwood Dome is unknown		*	
Historical earthquakes, if repeated, would not significantly affect Oakwood site	*		
Seismicity probably due to movement on Mount Enterprise fault, but seismic risk cannot be reliably assessed because reason for faulting is not yet understood		*	
No Quaternary igneous activity	*		
<u>HUMAN INTRUSION (Oakwood Dome)</u>			
Petroleum reserves below overhang and 4 km (2.4 mi) to SE			*
Intensive exploratory and production drilling through salt overhang, partly to level of hypothetical repository; sites of three holes have not been located			*
<u>SURFACE CHARACTERISTICS (Oakwood Dome)</u>			
Gently rolling terrain	*		
Dikes possibly required for flood protection		*	



## INTRODUCTION TO THE EAST TEXAS BASIN

### The East Texas Waste Isolation Program

*The East Texas Waste Isolation program began on January 1, 1978, and ended on March 30, 1983. The program goals were to assist in the selection of a suitable salt dome in the East Texas Basin through geologic and hydrogeologic characterization of the domes and surrounding strata and to provide generic information applicable to other salt-dome basins.*

This report summarizes results of the East Texas Waste Isolation program from January 1, 1978, to March 30, 1983. As part of the Area Characterization Phase of evaluating U.S. Gulf Coast salt-dome basins, the East Texas program was designed to characterize the geology and geohydrology of salt domes and surrounding strata in the East Texas Basin and to provide generic information applicable to other salt-dome basins. The data base for this program is extensive because the basin is a mature petroleum province that contains major fresh-water aquifers (table 2). Table 3 lists the 33 principal lines of geologic research, the scale of examination, and the pertinent sections of this report covering these aspects. Most of these lines of research are applicable to other salt-dome basins as well. The most important generic studies are listed in column 1 of table 3. References cited at the end of each unit provide sources of data and derivation of conclusions summarized in this report. This approach is a compromise between the need for adequate documentation and the need to avoid producing a text encumbered with multiple citations in each sentence. Full citations of all these papers are provided in the references at the end of this report.

Kreitler (1979); Kreitler and others (1980); Kreitler and others (1981a); Kreitler and others (1982a)

Table 2. Data base for the East Texas Waste Isolation program.

Surface

Geologic Atlas of Texas map sheets, scale 1:250,000

Geologic maps from unpublished theses

Topographic maps, scales 1:62,500 and 1:24,000

Texas general highway maps, scales 1:63,360 and 1:253,440

Aerial photographs, scales 1:12,000 to 1:25,500

Landsat imagery, scale 1:250,000, band-5

Re-leveling profile of 28 stations across Mount Enterprise fault zone

Microseismic monitoring data from one to three seismograph stations near Mount Enterprise fault zone

Subsurface

Geophysical logs from ~4,600 wells

Water-level data from >2,000 water wells

Water-chemistry data from ~1,500 water wells

29 shallow borings to depths of 7 to 120 m (20 to 400 ft) over Oakwood Dome, 9 of which were monitored for water levels

Hydrologic test data from five production wells, one of which was cored

TOG-1 412-m (1,352-ft) core through Oakwood Dome salt, cap rock, and overburden; TOH-2AO 563-m (1,847-ft) core through Wilcox Group near Oakwood Dome

13 cores borrowed from Bureau of Economic Geology Well Sample Library and from oil companies

475 km (295 mi) of 6-fold C.D.P. seismic reflection line

Residual gravity map, scale 1:96,000

Table 3. Studies in the East Texas Waste Isolation program. Columns 1 through 5 refer to the scales of examination in each study. Letters in each column refer to sections of this report that summarize the results of each study (see corresponding footnotes).

	(1) GENERIC	(2) BASINWIDE	(3) ALL 15 DOMES	(4) OAKWOOD, KEECHI, PALESTINE, BUTLER DOMES	(5) LOCAL NON-DOME
<b>SITE GEOMETRY</b>					
Measuring size and shape of salt domes to determine if criteria of minimum thickness and lateral extent are met. Measurement based on analysis of structure-contour maps from gravity, seismic, and well data.			e		
Measuring depth to salt and cap rock to determine if minimum-depth criterion is met. Measurement based on interpretation of well logs and seismic profiles.			e		
<b>SURFACE GEOLOGY</b>					
Calculating denudation rates by surveys of suspended-sediment loads and reservoir sedimentation to assess risk of erosional breaching of dome.		1			
Measuring stream and terrace profiles to determine the effects of possible dome uplift or collapse.		1		1	
Shallow drilling of Quaternary valley fill over Oakwood Dome to determine the effects of possible dome uplift or collapse.				1	
Analyzing slopes above domes to recognize possible dome uplift or collapse.				1	
Analyzing link lengths of drainage networks to determine the existence of possible dome uplift or collapse.			e	1	1
Stratigraphic and structural mapping, including fault zones, over domes to determine the effects of possible dome uplift or collapse.				1,n	
Lineament analysis of aerial photographs and Landsat imagery to study regional and over-dome fracture patterns.		1			1
Re-leveling over Mount Enterprise fault zone to measure elevation changes from faulting in the past 30 yr.					o
Microseismic monitoring of the Mount Enterprise fault zone to determine magnitudes and locations of earthquakes.					o



Table 3. (cont.)

	(1) GENERIC	(2) BASINWIDE	(3) ALL 15 DOMES	(4) OAKWOOD, KEECHI, PALESTINE, BUTLER DOMES	(5) LOCAL NON-DOME
SUBSURFACE GEOLOGY					
Interpreting geophysical logs to elucidate lithology, depositional systems, structure, tectonic evolution, and geometry of sedimentary units in the basin.	j k	a b c f	b c e		
Constructing 49 stratigraphic and structural regional cross sections to carry out basin analysis.		b c	b c		
Constructing structural cross sections around 15 domes to determine geometry of near-dome stratigraphic units.	i		e		
Interpreting seismic reflection data and time-to-depth conversion of events to examine seismic stratigraphy, especially of units below depth of abundant well control.		b c f h n		b c	
Interpreting residual gravity to define salt-related structures.		b f	e		
Analyzing regional fault systems to examine distribution, geometry, displacement history, and origin, especially for seismic potential.		n			
Examining subsurface data around 15 salt domes to infer times and patterns of salt movement over 64 Ma.	i j		e h i j k		
Measuring thickness changes around 15 salt domes to quantify rates of dome growth over 64 Ma to predict future dome growth.	m		e i m		
Oakwood salt-core studies of lithology, geochemistry, fluid inclusions, structure, and strain to evaluate host-rock characteristics.	w x y z			w x y z	

Table 3. (cont.)

	(1) GENERIC	(2) BASINWIDE	(3) ALL 15 DOMES	(4) OAKWOOD, KEECHI, PALESTINE, BUTLER DOMES	(5) LOCAL NON-DOME
Studies of Oakwood cap-rock lithology, geochemistry, isotopic chemistry, structure, and origin to evaluate the effects of geologic sealing by cap rock.	z a'			z a'	
General literature review of internal structure of salt glaciers and diapirs to evaluate host-rock characteristics.	*				
Literature review of mechanisms for initiating salt flow to understand structural evolution of host rock.	g	g			
Synthesizing petroleum potential of salt domes to evaluate probability of future exploration for resources.		e	e		
Documenting petroleum storage in salt domes to eliminate domes with prior economic use.			e		
Documenting hydrocarbon accumulation patterns.	p	p	p	p	p
GEOHYDROLOGY					
Documenting surface saline waters to determine their relation to shallow salt domes.	u		e u		
Monitoring ground-water levels to deduce ground-water flow paths.		d q		q	
Pumping tests of producing wells around Oakwood Dome to determine hydrologic properties of fresh-water aquifers.				q b'	
Analyzing water and existing water-chemistry data to determine geochemical evolution of fresh and saline aquifers.	r v	d r v		r v	r
Isotopic analysis of ground water to determine age, residence time, and source.		t		v	r

Table 3. (cont.)

	(1) GENERIC	(2) BASINWIDE	(3) ALL 15 DOMES	(4) OAKWOOD, KEECHI, PALESTINE, BUTLER DOMES	(5) LOCAL NON-DOME
Constructing hydrodynamic models around Oakwood Dome to evaluate the effects of changing several hydrologic variables on flow patterns around the dome.	s c' d'			s c' d'	
Examining petrography, isotopes, and stratigraphic relations of Butler Dome false cap rock to determine origin and age of alteration.				v	

\* See Jackson (1983).

- a. Tectonic Evolution (p. 13).
- b. Structural Framework (p. 15).
- c. Stratigraphic Framework (p. 17).
- d. Regional Hydrogeology (p. 21).
- e. Inventory of East Texas Salt Domes (p. 23).
- f. Present Distribution and Geometry of Salt Structures (p. 27).
- g. Mechanisms Initiating Salt Flow (p. 31).
- h. Initiation of Salt Flow (p. 33).
- i. Diapirism (p. 35).
- j. Effects of Dome Growth on Depositional Facies of Enclosing Strata (p. 39).
- k. Effects of Dome Growth on Structure of Enclosing Strata (p. 45).
- l. Effects of Dome Growth on Surface Processes (p. 47).
- m. Rates of Dome Growth (p. 51).
- n. Fault Tectonics (p. 53).
- o. Seismicity (p. 57).
- p. Petroleum Potential of Domes (p. 61).
- q. Ground-Water Hydraulics (p. 65).
- r. Ground-Water Chemistry (p. 69).
- s. Subsurface Salinity near Salt Domes (p. 71).
- t. Age of Ground Water (p. 75).
- u. Surface Saline Discharge (p. 79).
- v. Saline Aquifers (p. 83).
- w. Lithology of Salt (p. 87).
- x. Structure of Salt (p. 91).
- y. Strain in Salt (p. 95).
- z. Cap-Rock - Rock-Salt Interface (p. 97).
- a'. Cap Rock (p. 101).
- b'. Hydrogeologic Monitoring and Testing (p. 105).
- c'. Ground-Water Modeling: Wilcox Multiple-Aquifer System (p. 109).
- d'. Ground-Water Modeling: Flow Rates and Travel Times (p. 113).

## Tectonic Evolution

*The character of Mesozoic sedimentary fill in the East Texas Basin reflects underlying thermally induced tectonic processes characteristic of initial uplift, rifting, and thinning of Paleozoic continental crust. The subsequent tectonic subsidence allowed restricted-marine incursions accompanied by rift volcanism. Further subsidence resulted in the accumulation of open shallow-marine deposits followed by progradation of the continental margin by delta-dominated systems toward an oceanic-spreading center in the Gulf of Mexico.*

The East Texas Basin originated during the Triassic as an aulacogenic rift basin north of the principal rift zone that ultimately formed the Gulf of Mexico (fig. 1). During the pre-rift stage, lithospheric expansion and uplift exposed the Paleozoic Ouachita fold belt to erosion. After the onset of rifting, diverging zones of maximum uplift (upward arrows in fig. 1) migrated outward from the rift axes as the lithosphere rose and was stretched, probably as a result of an underlying thermal anomaly. These zones of uplift were followed by diverging zones of collapse (downward arrows). Upper Triassic red beds were deposited unconformably as continental rift fill on eroded basement. Widespread erosion formed the subsalt angular unconformity across Triassic strata and Paleozoic basement.

By the Middle Jurassic, the basin had subsided sufficiently to allow restricted incursion of seawater along the linear trough and its flanks, depositing the Louann Salt. Rift volcanism is recorded by lava flows and ash falls immediately above and below the salt.

In the Late Jurassic, open shallow-marine deposits accumulated on the subsiding continental shelf in the basin during continental breakup. The paucity of terrigenous sediment on this shelf suggests that the rift margin was still sufficiently elevated to divert rivers elsewhere. Continued, cooling-induced subsidence of the divergent continental margin eventually allowed progradation of large volumes of terrigenous clastics in the Late Jurassic and Early Cretaceous, when the Gulf of Mexico had completely formed. Rates of basin subsidence and sediment accumulation declined throughout the Cretaceous and had virtually ceased by the early Tertiary.

Jackson and Seni (1983); Jackson (1981b); Seni and Kreitler (1981); Jackson and others (1982)

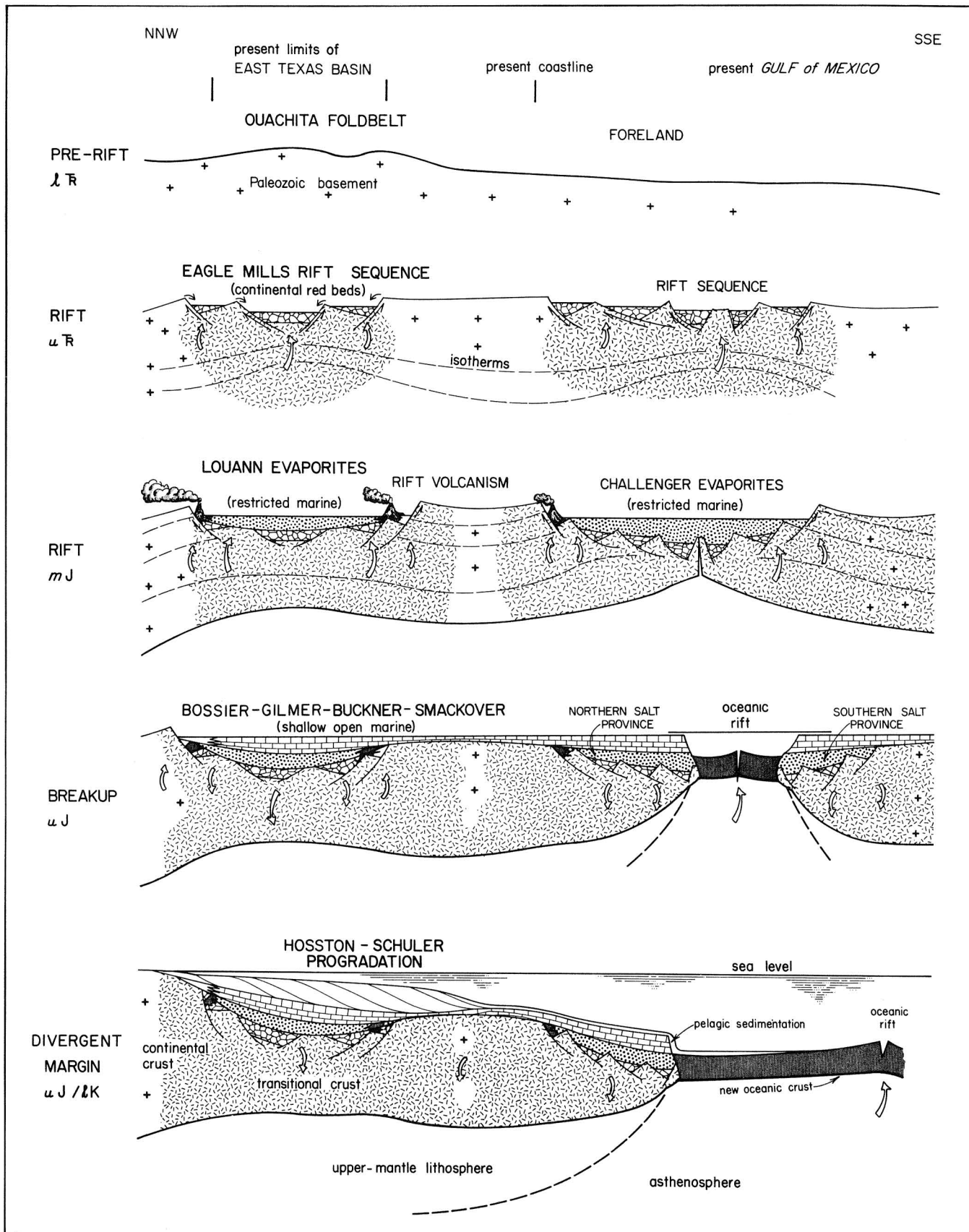


Figure 1. Schematic cross sections showing evolutionary stages in formation of East Texas Basin and adjoining Gulf of Mexico (from Jackson and Seni, 1983).

## Structural Framework

*The East Texas Basin has been distorted by second-order anticlines, including salt pillows, salt diapirs, and turtle structures, formed directly by gravity creep of salt. The basin is bounded by the Mexia-Talco fault zone on the north and west, by the Sabine Arch on the east, and by the Angelina Flexure on the south.*

The western and northern margins of the East Texas Basin coincide with other geologic structures varying from Pennsylvanian to Tertiary in age (fig. 2): (1) the Pennsylvanian Ouachita fold and thrust belt beneath Mesozoic cover and (2) the Triassic rift grabens and half grabens parallel to the Ouachita trend. This part of the basin margin is defined by the Mexia-Talco fault zone, a Jurassic to Eocene peripheral graben system that coincides with the updip limit of the Louann Salt.

The Sabine Arch (Uplift) forms the eastern margin of the basin (fig. 3). The southern margin of the basin is defined by the Angelina Flexure, a hinge line that is generally monoclinical at its ends and anticlinal in the middle. The Elkhart - Mount Enterprise fault zone extends from just north of the western end of the Angelina Flexure to the center of the Sabine Arch (fig. 2).

The gross structure of the East Texas Basin consists of regular basinward dips in the east, west, and north and a low rim in the south along the Angelina Flexure. Deformation within the basin appears to be related solely to large-scale, gravitationally induced creep of salt (halokinesis). The synclinal East Texas Basin was distorted by three types of second-order, salt-related anticlines: (1) salt pillows--large, low-amplitude, upwarping structures cored by salt; (2) salt diapirs--subvertical, cylindrical salt stocks that have pierced the adjacent strata; and (3) turtle structures--salt-free growth anticlines formed by subsidence of their flanks caused by collapse of underlying salt pillows during salt diapirism.

Jackson (1982); Agagu and others (1980b)

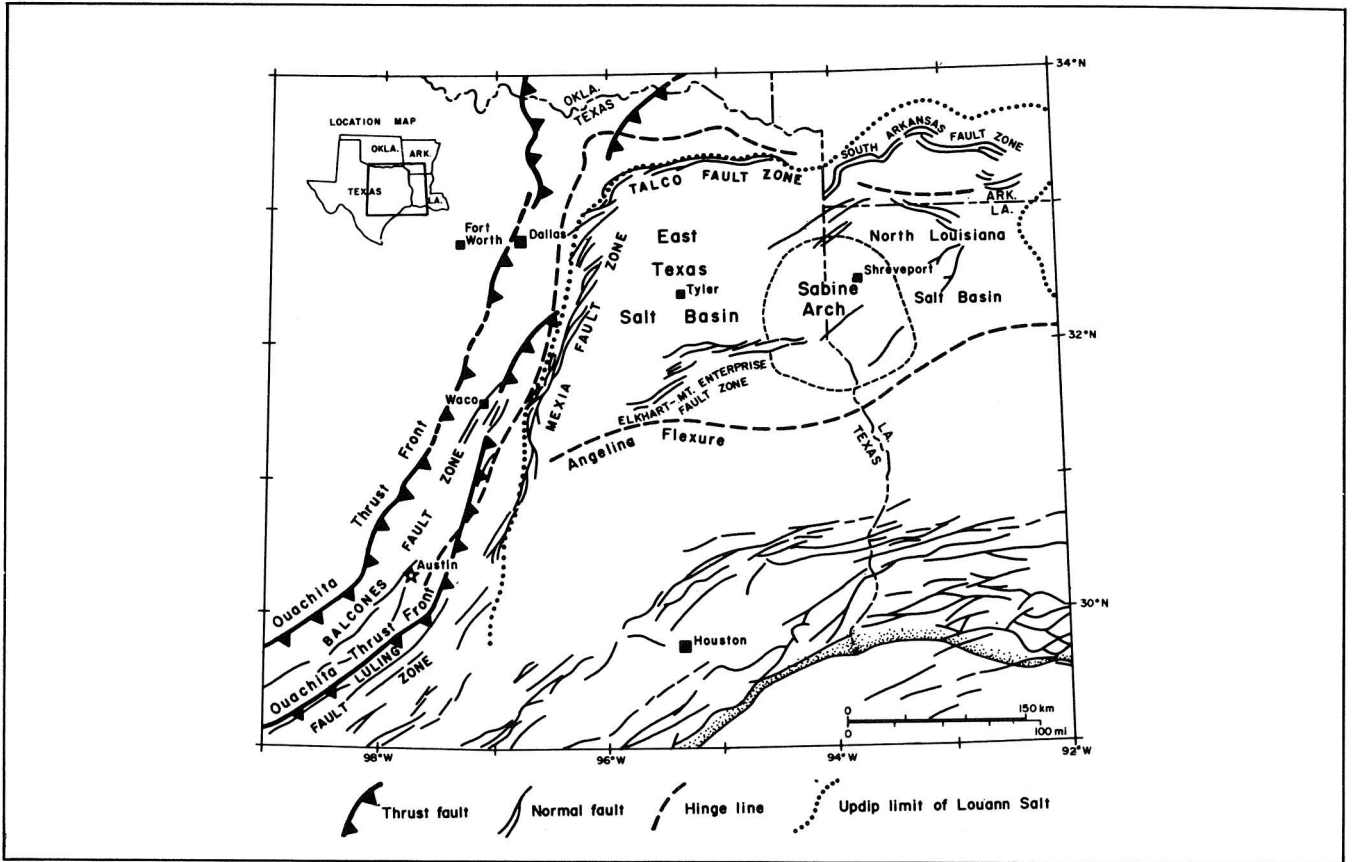


Figure 2. Map showing regional structural framework of the East Texas Basin (from Jackson, 1982, adapted from Martin, 1978).

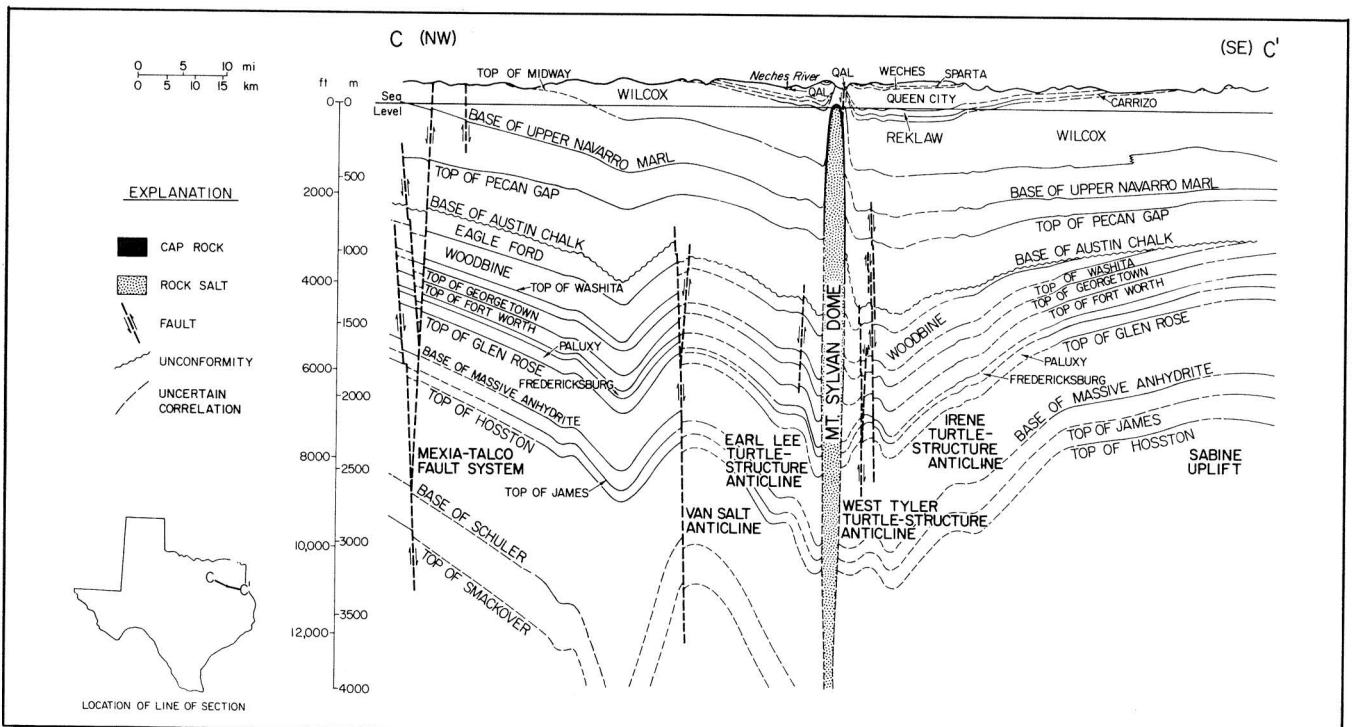


Figure 3. Structural cross section across East Texas Basin (from Wood and Guevara, 1981).

## Stratigraphic Framework

*The East Texas Basin contains 5,500 to 7,000 m (18,000 to 23,000 ft) of Mesozoic and Cenozoic evaporites, fluvial-deltaic sandstones, shales, and shelf carbonates. Apart from certain Upper Jurassic shales, deep-water (>300 m; >1,000 ft) facies are absent.*

The basin fill in East Texas followed a typical path from purely continental (Late Triassic) through restricted marine (Early Jurassic) to open shallow marine (Late Jurassic). This sequence was followed by episodes of terrigenous clastic and carbonate accumulation (Cretaceous), terminating with largely fluvial deposition (Tertiary) (figs. 4, 5, appendix). During the Late Triassic rift stage, Eagle Mills red beds were deposited unconformably on eroded basement. Middle Jurassic marine incursions along the rifts deposited the Werner Formation, consisting of red beds and evaporites and the overlying evaporitic Louann Salt.

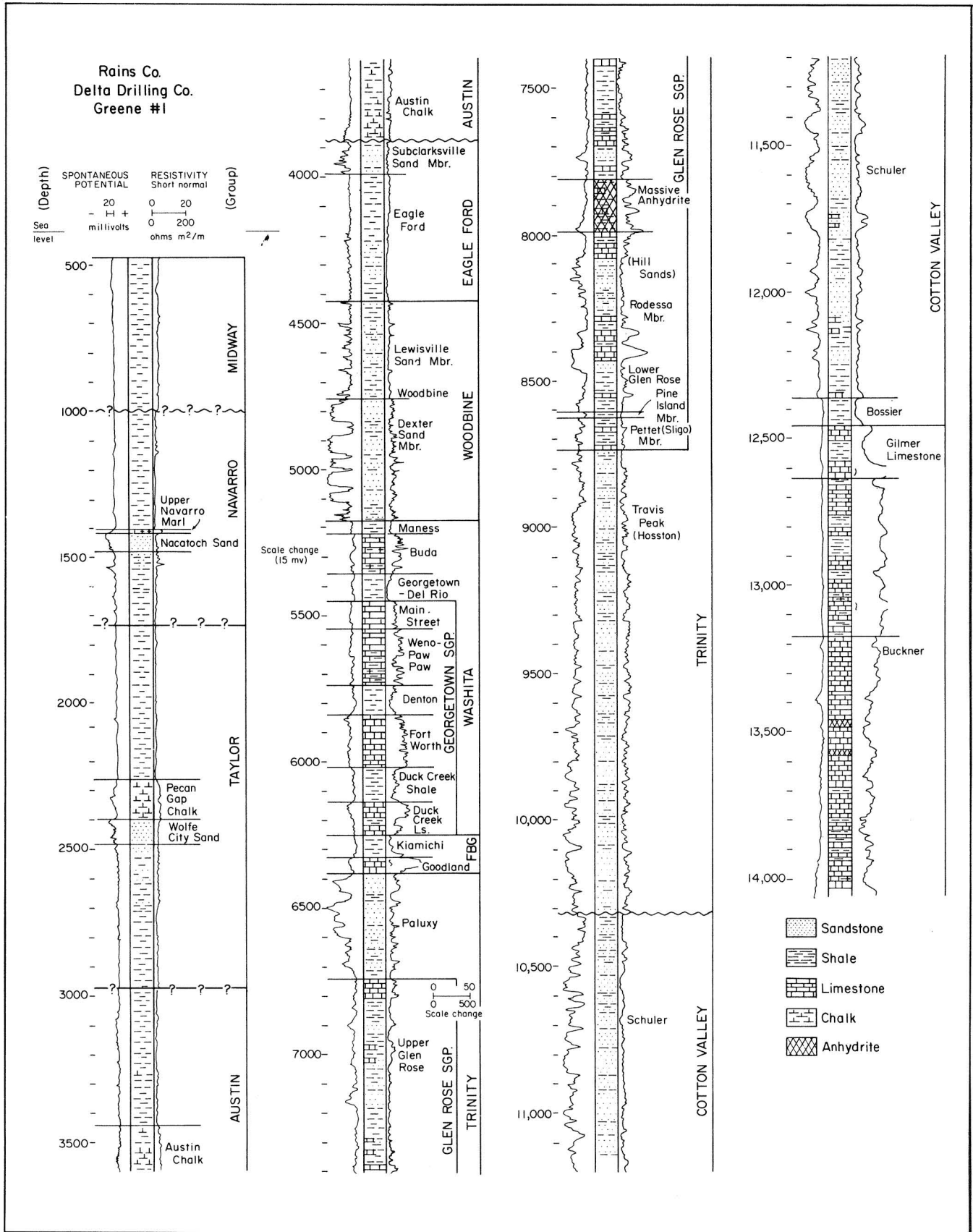
Open shallow-marine deposits in the Upper Jurassic Smackover, Buckner, and Gilmer Formations represent accumulations during continental breakup on the subsiding continental shelf. Sand-rich Schuler-Hosston deltas prograded across the divergent continental shelf during the Late Jurassic and Early Cretaceous. A rapid marine transgression resulted in the accumulation of Glen Rose carbonates, minor evaporites, and shale. In the Middle and Late Cretaceous, deltaic and fluvial sequences such as the Woodbine and Eagle Ford repeatedly prograded and built out the continental shelf. By the early Tertiary, the basin was essentially full, and fluvial systems prograded over the southern rim of the basin into the Gulf of Mexico. Net erosion has characterized the last 40 Ma of geologic time.

Wood and Guevara (1981); Agagu and others (1980a)



ERA-THEM	SYSTEM	SERIES	GROUP	FORMATION		
CENOZOIC	TERTIARY	EOCENE	CLAIBORNE	YEGUA		
				COOK MOUNTAIN		
				SPARTA		
		WECHES				
		QUEEN CITY				
		REKLAW				
					CARRIZO	
				WILCOX	UNDIFFERENTIATED	
			PALEOCENE	MIDWAY	UNDIFFERENTIATED	
	MESOZOIC	CRETACEOUS	UPPER CRETACEOUS	NAVARRO	UPPER NAVARRO CLAY	
					UPPER NAVARRO MARL	
					NACATOC SAND	
						LOWER NAVARRO
						UPPER TAYLOR
						PECAN GAP CHALK
					WOLFF CITY SAND	
					LOWER TAYLOR	
					GOBER CHALK	
					BROWNSTOWN BLOSSOM SAND	
					BONHAM CLAY	
					Glaucouitic Chalk Stringer	
				AUSTIN CHALK		
				Ector Chalk Mbr.		
				Sub-Clarksville Mbr.		
				EAGLE		
				Coker Sand Mbr.		
				FORD		
				Harris Sand Mbr.		
				WOODBINE		
				Lewisville Mbr.		
				Dexter Sand Mbr.		
				MANESS SHALE		
				BUDA LIMESTONE		
			GRAYSON SHALE			
			MAIN STREET LIMESTONE			
			WENO-PAW PAW LIMESTONE			
			DENTON SHALE			
			FORT WORTH LIMESTONE			
			DUCK CREEK SHALE			
			DUCK CREEK LIMESTONE			
			KIAMICHI SHALE			
			GOODLAND LIMESTONE			
			FREDERICKSBURG			
			PALUXY			
			UPPER GLEN ROSE			
			MASSIVE ANHYDRITE			
			RODESSO MEMBER			
			JAMES LIMESTONE MBR.			
			PINE ISLAND SHALE MEMBER			
			PETTET (SIGO) MEMBER			
			TRINITY			
			TRAVIS PEAK (HOSSTON)			
			COTTON VALLEY			
			SCHULER			
			BOSSIER			
			GILMER LIMESTONE (COTTON VALLEY LIMESTONE)			
			BUCKNER			
			SMACKOVER			
			NORPHLET			
			LOUANN			
			LOUANN SALT			
			WERNER			
			EAGLE MILLS			
PALEOZOIC				OUACHITA		

Figure 4. Stratigraphic column, East Texas Basin. Arrows show contacts on figure 3 (after Wood and Guevara, 1981). See also appendix.





## Regional Hydrogeology

*The Wilcox-Carrizo fresh-water aquifer system is separated from deeper saline aquifers by 600 to 1,200 m (2,000 to 4,000 ft) of aquitards and aquicludes. The proposed salt-dome repository would lie at the depth of aquitards and aquicludes between the fresh Wilcox-Carrizo and the saline Woodbine systems.*

Major fresh-water aquifers in the East Texas Basin are (youngest to oldest) the Queen City Formation, the Carrizo Formation, and the Wilcox Group. The Queen City is a water-table (unconfined) system in which topographic effects create a series of local ground-water basins. Immediately below is the leaky Reklaw aquitard, which causes artesian conditions in parts of the underlying Wilcox-Carrizo aquifer system. The Wilcox-Carrizo aquifer system includes (1) an artesian (confined) section overlain by the Reklaw aquitard and (2) a water-table (unconfined) system where the Wilcox-Carrizo crops out along the west, north, and east margins of the basin. The fresh-brackish water interface (1,000 mg/L) generally lies from 90 to 150 m (300 to 500 ft) above the base of the Wilcox Group. The major saline aquifer is the Woodbine Group, separated from the fresh-water systems by 600 to 1,200 m (2,000 to 4,000 ft) of aquitards and aquicludes. Deeper saline aquifers include the Paluxy Formation, the Glen Rose Subgroup, and the Hosston Formation ("Saline Aquifers," p. 83). A repository at a depth of 600 to 900 m (2,000 to 3,000 ft) would be situated at the depth of the 600- to 1,200-m (2,000- to 4,000-ft) interval between the Wilcox and Woodbine aquifers.

Regional ground-water flow patterns in the Wilcox-Carrizo system are shown in figure 6. Owing to a shallow water table (depth  $\approx$  12 m, 40 ft), flow in the large outcrop areas along the west and east margins of the basin correlates closely with topography. Ground-water flow lines in outcrops emanate from large recharge areas at watershed divides and either converge on streams or veer downdip. Topographic control on flow is also evident in the confined (artesian) section of the basin, where flow lines tend to veer away from watershed divides and generally converge toward the Trinity, Neches, and Sabine Rivers. This indicates that the Reklaw aquitard leaks in some areas and that the Wilcox-Carrizo aquifer may discharge upward through the Reklaw to streams. Both Oakwood and Keechi Domes are located within the artesian section. Pressure-depth relations ("Ground-Water Hydraulics," p. 65) indicate that upward leakage is confined to the area around the lower Trinity River.

Fogg and Kreitler (1982); Fogg and Kreitler (1981); Fogg (1980a); Fogg and others (1982a)

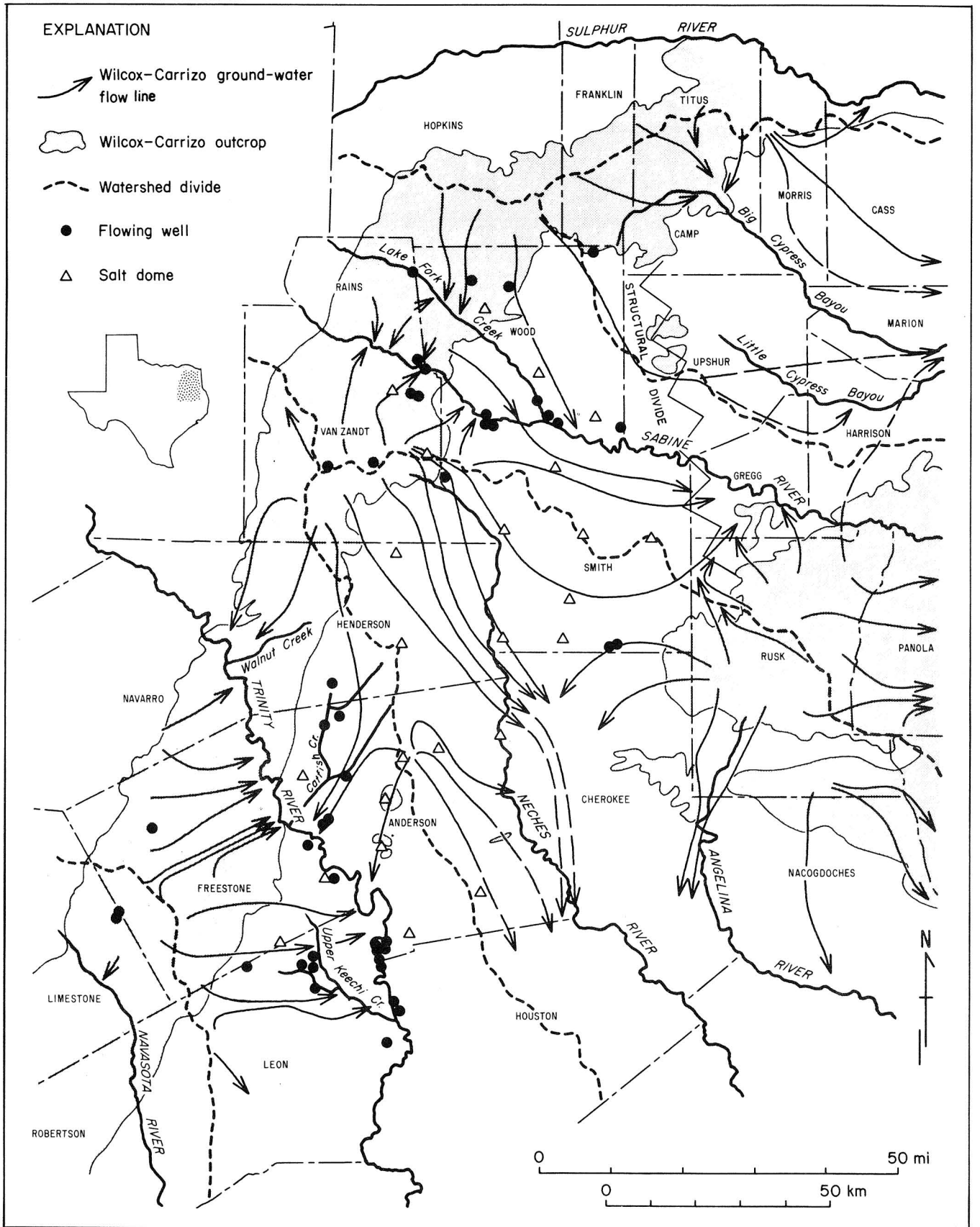


Figure 6. Map of ground-water flow lines for Wilcox-Carrizo system, East Texas Basin (from Fogg and Kreitler, 1981).

## Inventory of East Texas Salt Domes

*A wide range of pertinent geologic and economic data for all 15 shallow salt domes is summarized in this report. Salt-stock morphology provides a guide to structural maturity.*

This program was designed primarily to examine the feasibility of isolating nuclear waste in East Texas salt domes. The program collected pertinent geologic and economic data for all 15 shallow domes (fig. 7): location, residual-gravity expression, depths to cap rock and salt, orientation and lateral dimensions, shape, cap-rock thickness and composition, geometry of adjacent strata, faulting around dome, growth history, evidence of collapse, topographic expression, surface salines, resources, and uses of the domes. Graphics for each dome include structure contours of the salt stock on a topographic base, isometric block diagram of the salt stock, cross sections showing salt-stock shape along major and minor axes, and a cross section through the dome showing adjacent strata.

The orientation of precursor Jurassic - Lower Cretaceous salt ridges controlled the following aspects of the diapirs that evolved from them: major-axis orientation, diapir-family orientation, and overhang directions (figs. 8, 9). The following variables generally correlate with increasing structural maturity in salt stocks: decreasing axial ratio, increasing percentage overhang, and increasing planar crest area. The most reliable indications of structural maturity in salt stocks are axial ratio and percentage overhang (fig. 10). No one variable is totally reliable, and this approach should be treated with caution.

Jackson and Seni (1984); Giles and Wood (1983); Wood and Giles (1982); Giles (1980)

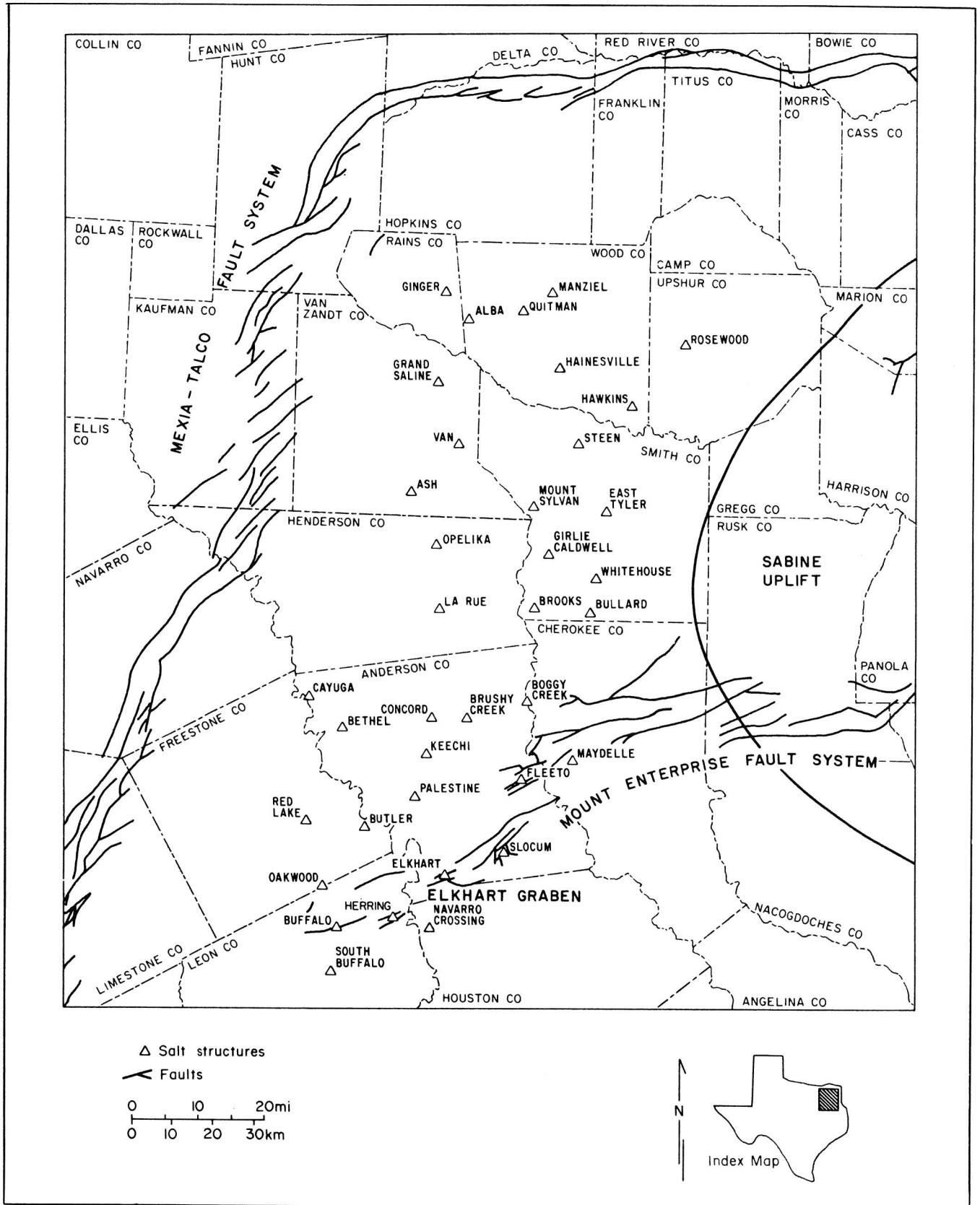


Figure 7. Map of the salt domes of the East Texas Basin. The 15 shallow salt domes (depth to salt < 1,220 m, < 4,000 ft) studied in detail are shown as triangles (after Kreitler and others, 1981a).

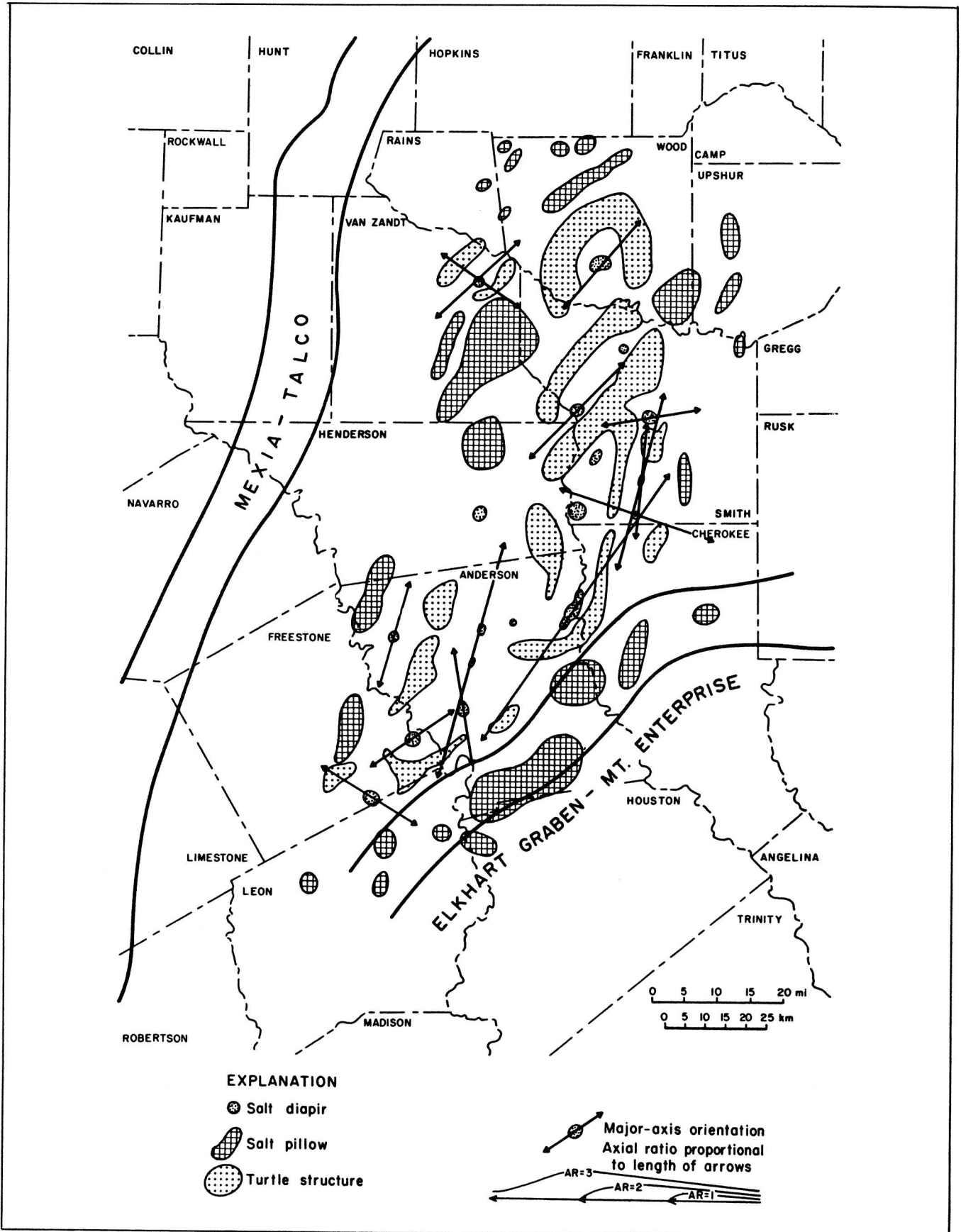


Figure 8. Map of major-axis orientation and proportional axial ratios of salt diapirs.



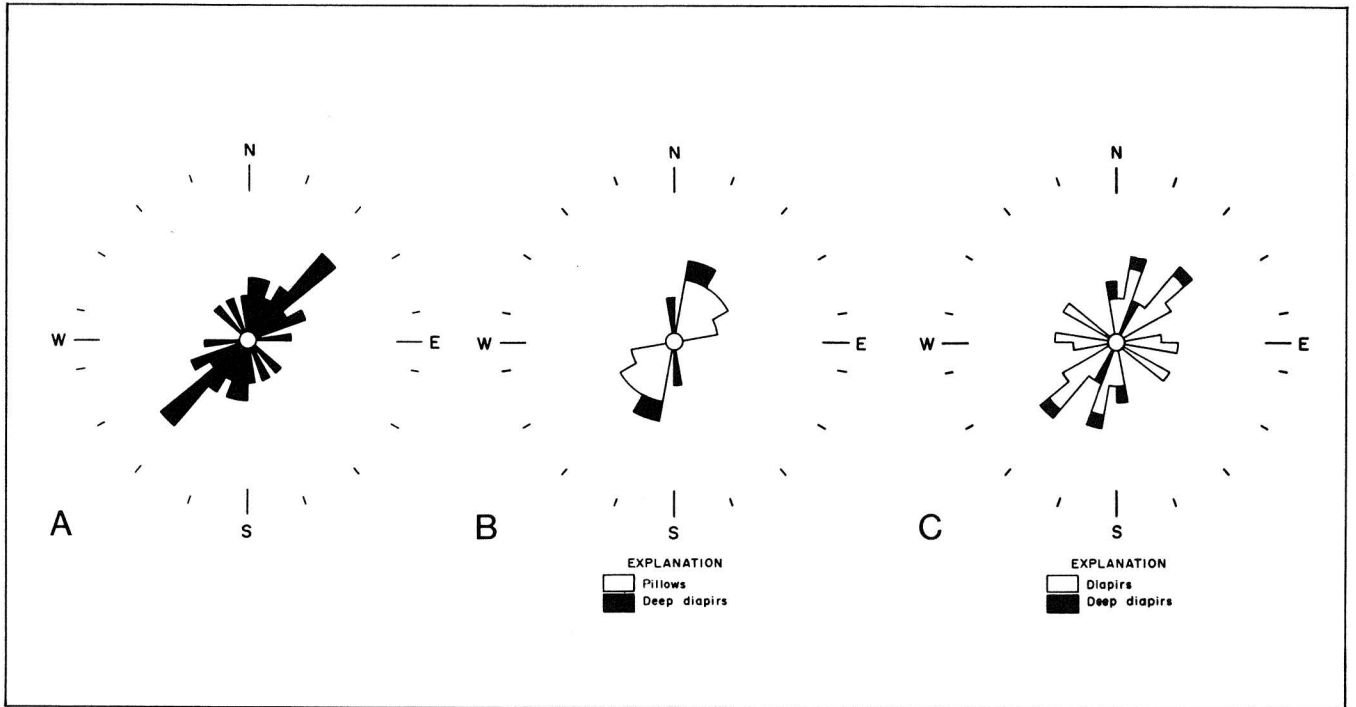


Figure 9. Rose diagrams of major-axis orientation of (A) turtle structures, (B) salt pillows, and (C) salt diapirs.

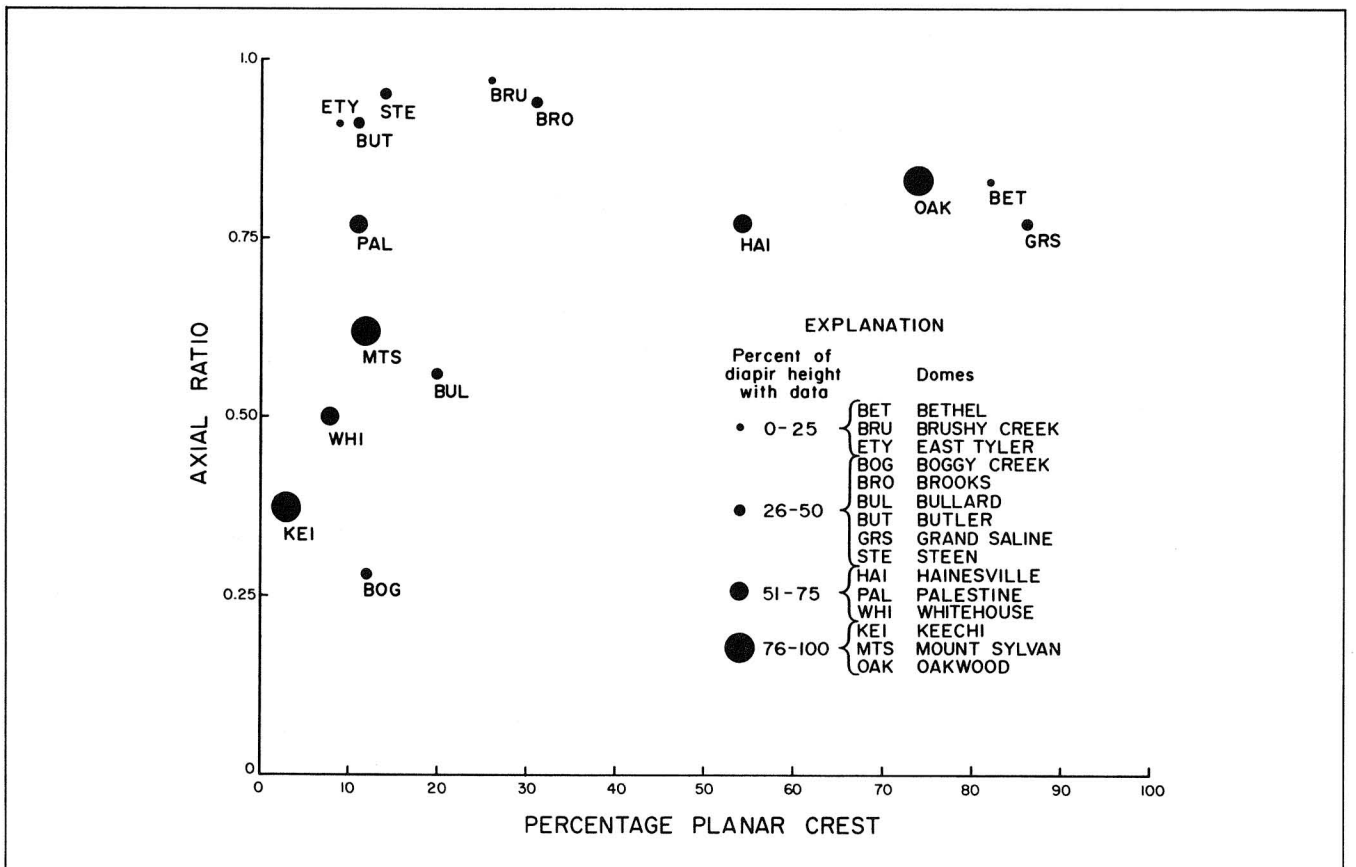


Figure 10. Graph of axial ratio versus percentage planar crest for 15 East Texas diapirs.

## REGIONAL GEOLOGIC STUDIES

### Present Distribution and Geometry of Salt Structures

*A central province of salt diapirs is surrounded by three other provinces: intermediate-amplitude salt pillows (inner), low-amplitude salt pillows, and a salt wedge (outer). These provinces reflect increasing thicknesses of the original salt source layer toward the basin center.*

The present distribution and morphology of salt structures in the East Texas Basin are portrayed in figure 11. A zone of undeformed salt, 2.7 to 4.6 km (8,800 to 15,000 ft) deep and 225 km (135 mi) long, encircles an array of salt structures. In much of the basin center, the Louann Salt is apparently absent. Salt structures (fig. 12) are classified into the following provinces.

(1) An outermost salt wedge consists of apparently undeformed salt from 0 to 340 to 640 m (0 to 1,115 to 2,100 ft) thick. Its updip pinch-out coincides with the Mexia-Talco fault zone.

(2) Periclinal salt structures with low amplitude/wavelength ratios are called low-amplitude salt pillows. These pillows are flanked by synclines of Louann Salt. The Louann Salt was originally at least 550 to 625 m (1,800 to 2,050 ft) thick before deformation, according to graphical reconstruction by unfolding of the pillows. Overburden thickness was about 500 m (1,640 ft) throughout provinces 1 through 3 at the start of salt movement.

(3) Intermediate-amplitude salt pillows are commonly separated by salt-evacuated synclines and are larger than pillows of province 2. Original thickness of the salt source layer here is estimated to be 550 to >760 m (1,800 to >2,500 ft), on the basis of graphical reconstruction by unfolding of the pillows.

(4) The salt diapirs of the diapir province in the basin center are the most mature salt structures. They have all partly "pierced" their overburden and have risen to within 23 m (75 ft) (Steen Dome) to about 2,000 m (6,560 ft) (Girlye Caldwell Dome) of the present surface.

Jackson and Seni (1983, 1984); Seni and Jackson (1983a,b, in press); Giles and Wood (1983); Giles (1980); Giles (1981); Wood and Giles (1982)

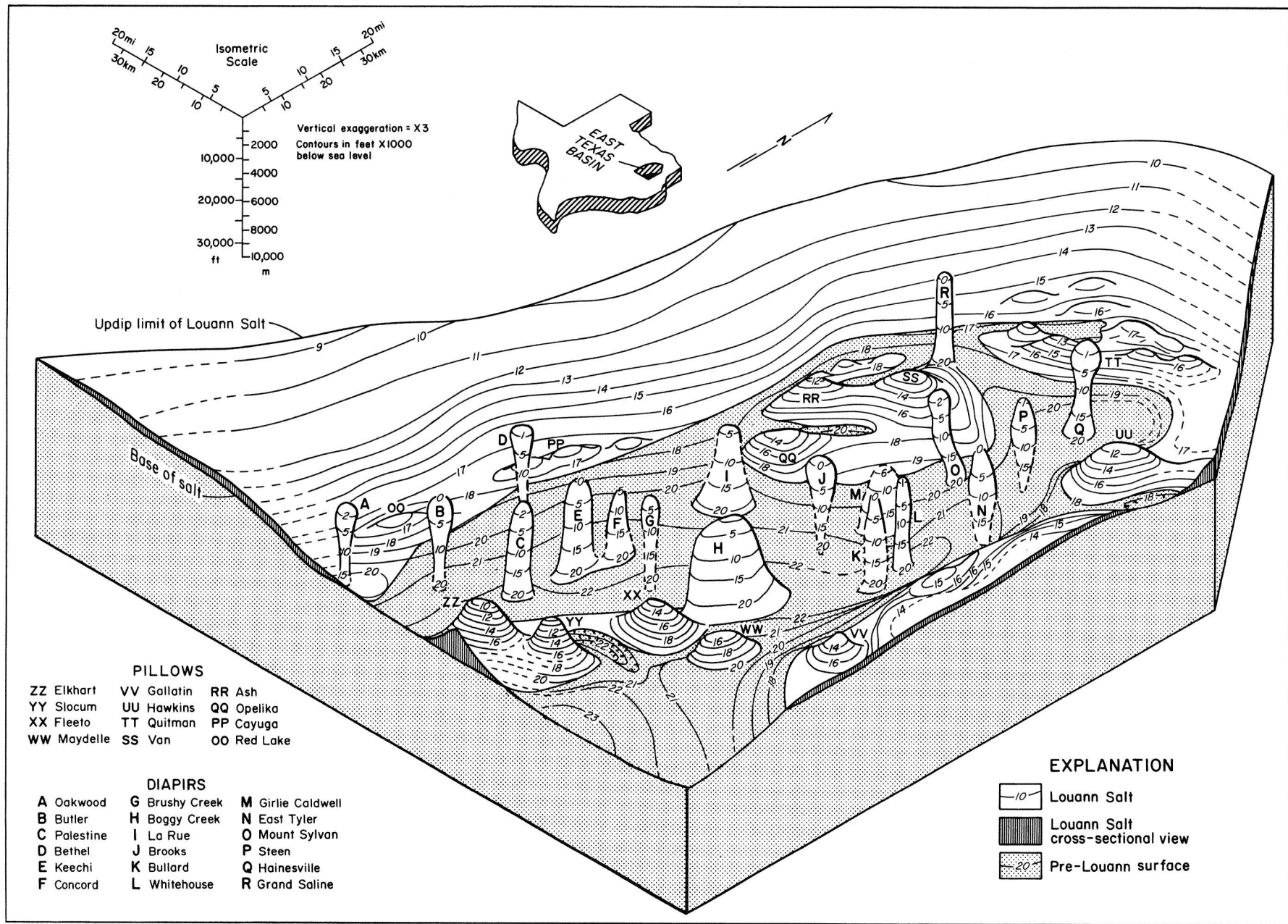


Figure 11. Isometric block diagram of salt structures in the East Texas Basin (from Jackson and Seni, 1983).

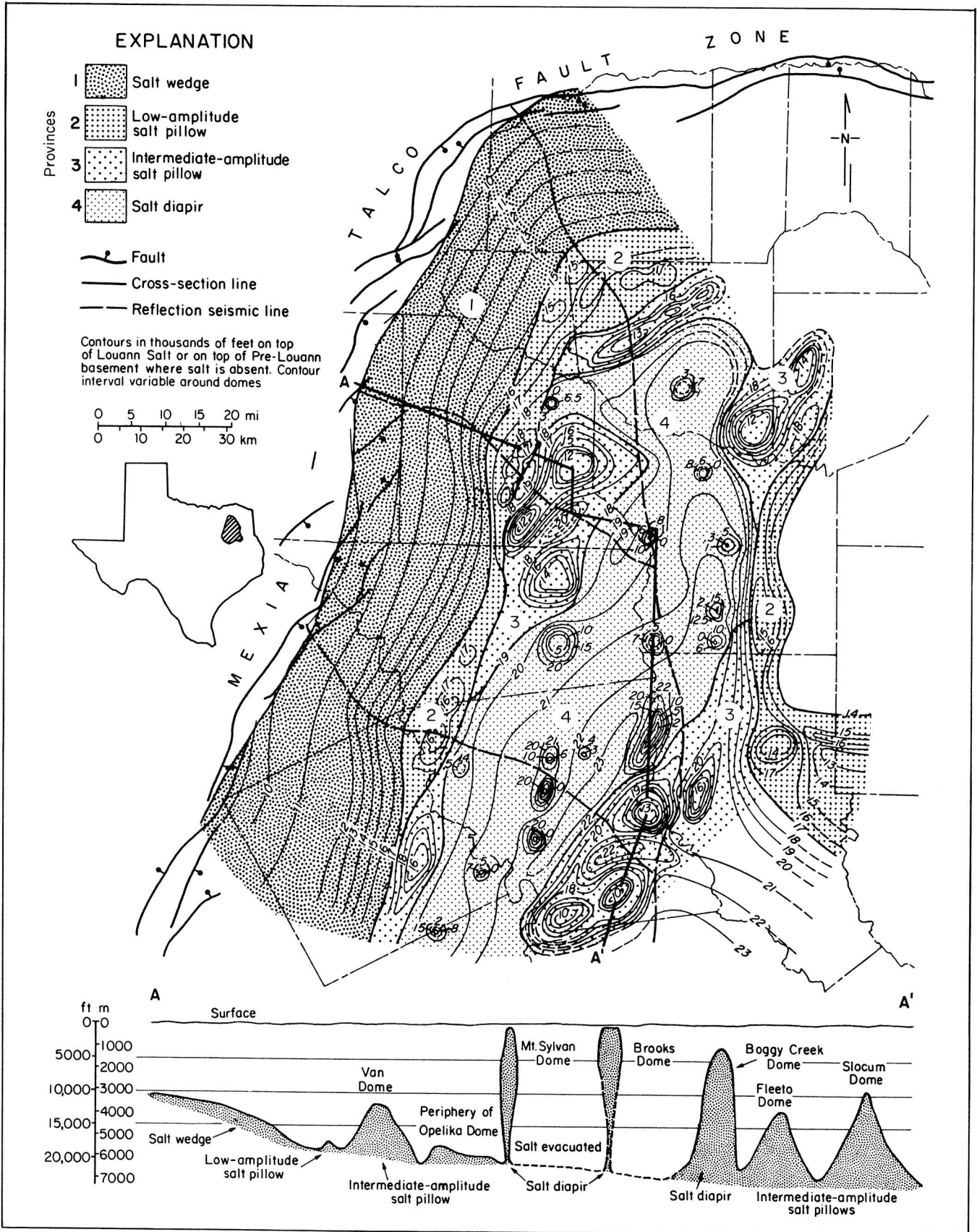


Figure 12. Map of salt provinces and salt-structure contours, East Texas Basin (from Seni and Jackson, 1984).



## Mechanisms Initiating Salt Flow

*Salt pillows formed by (1) differential loading by deltaic sediments over shallow salt; (2) passive rise of salt into gravity-glide anticlines; (3) buoyancy at depths <700 m (<2,300 ft), where salt was loaded by dense carbonates; (4) buoyancy at depths >700 m (>2,300 ft), where salt was loaded by compacted terrigenous clastics and most other sediments; and (5) possible thermal convection in thick salt masses >1,000 m (>3,280 ft) deep.*

For salt to undergo steady-state creep (rheid flow), several conditions must be present. Many combinations of factors, however, promote ductile behavior, such as increasing water content, high temperatures, and low strain rates. Differential stress (equivalent to hydraulic gradient in fluids) must exceed the elastic plastic-flow limit of the salt. Numerous geologic variations in thickness, density, viscosity, or temperature (such as folds, faults, and facies changes) provide differential stresses and trigger salt flow.

In the case of a dipping salt layer of uniform thickness overlain by horizontal, parallel layers of uniform thickness, salt will flow downhill, regardless of the overburden density. This causes updip thinning and downdip thickening of the salt; cover extends updip and shortens downdip by gravity-glide buckling. Where a dipping layer of uniformly thick salt is overlain by progressively thicker, denser cover downdip, updip salt flows downhill from  $P_3$ , and downdip salt flows uphill from  $P_1$ , converging at a point,  $P_2$ , where the gravity head is balanced by the pressure head (fig. 13); salt pillows can be nucleated at convergence points like  $P_2$ .

East Texas salt pillows initially grew by buoyancy because a density inversion was induced by dense Upper Jurassic carbonates overlying less dense salt (fig. 14). Salt rise was probably augmented by folding of the carbonates as they glided into the basin over the salt detachment zone. Younger, larger pillows grew from salt ridges formed by intense differential loading at the leading edge of prograding sand-rich deltas (fig. 15). In at least one dome (Hainesville), erosional breaching of a pillow triggered diapirism. After deep burial had compacted terrigenous sediments, diapir buoyancy was driven by density inversion. Salt may now be thermally convecting in the deepest parts of salt stocks.

Woodbury and others (1980); Kehle (in preparation); Jackson and Seni (1983); Jackson and Harris (1981)

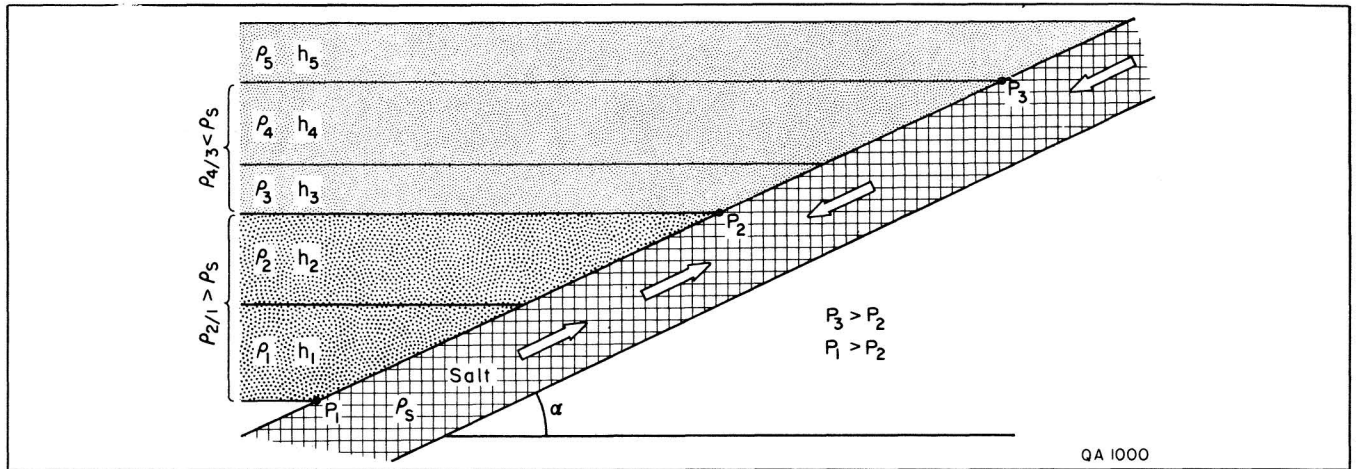


Figure 13. Schematic cross section showing salt-flow directions in dipping source layer overlain by uniform, onlapping overburden (R. O. Kehle, personal communication, 1982). The density of units 1 and 2 is greater than that of salt, and the density of units 3 and 4 is less than that of salt.

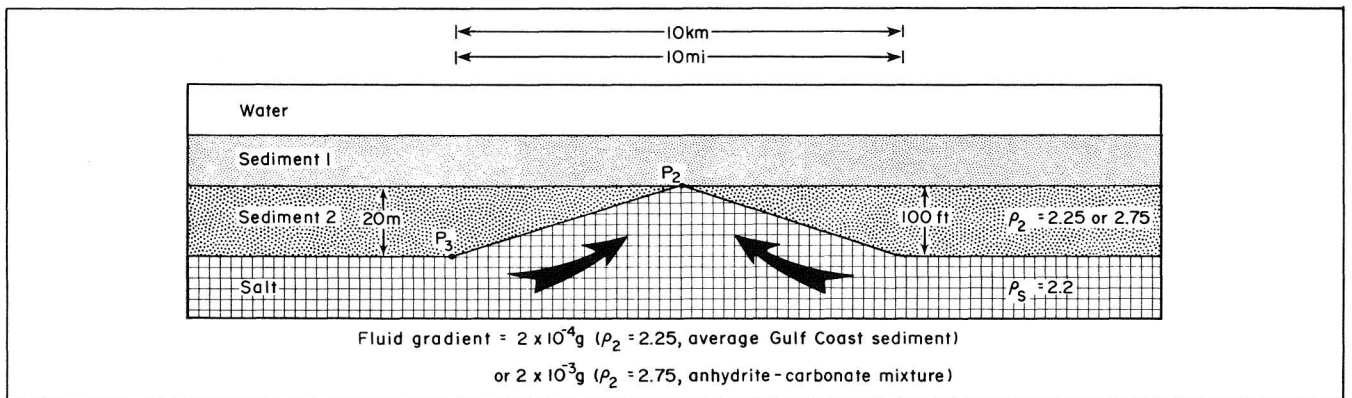


Figure 14. Schematic cross section showing fluid gradient between  $P_2$  and  $P_3$  in 10-mi-wide salt pillow below denser cover based on hydraulic head and slope of pillow flank (R. O. Kehle, personal communication, 1982).

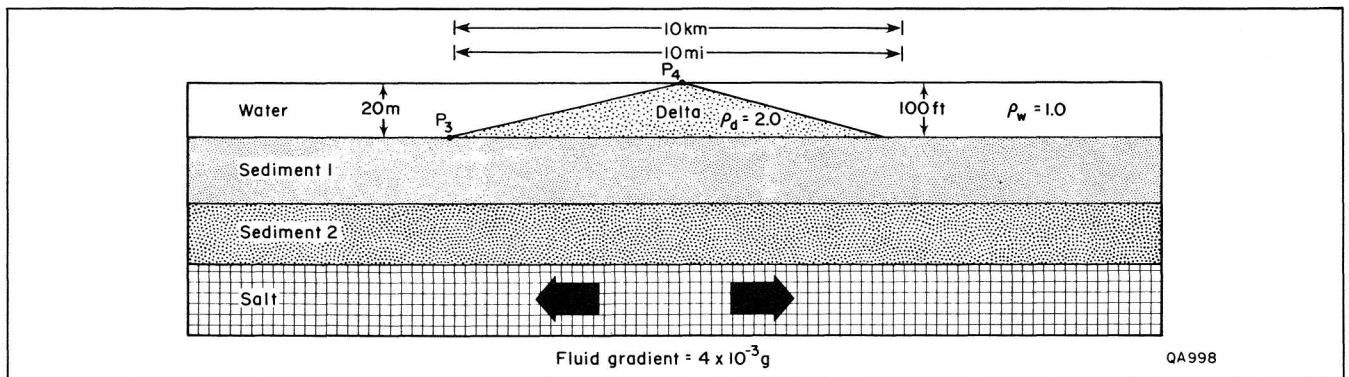


Figure 15. Schematic cross section showing fluid gradient in tabular salt below  $P_3$  and  $P_4$ , induced by differential loading by dense, sand-rich delta prograding toward viewer (R. O. Kehle, personal communication, 1982). Gradient is 20 or 2 times (for cover of specific gravity 2.25 to 2.75, respectively) the buoyancy force induced by density inversion shown in figure 14, although the size of the heterogeneities is the same.

## Initiation of Salt Flow

*Seismic data indicate that the oldest salt structures were low-amplitude pillows. The pillows grew beneath the Smackover-Gilmer carbonate platform. Subsequently Schuler-Hosston deltas prograded across the platform and formed more-distal salt anticlines.*

The earliest record of movement in the Louann Salt is in the overlying shallow-marine interval below the top of the Upper Jurassic Gilmer Limestone. This seismic unit thins over salt pillows of province 2, and overlying units onlap these pillows. Low-amplitude salt pillows therefore grew in pre-Gilmer time. Pillows grew along the western margin of the basin in pillow provinces 2 and 3 ("Present Distribution and Geometry of Salt Structures," p. 27). Oakwood Dome and possibly Grand Saline Dome, on the southwestern fringe of the diapir province 4, also began to grow as pillows in pre-Gilmer time.

The overlying Upper Jurassic marine strata formed an aggrading, slowly prograding, carbonate wedge that loaded the salt fairly uniformly. The evaporitic Buckner Anhydrite wedges out seaward in pillow provinces 2 and 3 (fig. 16A), possibly because topographic swells over pillows restricted circulation of seawater. The carbonate shelf break is inferred from abrupt thickening of overlying terrigenous clastics along this line. In Gilmer time, the basin was still starved and the slope sediments were thin (fig. 16A). This accounts for the lack of contemporaneous halokinesis in the central basin, despite its having the great thickness of salt.

In the Late Jurassic and Early Cretaceous, the Schuler-Hosston clastics prograded rapidly across the carbonate platform as coalescing sand-rich deltas. Progradation slowed on crossing the shelf break, but the thick deltas continued to advance as a linear front into the previously starved basin (fig. 16B). Subsurface mapping delineates strike-parallel thicks in provinces 3 and 4, indicating the existence of parallel ridges and troughs. Loading of the pre-Schuler substrate by the advancing linear depocenters would have squeezed salt ahead as a frontal bulge to form salt pillows (fig. 16B). An increase in sediment supply or progradational rate would have buried the frontal pillows, thereby initiating parallel, but more distal, salt pillows, ridges of salt from which the salt diapirs would have grown by budding upward.

Jackson and Seni (1983); McGowen and Harris (in press); Jackson and Harris (1981); Kehle (in preparation)



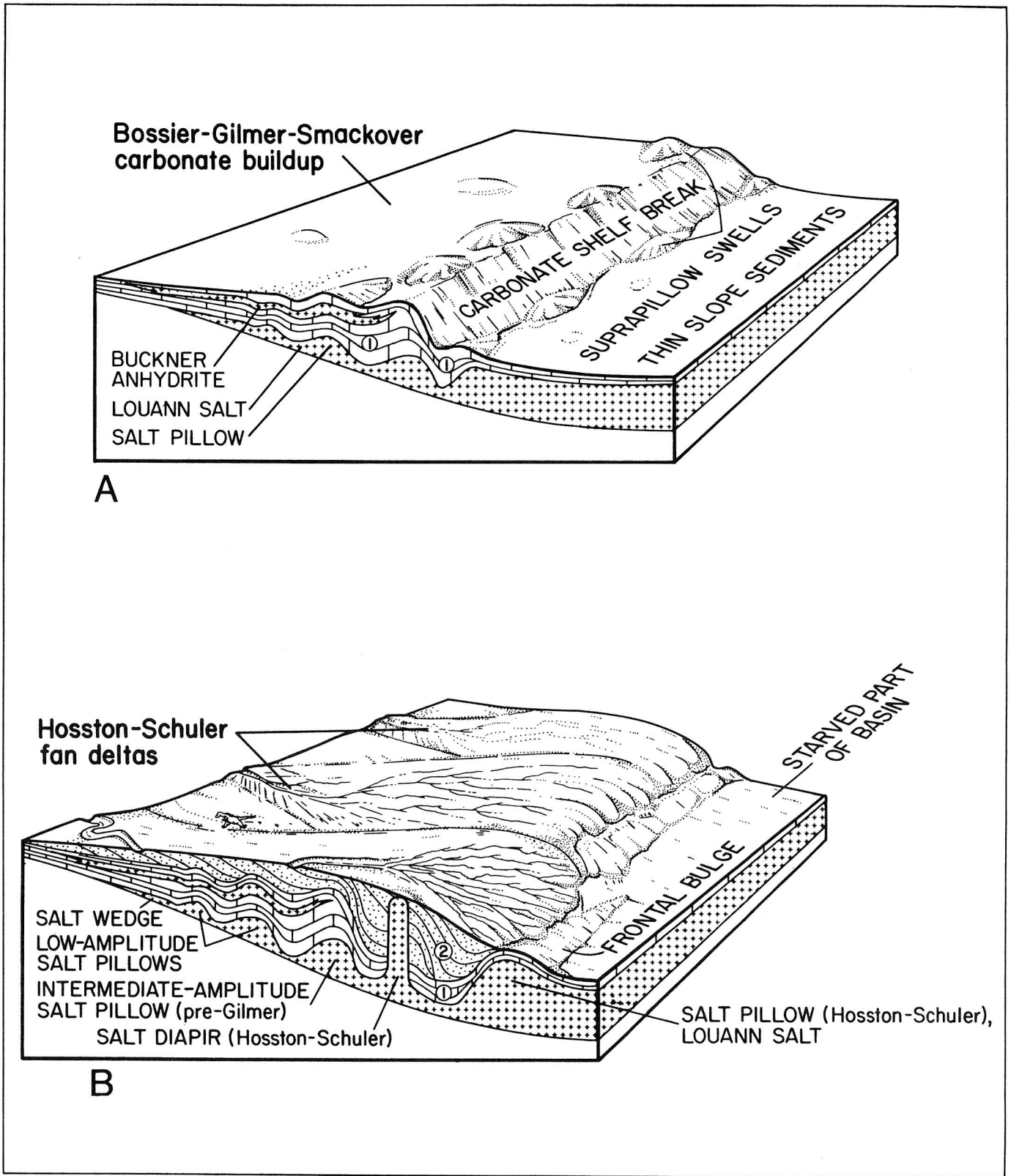


Figure 16. Models of Late Jurassic - Early Cretaceous salt mobilization. (A) Schematic block diagram of depositional facies during Bossier-Gilmer-Smackover time (after Jackson and Seni, 1983). (B) Schematic block diagram of depositional facies during Hosston-Schuler time (after Jackson and Seni, 1983). Numbers 1 and 2 refer to primary and secondary peripheral sinks, respectively.

## Diapirism

*Group 1 diapirs grew along the margins of the diapir province in Late Jurassic - Early Cretaceous time. Group 2 diapirs grew along the basin axis in the mid-Cretaceous. Group 3 diapirs grew along the northwestern margins of the diapir province in the Late Cretaceous.*

By Glen Rose time (Early Cretaceous), salt diapirs were growing in three areas around the periphery of the diapir province (fig. 17), starting at about 130 Ma ago. Two areas coincide with known Schuler-Hosston clastic depocenters. The significance of the third area on the eastern margin of the basin is obscure. These group 1 diapirs thus appear to have been localized by loading on the salt-cored pillows in front of the prograding Schuler-Hosston deltas.

By mid-Cretaceous, when maximum sedimentation was taking place in the basin center, a second generation of diapirs evolved through a pillow stage from the thick salt (fig. 18). Sites of group 2 diapir initiation migrated from the basin center northward along the basin axis.

The group 3 diapirs on the northern and western margin of the diapir province had a different origin. In the Late Cretaceous, subsidence of the East Texas Basin had declined exponentially to relatively low rates. Tilting of the basin margins by loading of the basin center would have promoted basin-edge erosion, a common process during the end of basin evolution. Alternatively, erosion may have been fostered by the rise of a large salt pillow, which would have caused shoaling and exposure of the overlying sea floor. Local unconformities exist over Hainesville Dome, and 150 to 200 km<sup>3</sup> (37 to 49 mi<sup>3</sup>) of salt are calculated to be missing. The precursor salt pillow was breached by erosion; salt extrusion formed the largest secondary peripheral sink in the East Texas Basin. Erosional breaching of the faulted crests of salt pillows might also have initiated piercing by the first and second generations of diapirs.

Seni and Jackson (1983a, b, 1984); Jackson and Seni (1983, in press); Giles (1981); Loocke (1978)

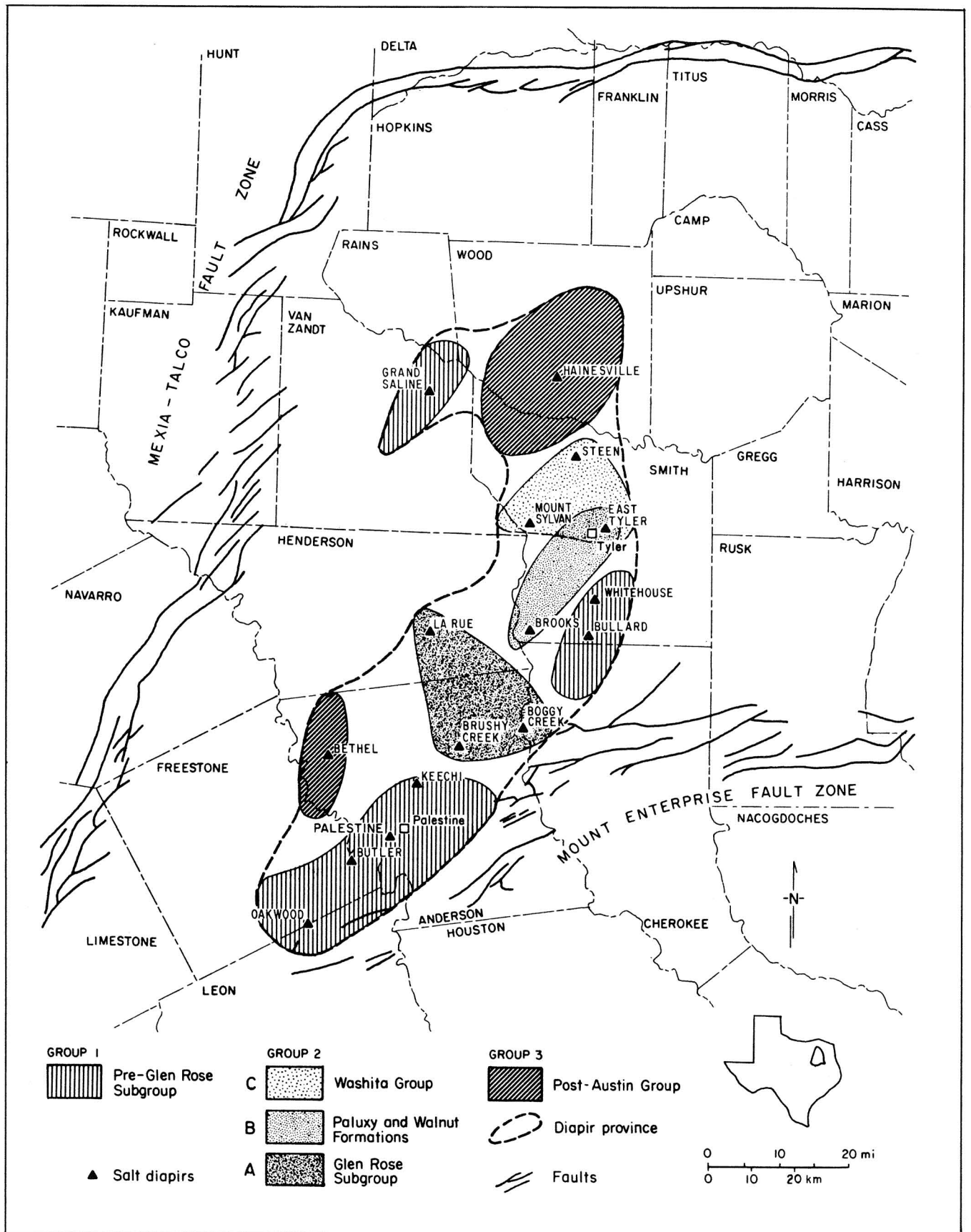
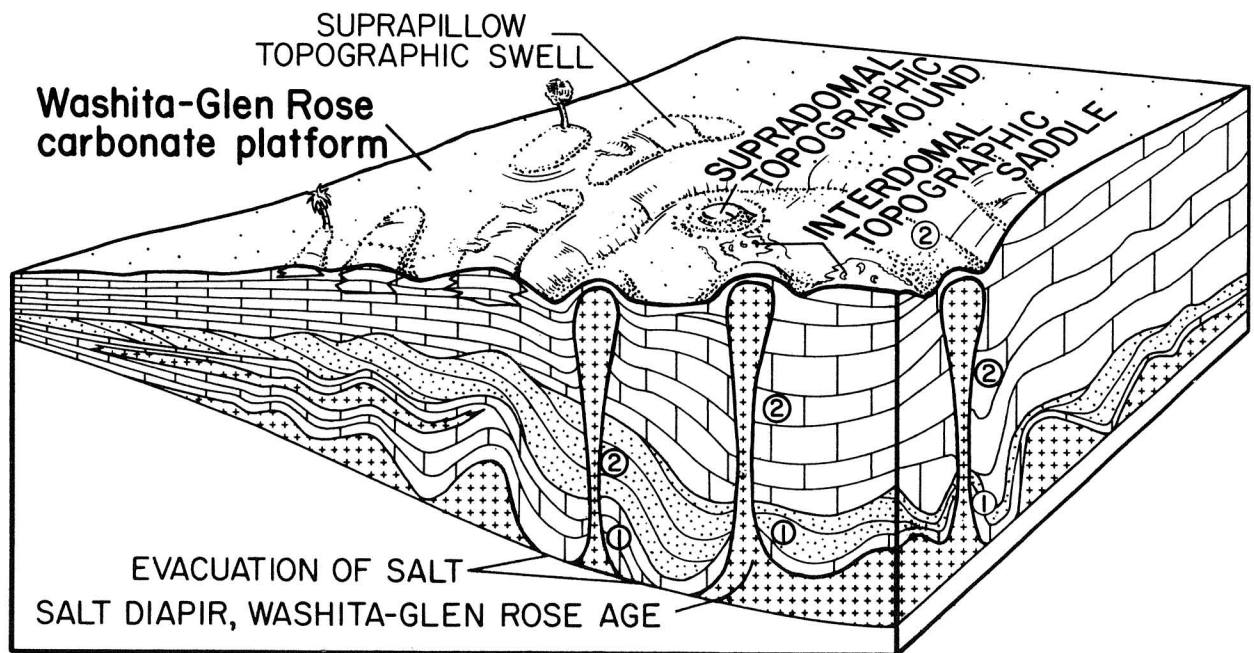


Figure 17. Map of diapir groups in the East Texas Basin (from Seni and Jackson, 1983b).



### EXPLANATION

- ① Primary peripheral sink
- ② Secondary peripheral sink
- ③ Tertiary peripheral sink

Figure 18. Block diagram of depositional facies during Washita - Glen Rose and Wilcox time (after Jackson and Seni, 1983).



## Effects of Dome Growth on Depositional Facies of Enclosing Strata

*Studies of paleoenvironments of the East Texas Basin and of modern environments elsewhere show that growing salt structures formed topographic mounds and depressions. The topographic influence on sedimentation patterns is characteristic of different dome-growth stages and sedimentary environments.*

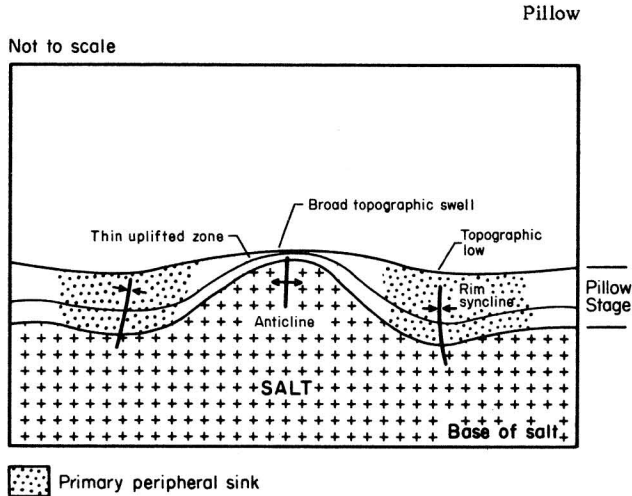
Syn depositional lithostratigraphic variations in response to salt flow highlight the interdependence between sediment accumulation and dome evolution (fig. 19). These lithostratigraphic variations were primarily controlled by paleotopography. Salt uplift formed broad swells over salt pillows and small mounds over diapirs. Concurrently, topographic and structural basins formed over zones of salt withdrawal, leaving saddles with residual elevation between the basins (fig. 20). This salt-related topography influenced sedimentation patterns, which, in turn, enhanced continued salt flow because of increased loading by vertically stacked facies in the peripheral sink.

In the East Texas Basin, salt-pillow growth uplifted and thinned broad areas over the crest and flanks of the pillows, whereas diapir growth uplifted and thinned smaller areas (fig. 19). During diapirism, the effect of the topographic depression in the large peripheral sink was much greater than the effect of the diapir mound. Continued domal "piercement" commonly destroyed the uplifted strata by erosion or by shoving the uplifted units aside. In contrast, much of the broad, thinned zone over pillow crests was preserved when during diapirism the underlying pillow collapsed and was buried deep below secondary and tertiary peripheral sinks (fig. 20). The locations of sinks are related to evolutionary stage and regional dip. Axial traces of primary peripheral sinks tend to be updip of the salt pillow. In contrast, secondary and tertiary peripheral sinks commonly encircle the diapir. This change in position results from the transition from predominantly downdip lateral flow in the pillow stage to a combination of centripetal and upward flow in the diapir stage.

The sedimentary response of fluvial and deltaic environments to salt-influenced topography was different from the response of marine and shelf environments. Fluvial systems bypassed topographic mounds above domes and pillows (fig. 21). Sediments deposited in uplifted areas, therefore, tend to be thin and sand poor (fig. 22). Subsidence of the peripheral sinks promoted aggradation of sand-rich fluvial-channel facies.

In siliciclastic shelf and shallow-marine carbonate environments, sand can accumulate by winnowing on bathymetric shoals, so that salt domes with sufficient surface expression, such as those in the modern Persian Gulf, are overlain by sand-rich sediments. Lower Cretaceous reefs have been found in East Texas on saddles with residual elevation between salt-withdrawal basins (fig. 20). Dome-crest reefs have been recognized in Oligocene sediments of the Texas Gulf Coast, in Holocene strata in the northwestern Gulf of Mexico, and in the modern Persian Gulf, but not in East Texas.

Seni and Jackson (1984); Jackson and Seni (1983); Seni and Fogg (1982); McGowen and Harris (1981); Seni (1981)



#### Pillow

Sediments above pillow are thin over broad, equidimensional to elongate area. Maximum thinning over crest. Area extends 100-400 km<sup>2</sup> (40-150 mi<sup>2</sup>), depending on size of pillow. Percentage thinning, 10-100%.

#### Withdrawal basin

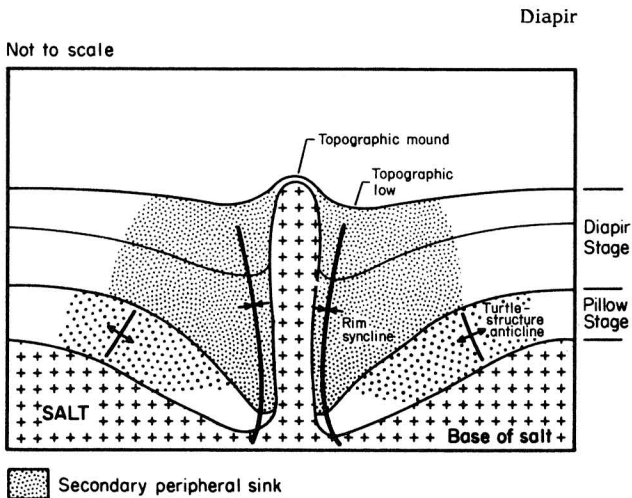
Sediments are thickened in broad to elongate primary peripheral sink, generally located on updip side of salt pillow. Axial trace of sink parallels axial trace of elongate uplift; axial traces are generally separated by 5-20 km (3-12 mi). Sink attains 300 km<sup>2</sup> (120 mi<sup>2</sup>) in extent, depending on size of pillow. Percentage thickening, 10-30%. Recognition of primary peripheral sink may be hindered by interference of nearby salt structures.

#### Facies

Thin, sand-poor, fluvial-deltaic deposits over crest of pillow include interchannel and interdeltatic facies. Erosion common. Carbonate deposits on crest include reef, reef-associated, and high-energy facies.

#### Facies

Thick, sand-rich fluvial-deltaic deposits in primary peripheral sink include channel axes and deltaic depocenters. Aggradation common in topographically low area of sink. Carbonate deposits in sink include low-energy facies caused by increase in water depth.



#### Diapir

Strata largely absent above dome. An 8- to 50-km<sup>2</sup> (3- to 20-mi<sup>2</sup>) area around diapir is thinned, depending on size and dip of flanks of dome.

#### Withdrawal basin

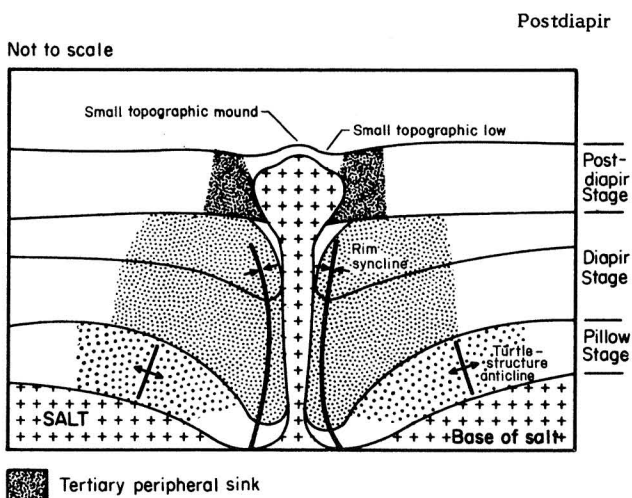
Sediments are thickened up to 215% in secondary peripheral sink. Sinks up to 1,000 km<sup>2</sup> (390 mi<sup>2</sup>) in extent are equidimensional to elongate and preferentially surround single or multiple domes; several sinks flank domes; percentage thickening, 50-215%.

#### Facies

Facies immediately over dome piercing by diapir of all but the youngest strata. Sand bodies commonly pinch out against dome flanks.

#### Facies

Expanded section of marine facies dominates, including limestones, chinks, and mudstones; generally sink is filled with deeper water, low-energy facies caused by increased water depth. Elevated saddles between withdrawal basins are favored sites of reef growth and accumulated high-energy carbonate deposits.



#### Postdiapir

Strata thin or absent in small 10-50 km<sup>2</sup> (6-20 mi<sup>2</sup>) area over crest and adjacent to dome; area depends on size of dome and dip of flanks.

#### Withdrawal basin

Sediments within 20-200 km<sup>2</sup> (8-80 mi<sup>2</sup>) of the tertiary peripheral sink are thickened up to 50%, commonly by > 30 m (100 ft). Axial trace of elongate to equidimensional sink surrounds or flanks a single dome or connects a series of domes.

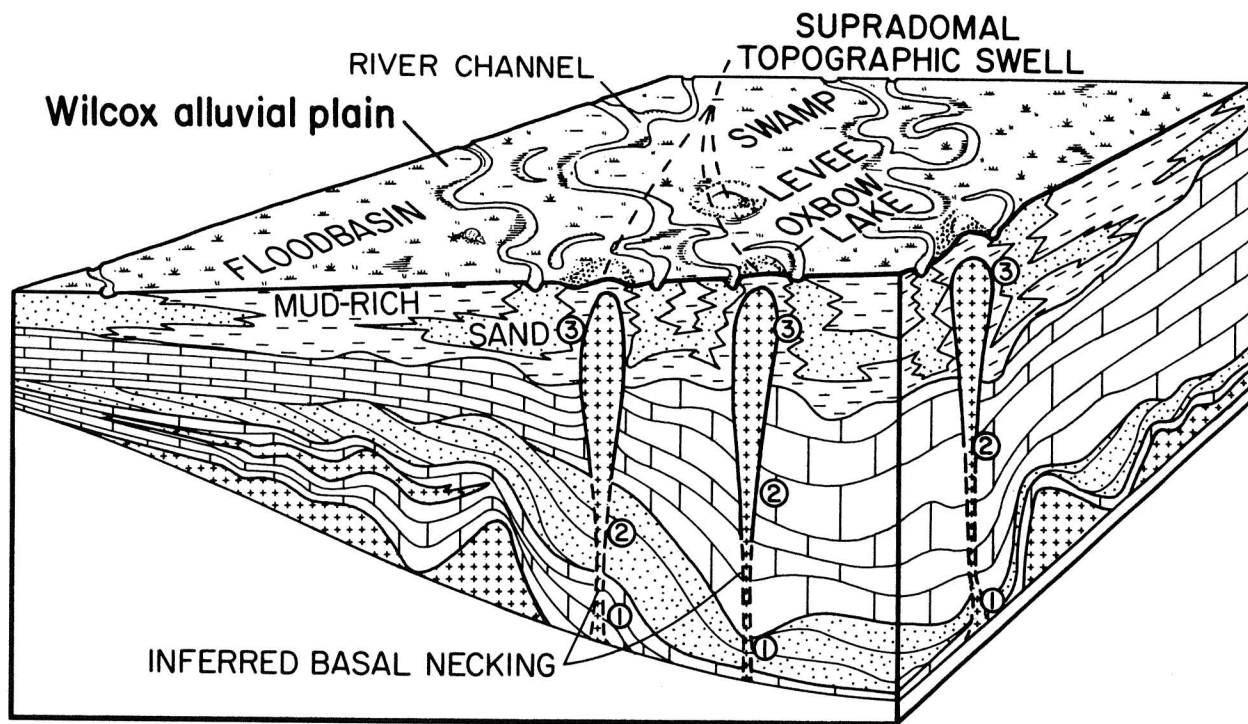
#### Facies

Facies and strata over crest of dome not preserved in cases of complete piercement. Modern analogs have interchannel and interdeltatic facies in uplifted area. Mounds above dome include thin sands. Carbonate strata include reef or high-energy deposits; erosion common.

#### Facies

Modern analogs have channel axes in sink. Aggradation of thick sands common in subsiding sink. Carbonate strata include low-energy facies.

Figure 19. Schematic cross sections showing stages of dome growth (from Seni and Jackson, 1983a).



### EXPLANATION

- ① Primary peripheral sink
- ② Secondary peripheral sink
- ③ Tertiary peripheral sink

Figure 20. Block diagram of depositional facies during Wilcox time (after Jackson and Seni, 1983).



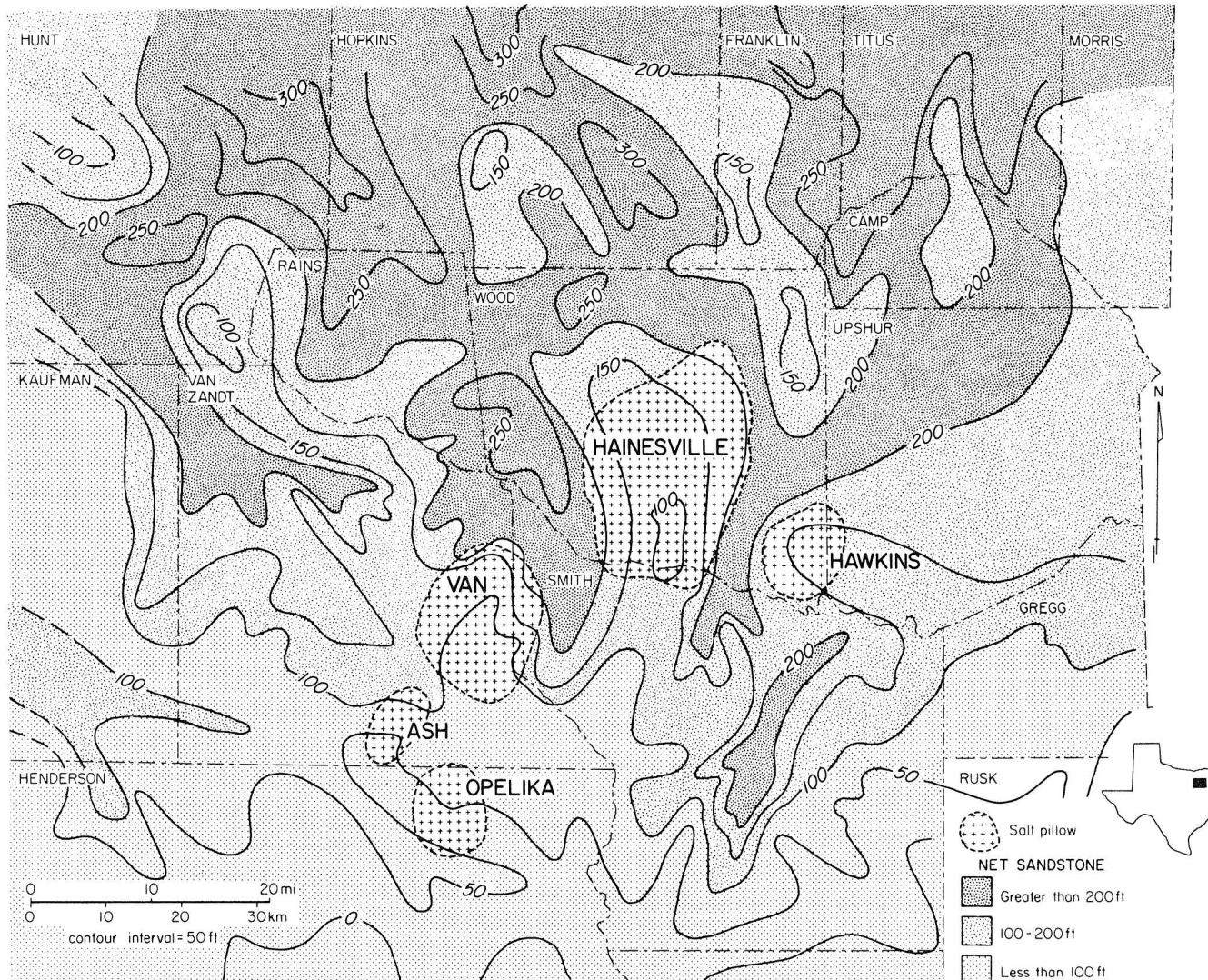


Figure 21. Net-sandstone map, Paluxy Formation, showing decrease in sandstone thickness over crests of pillows (from Seni and Jackson, 1984).

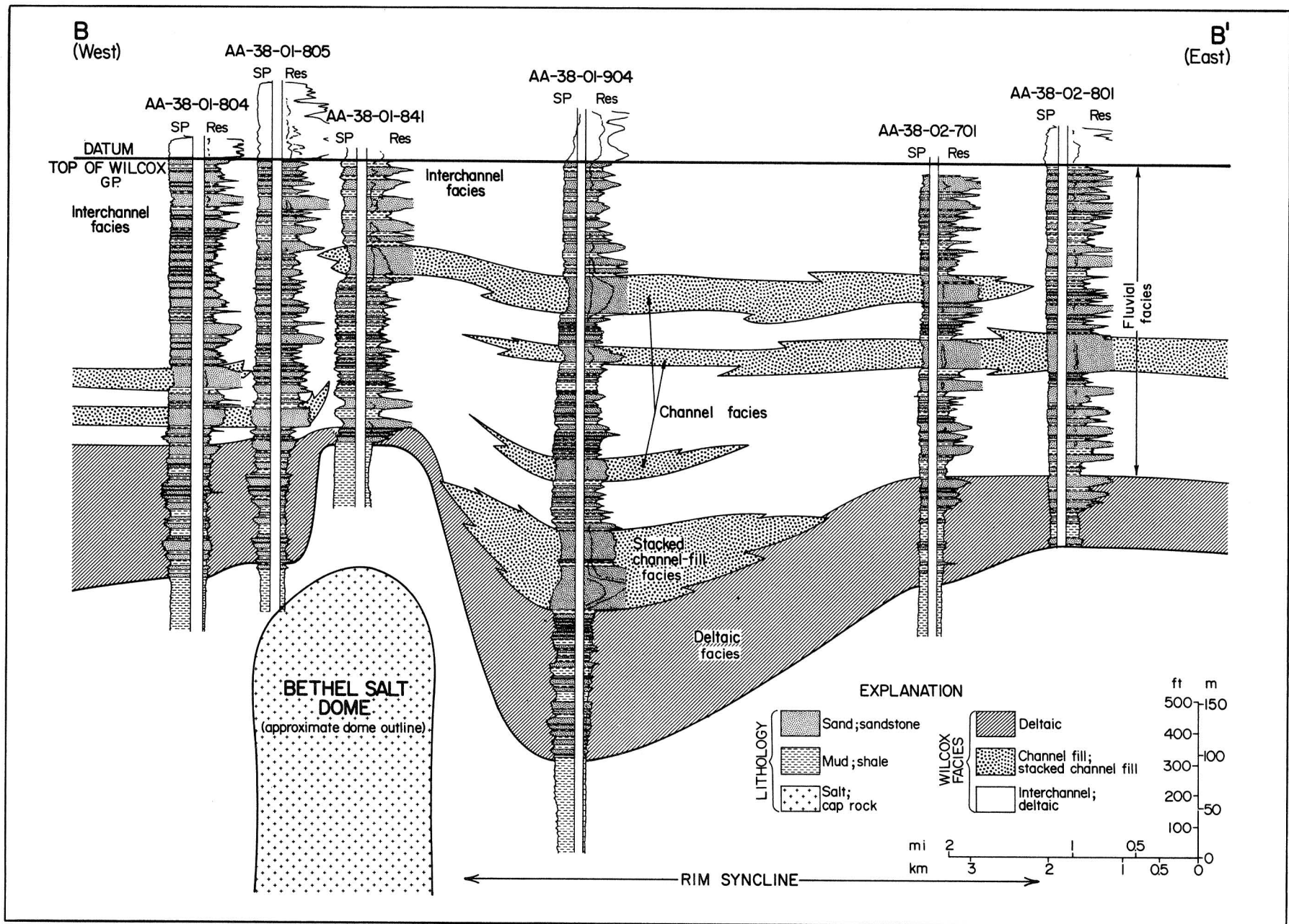


Figure 22. Cross section B-B' through Wilcox Group around Bethel Dome (from Seni and Jackson, 1983a).



## Effects of Dome Growth on Structure of Enclosing Strata

*Strata immediately adjacent to diapirs invert from anticlinal to synclinal, whereas interdomal strata invert from synclinal to anticlinal, creating a turtle-structure anticline.*

During the pillow stage of growth, strata over the pillow crest and flanks are anticlinal, whereas strata in the primary peripheral sink over the area of salt withdrawal are synclinal (fig. 23). Sediments over the pillow crests undergo extension, commonly with antithetic faults and central grabens, drape compaction, and differential compaction. Most thinning of strata above pillows, however, is syndepositional and caused by salt flow.

During the subsequent diapir stage, the flanks of the pillow deflate because of salt withdrawal into the diapir growing from the center of the pillow. Pillow deflation results in collapse of the originally anticlinal strata, forming a synclinal secondary peripheral sink (such as Bethel and Hainesville Domes, fig. 23). The core of the primary peripheral sink remains unaffected by collapse. However, the flanks of the sink, which overlie the pillow flanks, collapse during diapirism, thereby forming a turtle-structure anticline. Stratal thickening in secondary peripheral sinks is due mainly to syndepositional salt flow rather than to post-depositional distortion by folding. Diapiric piercement is commonly assisted by erosional breaching of a salt pillow, as evidenced by angular unconformities centered around diapirs like Hainesville Dome.





Salt stocks with upward-converging sides (such as Palestine and Boggy Creek Domes) drag up adjacent strata. In contrast, stocks with upward diverging or vertical sides (such as Bethel and Grand Saline Domes) have negligible effect on adjacent strata. This suggests that friction along the salt contact has only a local effect. All salt stocks examined are bounded by ring faults along their sides. Antithetic faults are more abundant than homothetic faults over diapirs. Thus the effects of lateral extension and collapse predominate over uplift.

Jackson and Seni (1983, 1984); Seni and Jackson (1983a); Jackson (1982); Wood and Guevara (1981); Jackson and Harris (1981); McGowen and Harris (1981); Wood (1981); Wood and Giles (1982)

TOP OF WOODBINE  
EAST TEXAS DIAPIR PROVINCE

- SALT DIAPIRS  
 A Oakwood  
 B Butler  
 C Palestine  
 D Bethel  
 E Keechi  
 F Boggy Creek  
 G Brooks  
 H Bullard  
 I Whitehouse  
 J Mount Sylvan  
 K East Tyler  
 L Steen  
 M Hainesville  
 N Grand Saline

EXPLANATION

-  Salt diapir (pierces top of Woodbine)
-  Fault trace (plane dips away from viewer)
-  Fault plane with separation (plane dips toward viewer)
-  Contours in feet X 100 below sea level. Contour interval variable

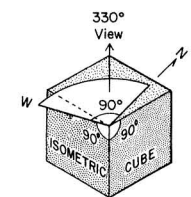
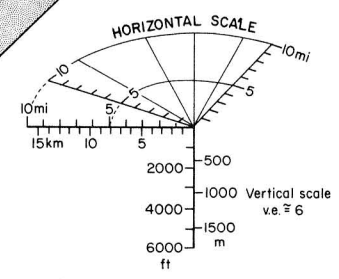
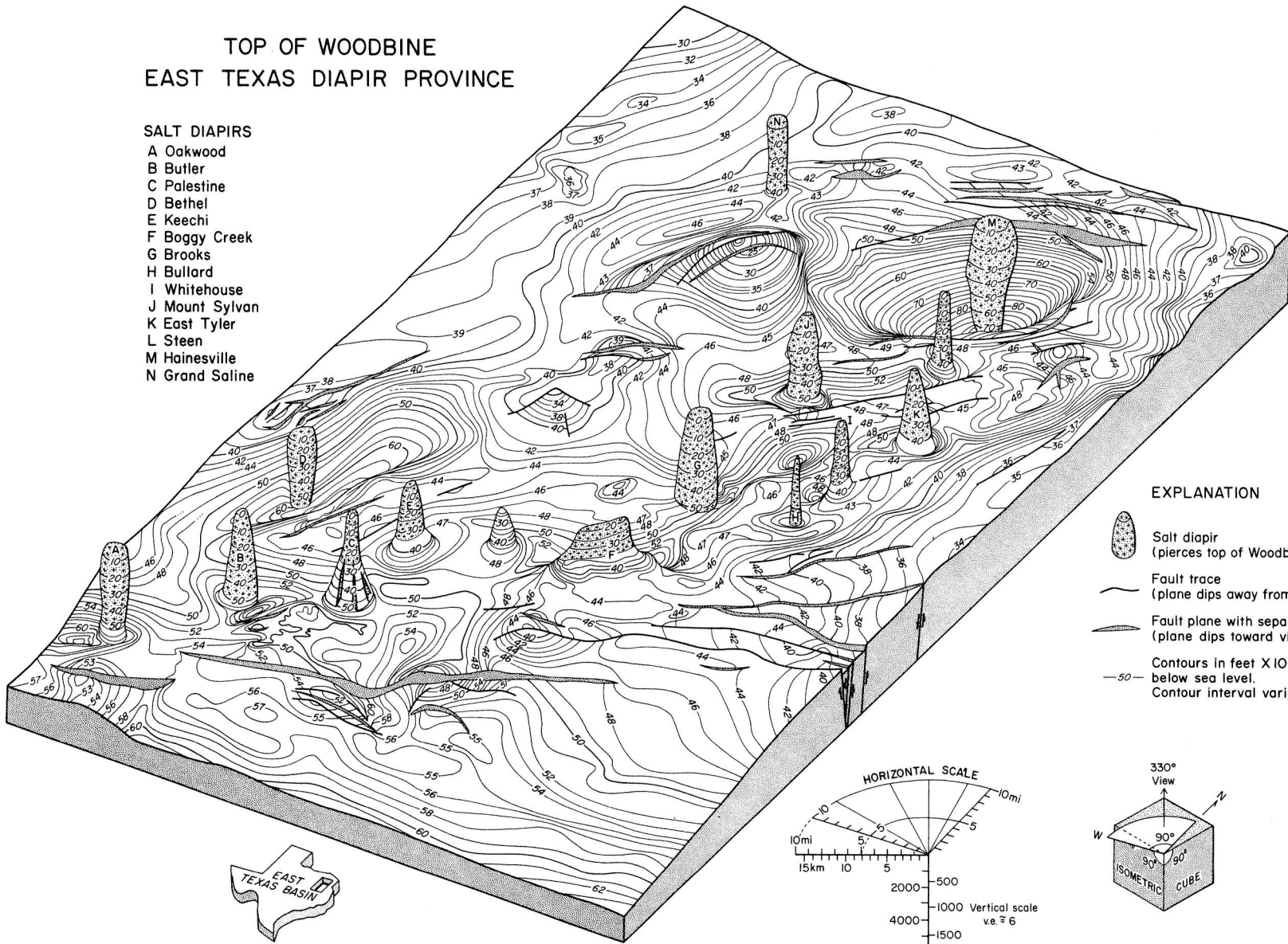


Figure 23. Isometric block diagram of salt diapirs and structure contours on top of Woodbine Group.

## Effects of Dome Growth on Surface Processes

*Anomalous geomorphic features over Oakwood Dome include a central depression, relatively steep, incised channels, cut-off channels, and erosional slopes that are steeper than those over Keechi and Palestine Domes. These features are equivocal and do not preclude Quaternary uplift. Scattered depositional terraces show no evidence of dome-related uplift. On the contrary, the southern part of Oakwood Dome may have subsided in Quaternary time.*

Fracturing induced by dome growth is apparently recorded in the pattern of lineaments above salt domes. Shallower domes have lineament distributions with lower degrees of preferred orientation than do deeper domes (fig. 24). Southern domes (Bethel, Boggy Creek, Butler, Keechi, Oakwood, and Palestine) tend to have lower degrees of lineament preferred orientation than do northern domes of the same depth. The lower preferred orientations are ascribed to a higher proportion of radial and concentric fractures induced by dome growth. Southern domes have a significantly higher lineament density than do the northern domes.

Channels over the central part of Oakwood Dome are incised as much as 4 m, unlike the shallow channels over the dome flanks. Migration of some creek channels away from the dome, leaving cut-off channels, may have been caused by dome uplift. Link-length-distribution analysis (Shreve, 1967) of East Texas drainage networks over various salt domes suggests that Oakwood Dome has a less mature drainage system than do other domes.

Morphologic maps of Palestine, Keechi, and Oakwood Domes distinguish between slopes formed by erosional processes and slopes formed by depositional processes. Hillside erosional slopes above Oakwood Dome are considerably steeper than those above the other two domes. Furthermore, erosional slopes above Oakwood and Palestine Domes are steeper than adjacent slopes outside the dome area. All three domes display depositional slopes, commonly in a central depression. Above Palestine Dome, a ring of hills surrounds a man-made lake. In the south-central part of Oakwood Dome, alluvium twice as thick as in adjacent downstream areas fills a relatively large floodplain (fig. 25). Topographic lows suggest subsidence over domes, possibly caused by ground-water dissolution of cap rock or salt.

Palestine, Keechi, and Oakwood Domes are located in the Trinity River drainage basin, where four Quaternary terrace levels have been identified. The regional gradient of these terraces shows no significant domal uplift. On a local scale, outcrop and borehole data from Quaternary terrace deposits at Oakwood and Palestine Domes show no indication of warping owing to dome uplift. However, these deposits are of limited extent, and determination of relative movement is difficult.

Extrapolation of suspended-sediment-load data (Trinity, Neches, and Sabine River basins, 20-yr mean duration of record) and of sedimentation resurvey data from four reservoirs (13-yr

mean duration of record) yields average denudation rates of 0.9 m/10<sup>4</sup> yr (3 ft/10<sup>4</sup> yr) and 1.7 m/10<sup>4</sup> yr (5.6 ft/10<sup>4</sup> yr), respectively. These rates are slightly higher than the estimated maximum rates of dome uplift (see "Rates of Dome Growth," p. 51).

Collins and others (1981); Collins (1982); Dix and Jackson (1981a); Collins and Hobday (1980); Dix (1980); Collins (1981a); Dix and Jackson (1981b); Collins (1981b); Collins (1981c)

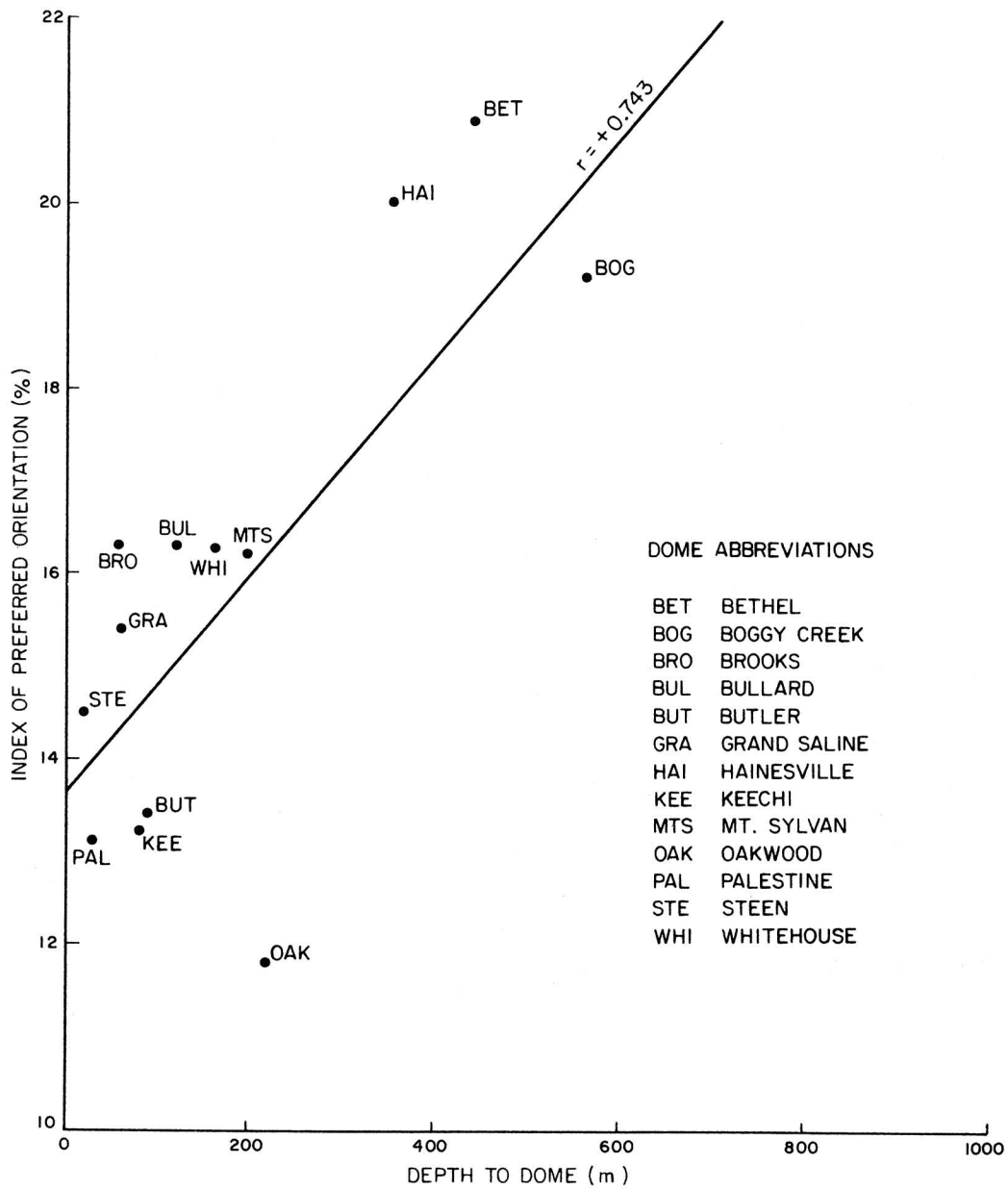


Figure 24. Graph showing significant correlation (99-percent confidence level) between depth to dome and index of preferred orientation of lineaments (from Dix and Jackson, 1981b).



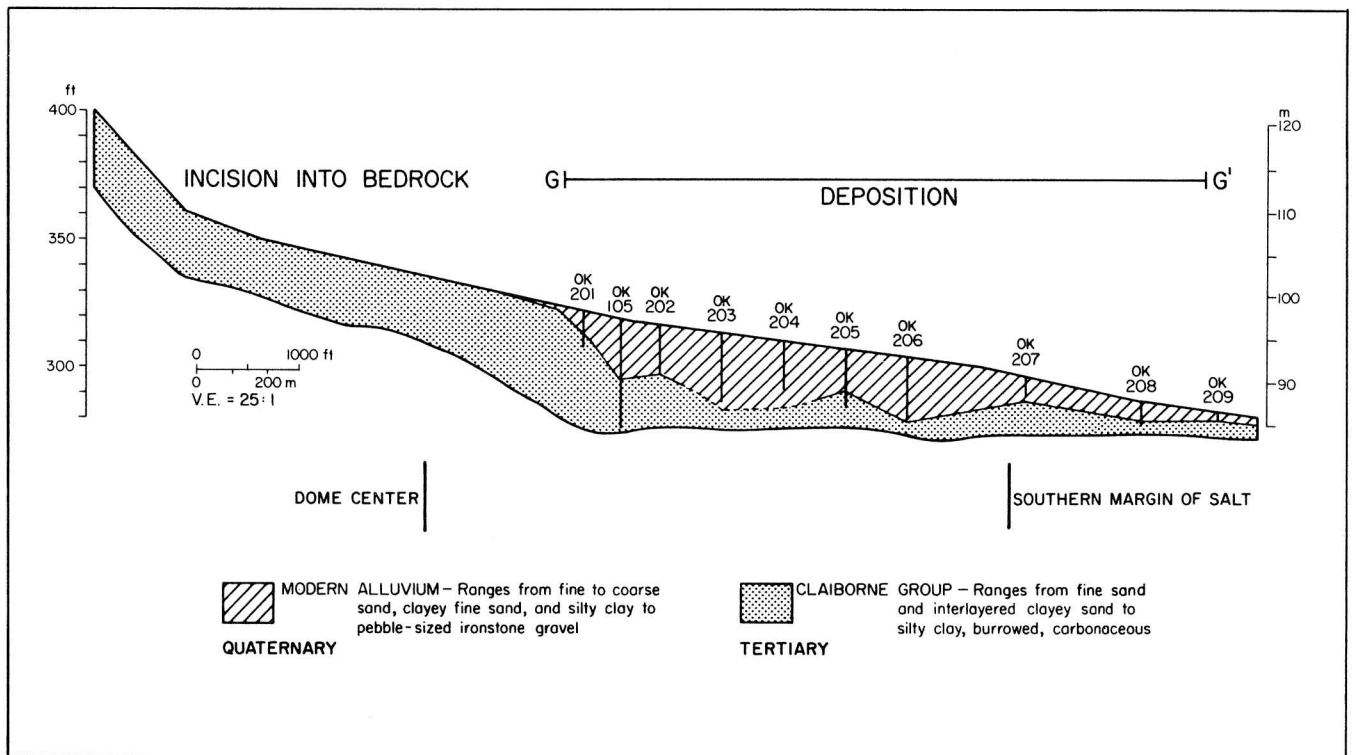


Figure 25. Cross section of Quaternary floodplain deposits above Oakwood Dome (from Collins and others, 1981).

## Rates of Dome Growth

*Three different techniques of calculating dome-growth rates show that growth declined exponentially from 112 to 48 Ma ago. Extrapolation indicates that none of the East Texas salt domes is likely to rise more than 0.6 m (2 ft) in the next  $10^4$  yr.*

Syn depositional thickness variations in surrounding strata allow measurement of the volumes and rates of salt flow during the growth of salt pillows and salt domes.

The concept of gross rate of growth versus net rate of growth is of fundamental importance to the potential isolation of nuclear waste in salt domes. Gross rates are a function of the volume of salt evacuated from the withdrawal basin and mobilized up the diapir. Net rates are a function of this process and all other processes that affect diapir growth rate and height, such as salt dissolution, extrusion, and lateral intrusion. Thus gross rates of growth approximate the true rate of salt flow regardless of the independent motion of the diapir crest. On the other hand, net rates of growth approximate the actual movement of the diapir crest.

Average growth rates were calculated for 16 salt domes for successive periods of 1 to 17 Ma and combined to yield curves of long-term growth over 64 Ma (fig. 26). Maximum gross rates of dome growth (400 to 530 m/Ma; 1,310 to 1,740 ft/Ma) coincided with maximum regional rates of deposition in the Early Cretaceous from 112 to 104 Ma ago. Rapid gross rates of dome growth (180 to 460 m/Ma; 590 to 1,510 ft/Ma) recurred along the northern and western margins of the diapir province in the Late Cretaceous from 86 to 56 Ma ago during growth of Hainesville and Bethel Domes.

All three growth-rate curves show the same trend of exponential decline with time, regardless of whether they are based on compacted or decompact sediment thicknesses. Extrapolation of the most recent, well-documented episode of dome growth 65 Ma ago indicates that none of the East Texas domes is likely to rise more than 0.6 m (2 ft) in the next  $10^4$  yr.

Seni and Jackson (1983b, 1984); Giles and Wood (1983); Giles (1981); Netherland, Sewell, and Associates (1976); Kumar (1977); Trusheim (1960); Jaritz (1980)

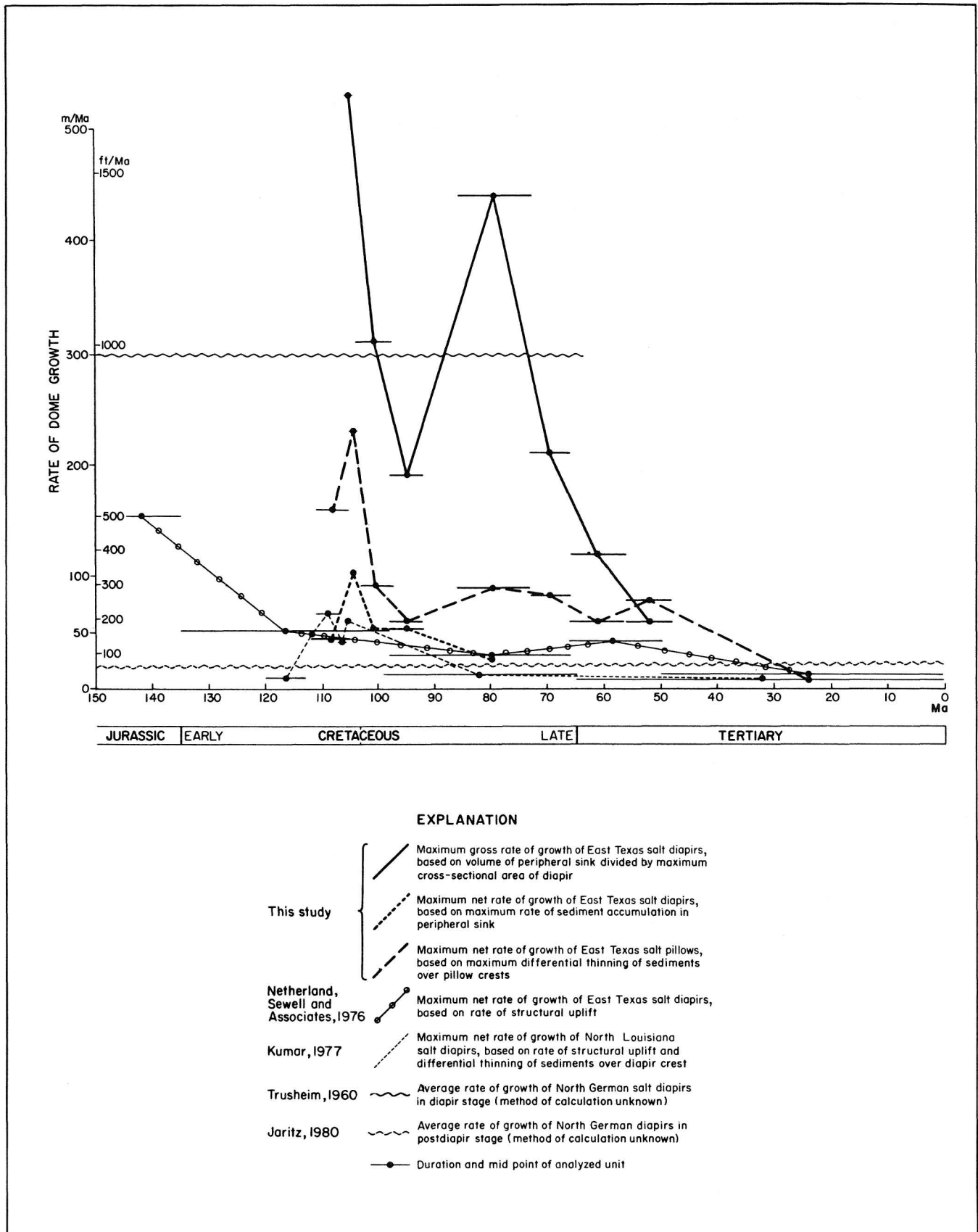


Figure 26. Comparison of long-term rates of dome growth for East Texas, North Louisiana, and North German salt domes (from Seni and Jackson, 1983b).

## Fault Tectonics

*All the regional faults studied (1) are normal, (2) moved steadily during the Mesozoic and early Tertiary, and (3) appear to be related to salt mobilization.*

All the regional fault systems were examined in terms of their distribution, geometry, displacement history, and possible origins. Figure 27 shows their relation to salt structures.

The Mexia-Talco fault zone is a graben between salt-free strata and strata underlain by mobile salt that allowed overburden creep into the East Texas Basin. The Elkhart Graben and the central-basin faults formed by crestal stretching and collapse of strata above salt pillows and turtle structures (fig. 28). At least one western fault in the Mount Enterprise fault zone is a long-active, listric-normal growth fault, downthrown to the north and based in the Louann Salt. Once initiated, its growth would have been perpetuated by loading induced by sediments trapped on the downthrown side and by the tensile stress regime near the basin margins.

The absence of displaced terraces suggests that faulting ceased before the Quaternary, except for a westward extension of the north flank of the Elkhart Graben and small faults south of the Mount Enterprise fault zone.

Jackson (1982); Jackson and others (1982); Collins and others (1980)

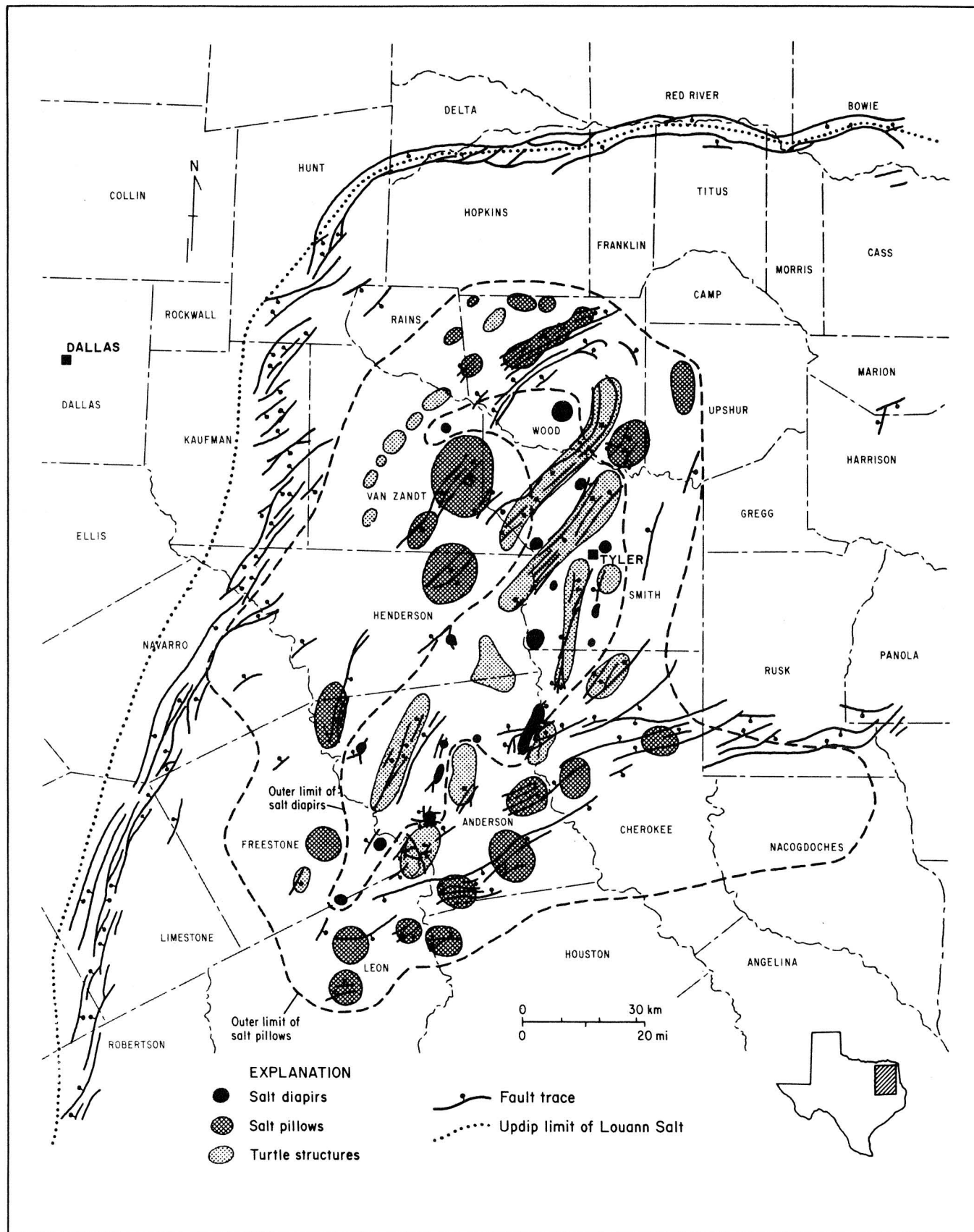


Figure 27. Map of fault traces on base of Austin Chalk and their relation to salt diapirs, salt pillows, and turtle structures (from Jackson, 1982).

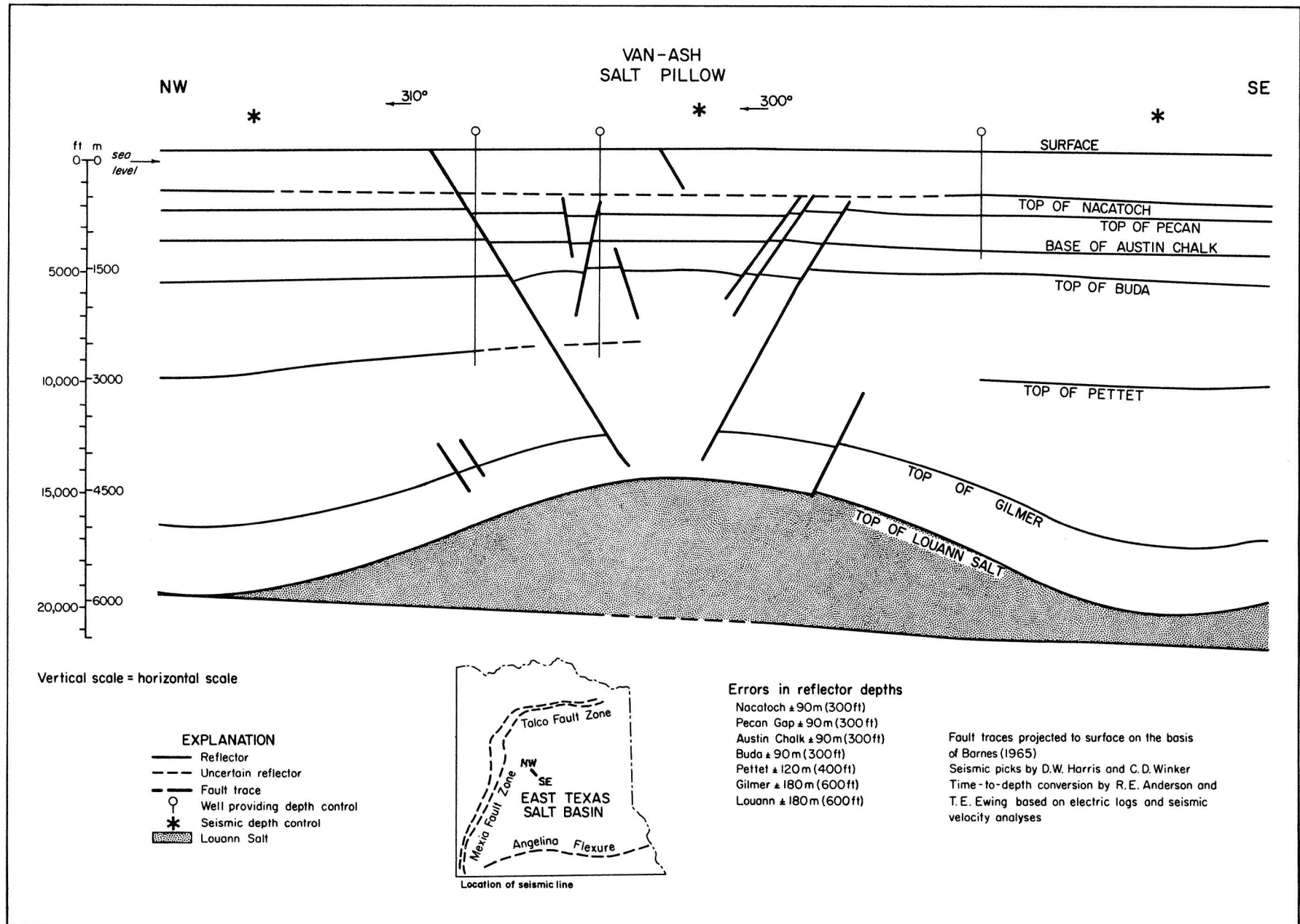


Figure 28. Time-to-depth-converted seismic section showing symmetric buried graben over crest of Van-Ash salt pillow (from Jackson, 1982).



## Seismicity

*At least eight earthquakes were recorded by microseismic stations in the Mount Enterprise fault zone, East Texas, from June 1981 to August 1982. The Jacksonville main shock on November 6, 1981, registered 3.0 to 3.2  $m_bLg$ , Richter magnitude 3.5 to 4.0, Mercalli intensity III-V, and was felt over 500 km<sup>2</sup> (200 mi<sup>2</sup>). It is ascribed to normal faulting in the Mount Enterprise fault zone.*

The East Texas Basin is generally considered an area of low seismic risk. However, historic evidence of apparent earthquakes in 1891 (near Rusk), in 1932 (near Wortham), in 1957 (near Mount Enterprise), and in 1964 (near Hemphill) suggested that seismic monitoring should be carried out because the area is a potential site for nuclear waste storage. The first stage of monitoring consisted of a single-channel, smoked-paper seismograph, which operated from February 1980 to May 1981. The second stage comprised a three-station, telemetered network from June 1981 to August 1982.

The following four earthquakes were recorded and located: (1) 3.0  $m_bLg$  (approximates Richter magnitude [ $m_b$ ] by using high-mode Love waves [ $Lg>$ ], Center, Texas, June 9, 1981, Universal Corrected Time (UTC); (2) 3.2  $m_bLg$ , Jacksonville, Texas, November 6, 1981, UTC; (3) 1.7  $M_{Coda}$  ( $\approx m_bLg$ ) aftershock, Jacksonville, Texas, November 9, 1981, UTC; and (4) 1.8  $M_{Coda}$ , Mount Enterprise, Texas, December 11, 1981, UTC. The following four earthquakes were recorded but not precisely located: (1) 2.1  $M_{Coda}$ , probable aftershock of Jacksonville, November 6, 1981, event, November 6, 1981, UTC; (2) 1.6  $M_{Coda}$ , possible aftershock of Jacksonville, November 6, 1981, event, January 5, 1982, UTC; (3) 2.3  $M_{Coda}$  and 1.9  $M_{Coda}$ , May 13, 1982, UTC.

The Jacksonville main shock was felt over 500 km<sup>2</sup> (200 mi<sup>2</sup>) and the aftershock over 75 km<sup>2</sup> (30 mi<sup>2</sup>) (fig. 29). This event is ascribed to normal faulting along the Mount Enterprise fault zone, which surrounds the epicenter (fig. 30). The Mount Enterprise fault zone is the least understood zone in East Texas because of poor subsurface information. Nevertheless, at least one seismic profile (fig. 31) indicates that, like the Mexia-Talco fault zone, the Mount Enterprise fault zone is based in the Louann Salt. This suggests that the Mount Enterprise fault zone is also related to salt creep, indicating a low seismic potential. A releveled profile across a fault immediately south of the Mount Enterprise fault zone indicates approximately 14 cm (5.5 inches) displacement in the past 30 yr.

Pennington and Carlson (1983); Jackson and others (1982); Collins and others (1980)



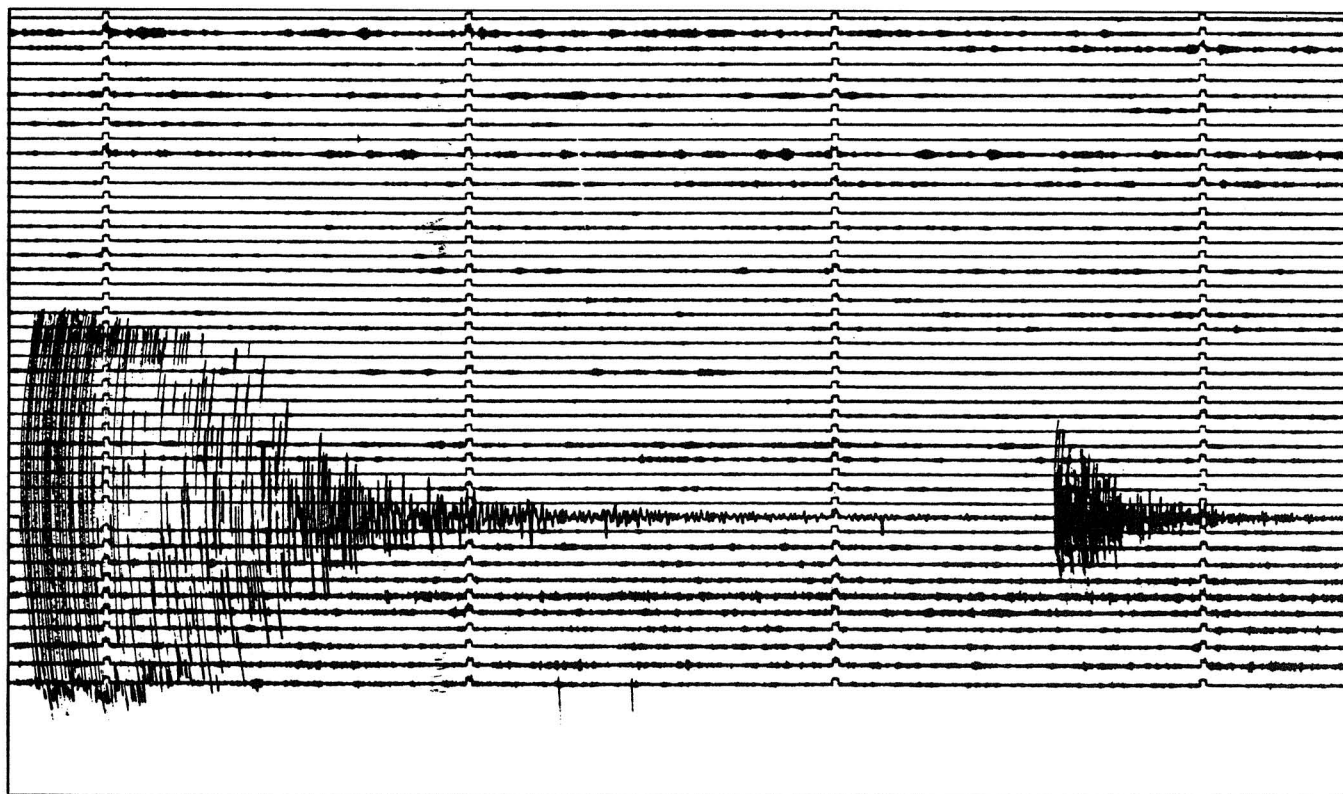


Figure 29. Seismogram of Jacksonville main shock (left), magnitude 3.2, and aftershock (right) from Mount Enterprise fault zone (from Pennington and Carlson, 1983).

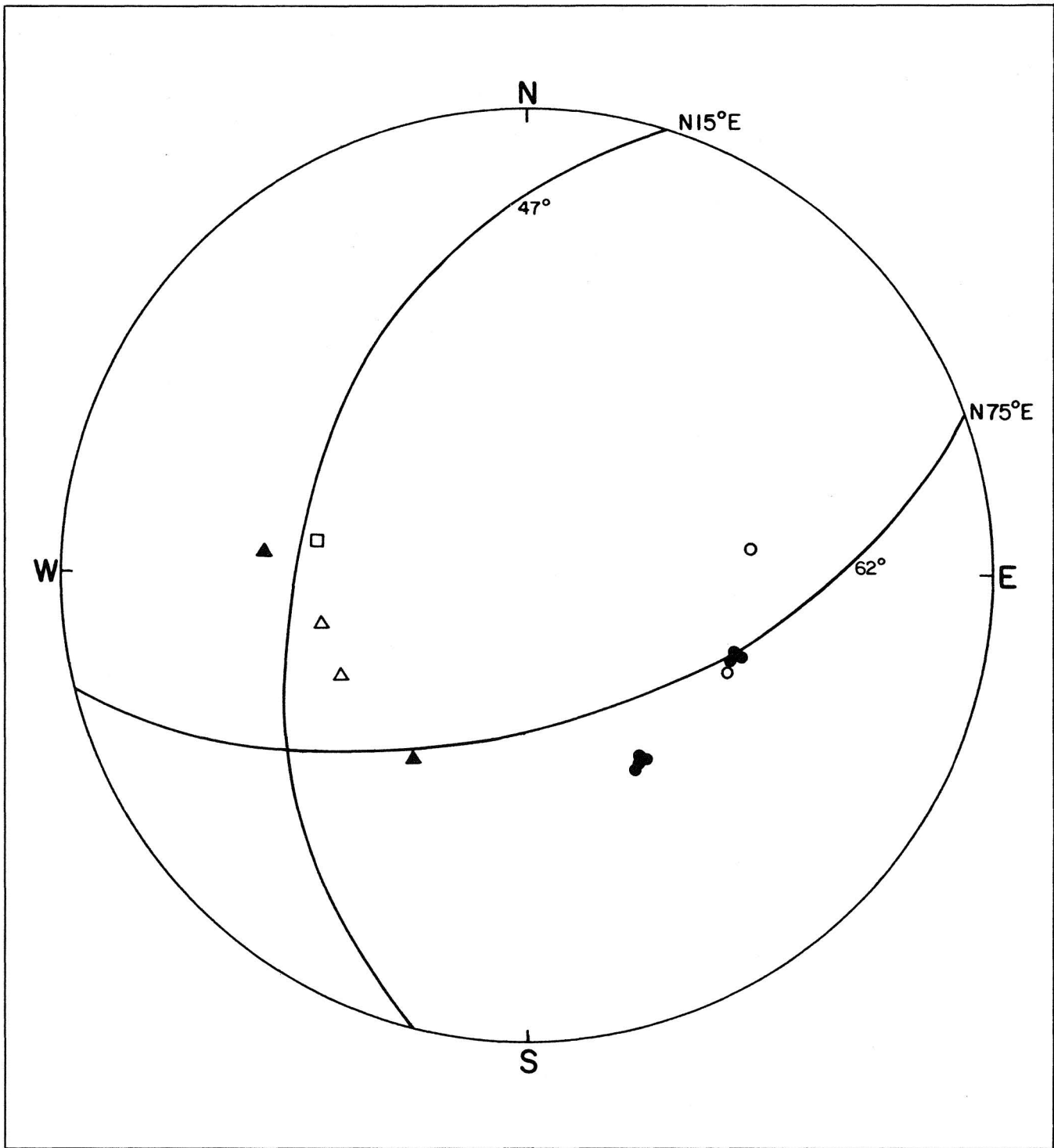


Figure 30. Composite focal mechanism for the located earthquakes and probable aftershocks in East Texas. Projection is lower-hemisphere equal-area; solid symbols represent compressional-wave arrivals, open symbols represent dilational-wave arrivals. Circles, Jacksonville earthquakes; triangles, Mount Enterprise earthquakes; square, Center earthquake. Data do not allow discrimination between normal faults, thrust faults, and strike-slip faults, but only the normal-fault solution has a nodal plane parallel to the Mount Enterprise faults striking ENE and is consistent with geologic evidence (after Pennington and Carlson, 1983).

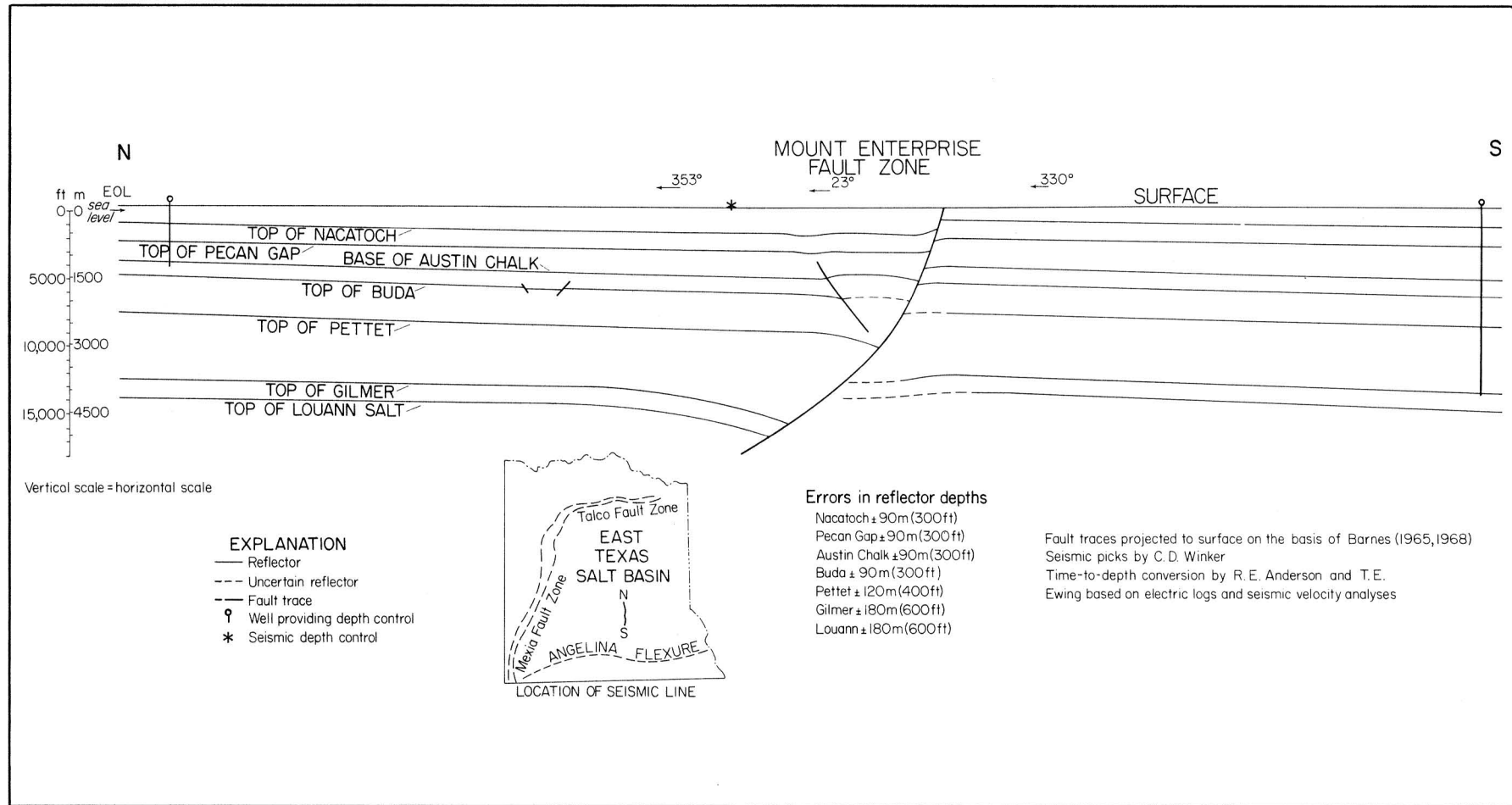


Figure 31. Time-to-depth-converted seismic section across Mount Enterprise listric-normal growth fault (from Jackson, 1982).

## Petroleum Potential of Domes

*In the central part of the East Texas Basin, most oil and gas have been produced from anticlines over salt pillows because of their large structural closure. In contrast, little oil and gas have been produced near salt diapirs because of their much smaller traps.*

Petroleum in the East Texas Basin is produced from three types of salt-related anticlines, listed in order of highest production: salt pillows, turtle-structure anticlines, and salt diapirs (fig. 32). Production statistics for the central part of the basin are shown in figure 33. Salt pillows have trapped more hydrocarbons than have turtle-structure anticlines because pillows formed earlier and uplifted thicker sections, thereby creating multiple-zoned fields.

Only relatively small ( $<10^7$  bbl) hydrocarbon reservoirs have been discovered at the shallow salt diapirs, despite intense exploration drilling for traps similar to those around productive shallow salt domes in the Gulf Coast Basin. The paucity of hydrocarbons is probably due to the relatively small structural closure characteristic of mature East Texas diapirs. Boggy Creek Dome, a large, immature, ridgelike diapir, uplifts a large stratigraphic section and contains the greatest known accumulation of oil associated with an East Texas dome. Additional hydrocarbon reserves might be discovered by deep drilling of dome flanks below the Woodbine Group. Thus the current apparent scarcity of petroleum around salt domes does not necessarily preclude future drilling near domes or through dome overhangs.

Wood and Giles (1982); Giles and Wood (1983); Jackson and Seni (1984)

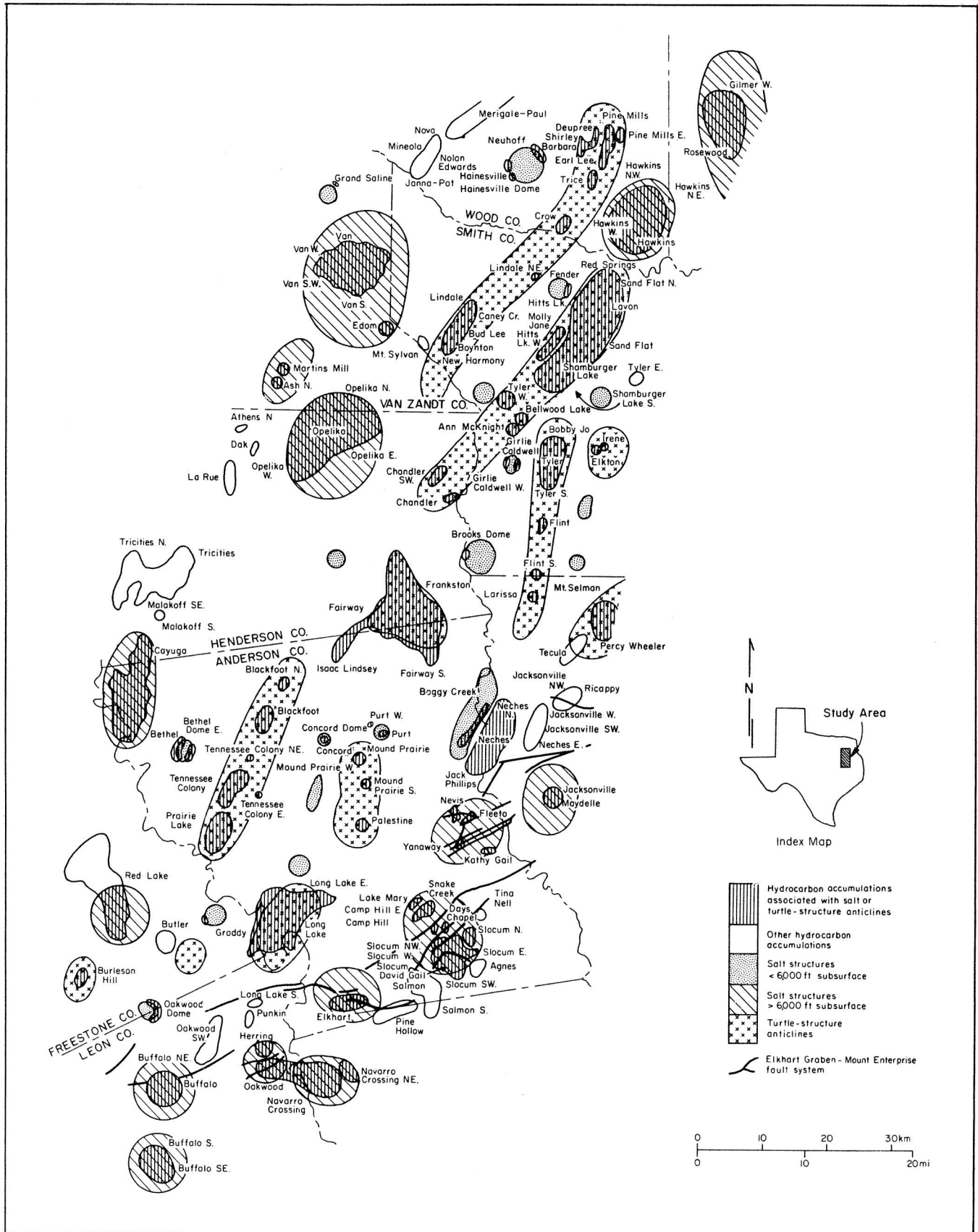
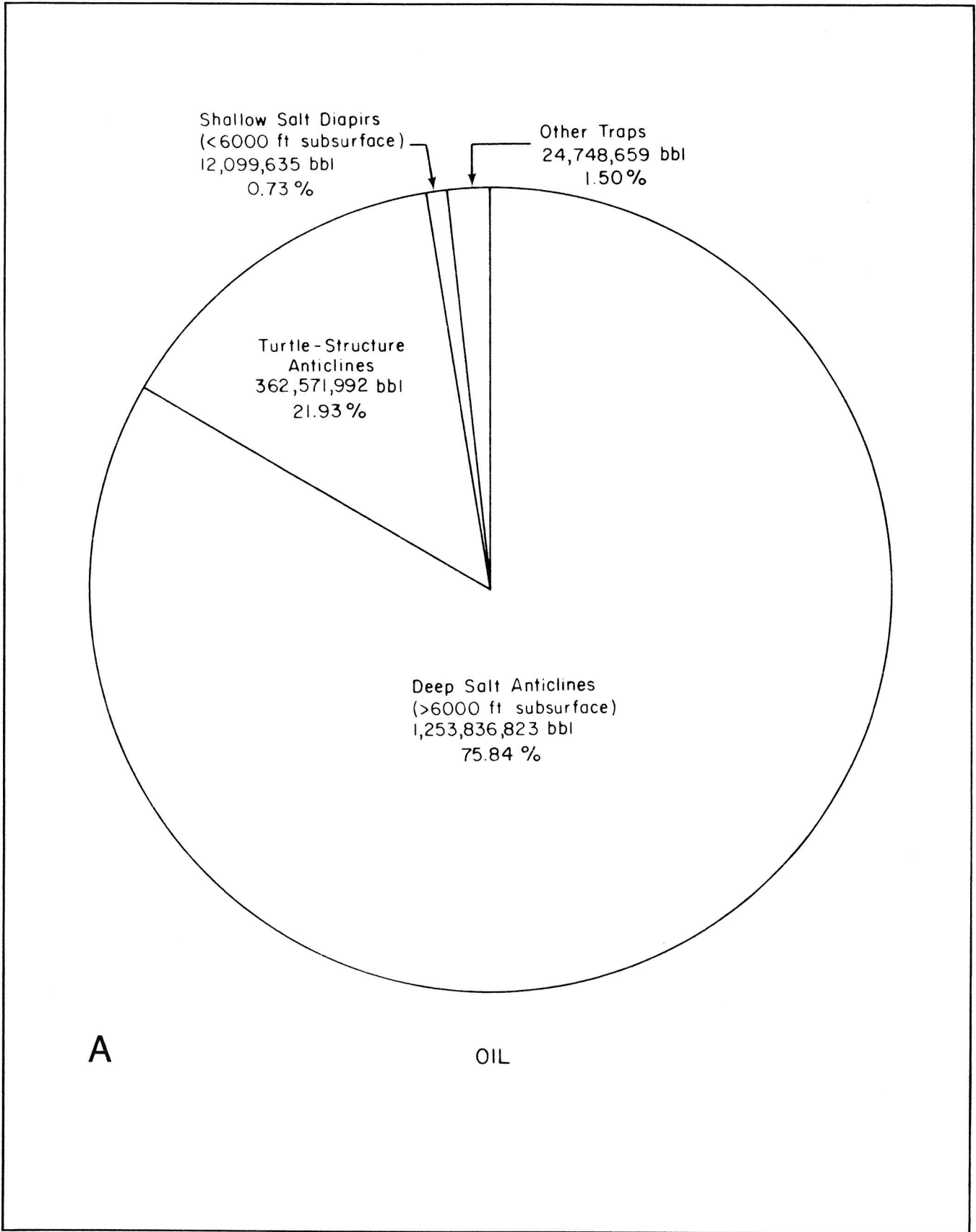


Figure 32. Map of salt-related structures and petroleum fields in central part of East Texas Basin (from Wood and Giles, 1982).



Figures 33 A and B. Oil (A) and gas (B) production statistics for central part of East Texas Basin (from Wood and Giles, 1982). (Continued on next page.)

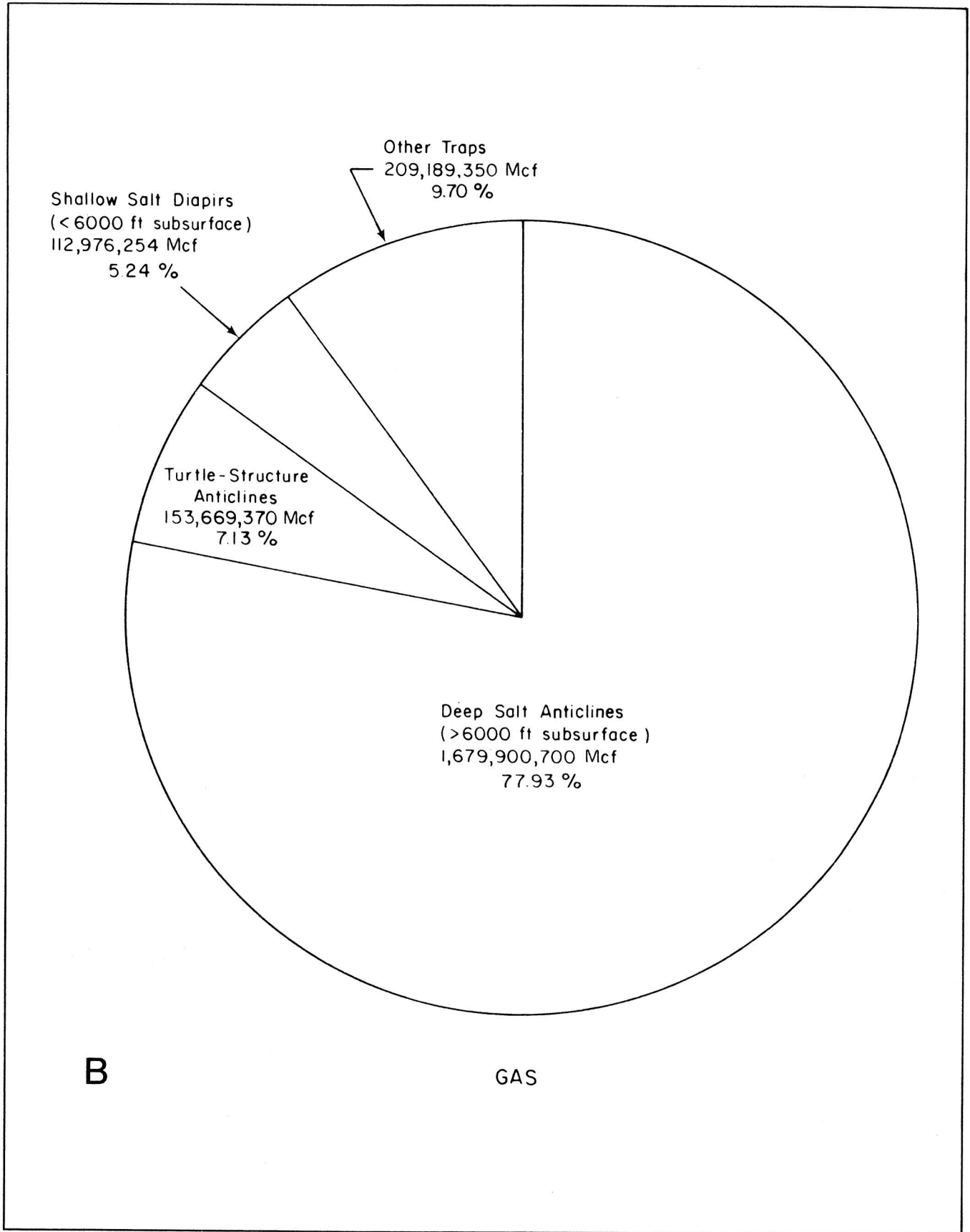


Figure 33B.

## REGIONAL HYDROGEOLOGIC STUDIES

### Ground-Water Hydraulics

*Regional ground-water circulation in the Wilcox-Carrizo aquifer system correlates closely with topography and geologic structure. A potential for downward vertical flow prevails except beneath the major streams and their tributaries. Potential for upward flow is greatest beneath the Trinity River floodplain.*

Regional potentiometric surfaces in Eocene aquifers are controlled primarily by topography and structure. Outcrop flow patterns closely follow topography as water moves away from high recharge areas to low discharge areas (fig. 34). Thus the Queen City does not form a regionally coherent flow system but, instead, a series of smaller flow cells of closely spaced recharge and discharge areas. In the confined Wilcox-Carrizo system, flow approximately follows the structural dip as ground water moves eastward in the northern half of the basin and southward in the southern half. The ground-water divide lies in southern Smith County.

Topography affects flow in the confined Wilcox-Carrizo indirectly through leakage between the Queen City and Wilcox-Carrizo. The leakage is indicated by a subtle correlation between the Wilcox-Carrizo potentiometric surface and topography (fig. 35). Analyses of vertical head differentials and the distribution of flowing wells confirm the occurrence of leakage and show its direction. The leakage is predominantly downward, except beneath the Trinity and Sabine Rivers, which appear to be discharge areas for the confined section (fig. 35). In comparison, the Neches River is not a discharge area because it does not incise deeply enough to intersect the Wilcox-Carrizo potentiometric surface.

Fluid pressure versus depth (P-D) relations in the Wilcox-Carrizo aquifers (fig. 36), measured by well-screen depths and depths to water levels, help locate areas of hydraulic potential for vertical flow. Almost all the 598 points plot below the hydrostatic pressure line (slope <1.0), indicating that, on the whole, vertical flow is downward (fig. 36). A high correlation coefficient shows that the P-D relationship is predictable. This hydraulic potential for downward flow increases toward higher elevations and from the artesian section to the outcrops.

Fogg and Kreitler (1982); Fogg and Kreitler (1981); Fogg (1981c)



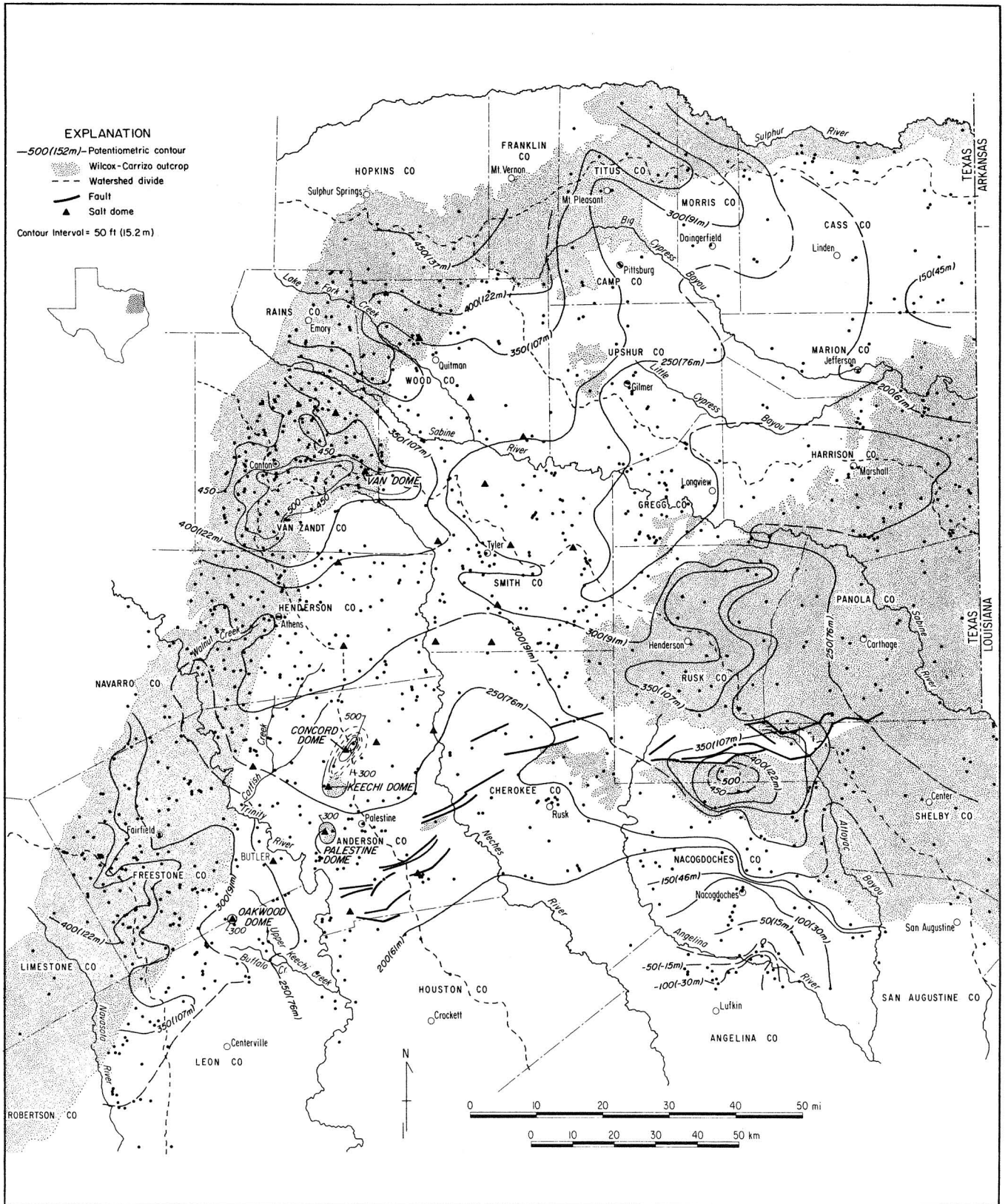


Figure 34. Map of regional potentiometric surface of Wilcox-Carrizo aquifer in East Texas (from Fogg and Kreitler, 1982).

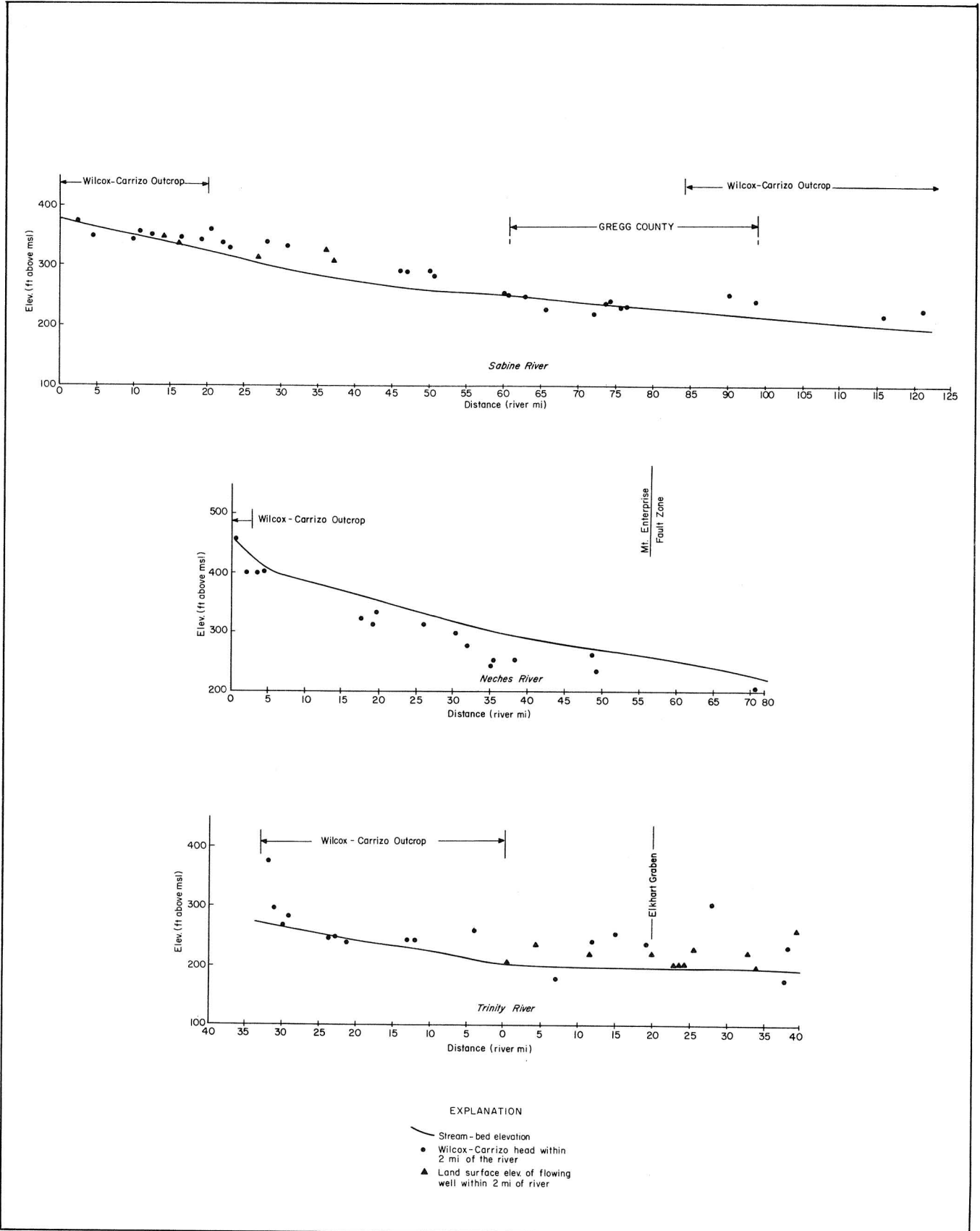


Figure 35. Elevations of Wilcox-Carrizo water levels and major stream beds (from Fogg and Kreitler, 1982).

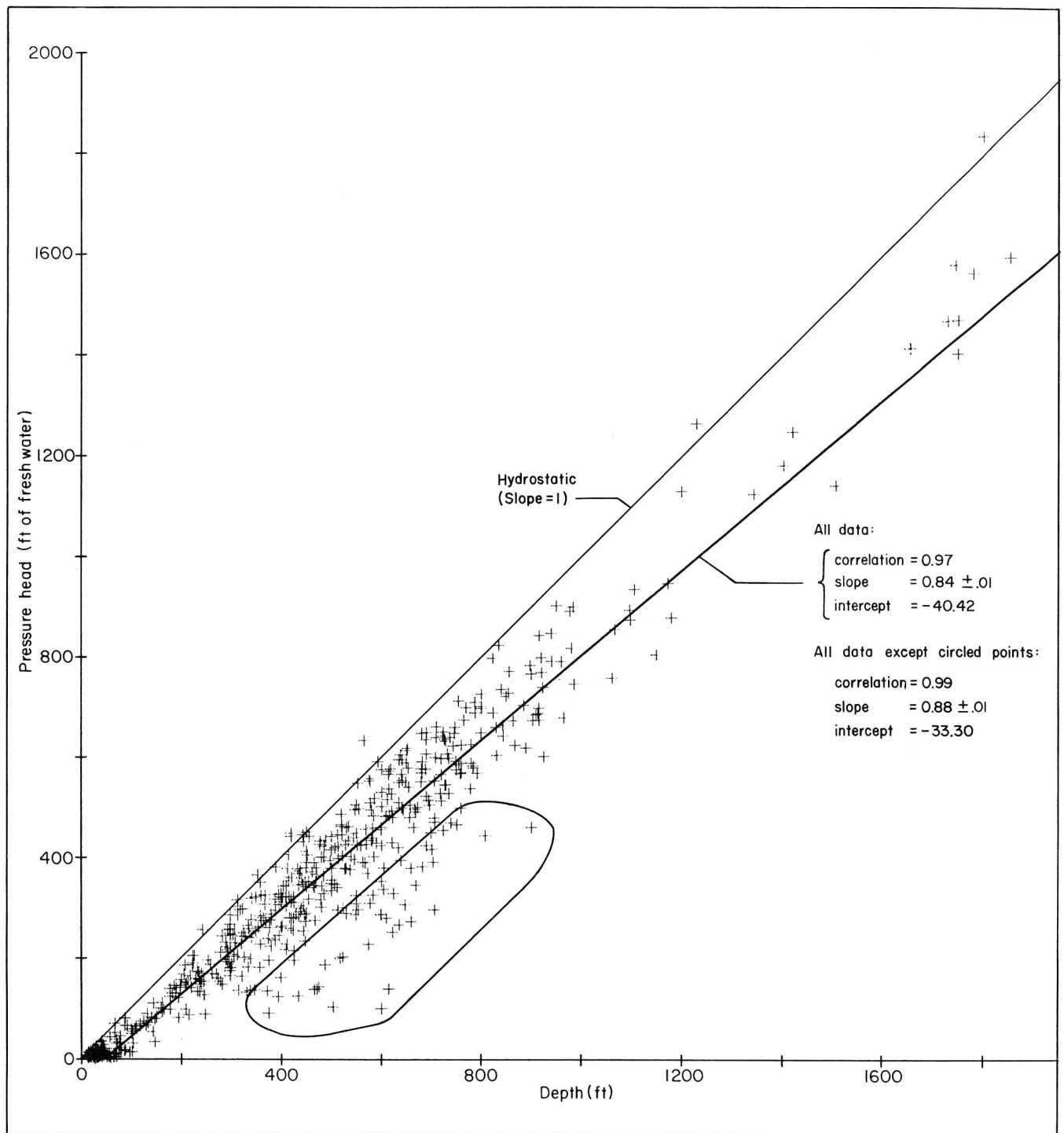


Figure 36. Graph of fluid pressure versus depth in fresh-water Wilcox-Carrizo aquifers (from Fogg and Kreitler, 1982).

## Ground-Water Chemistry

*Ground water is fresh in the Wilcox-Carrizo aquifer around most domes in the basin. Analysis of Carrizo water indicates recharge over Oakwood and Keechi Domes.*

As ground water flows from recharge areas to discharge areas in the Wilcox-Carrizo aquifer, it generally is altered from an acidic, oxidized calcium-magnesium-bicarbonate-sulfate water to a basic, reduced sodium-bicarbonate water (fig. 37). This change in water chemistry is controlled predominantly by calcite dissolution and cation exchange with smectitic clays. Water that differs from regional chemical patterns indicates anomalous hydrologic conditions such as possible dissolution of salt domes or relatively high rates of recharge to the artesian part of the Wilcox-Carrizo aquifer.

Water from the Carrizo aquifer at Oakwood Dome characteristically displays low pH and low anion and cation concentrations typical of a recharge zone. This is supported by light  $\delta^{13}\text{C}$  values (derived from soil carbon dioxide) from the same waters. Carrizo water at Keechi Dome has similar anomalous chemistry, indicating shallow recharge. Water from deeper Wilcox wells near the dome does not indicate recharge or vertical mixing with overlying Carrizo waters. The continuous rise of pH with depth demonstrates the existence of a closed carbonate system. Deep Wilcox artesian waters are strongly reducing, probably from coalification of organic material. Smectite and kaolinite are common clay minerals in Wilcox core near Oakwood Dome. Ca-smectite is the most abundant montmorillonite type above -457 m (-1,500 ft), and Na-smectite is common below -457 m (-1,500 ft). Both Na- and Ca-smectite are characterized by high cation exchange capacity.

The Wilcox Group is pierced by Oakwood Dome, but Wilcox ground water around the dome is primarily fresh (<1,000 mg/L total dissolved solids). The same is also true of most other domes in the basin, suggesting that the domes are generally isolated from ground-water circulation in the Wilcox by cap rocks or muddy facies around the domes.

Fogg and Kreitler (1982); Fogg and Kreitler (1981); Fogg and others (1982a); Kreitler and Wuerch (1981); Kreitler and Fogg (1980); Fogg (1980b)

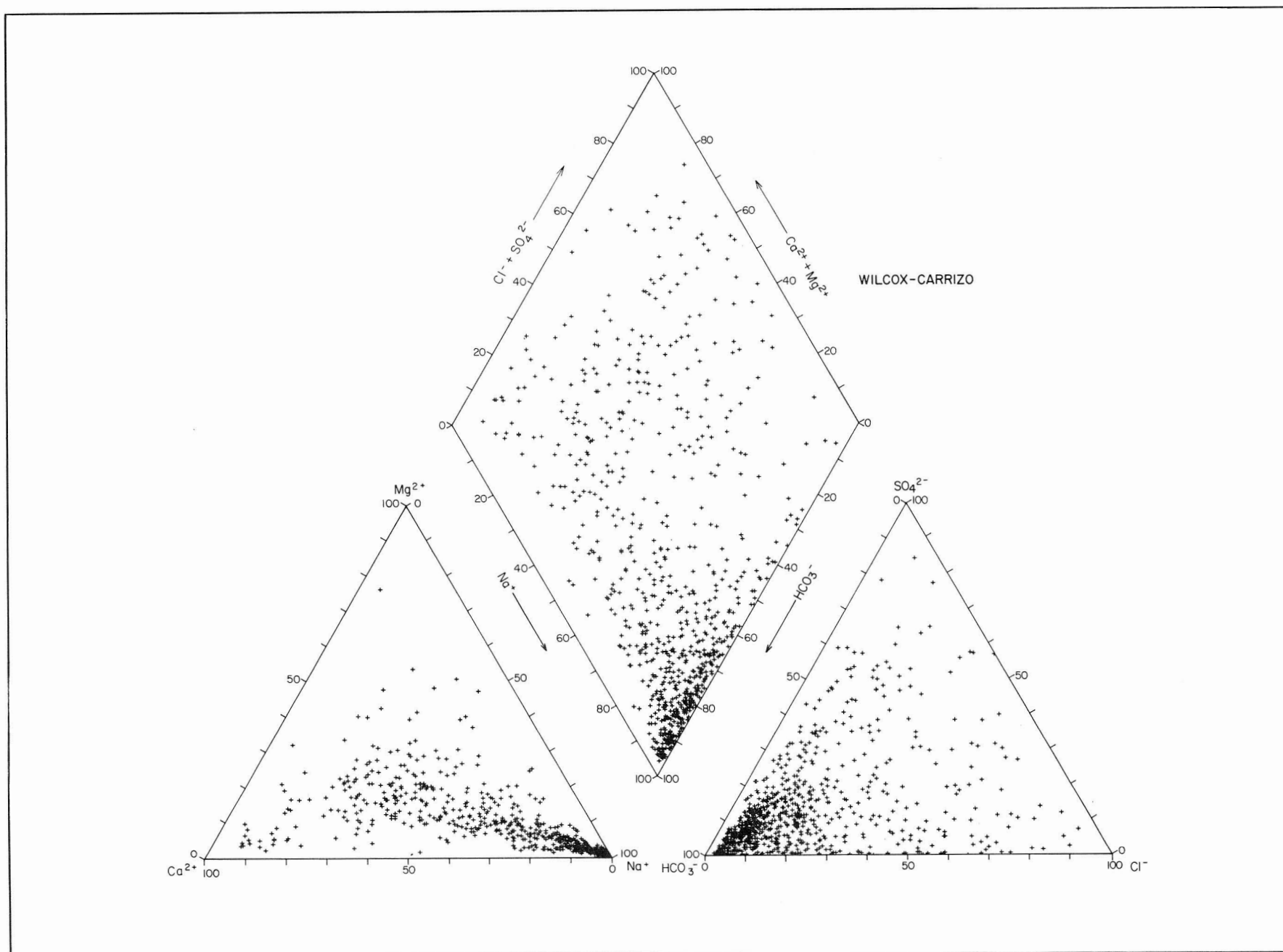


Figure 37. Piper diagram of Wilcox-Carrizo water chemistry (from Fogg and Kreitler, 1982).

## Subsurface Salinity Near Salt Domes

*Estimates of the salinities of formation water in the Woodbine, Nacatoch, and Wilcox stratigraphic units have been determined using electric log interpretation (SP and resistivity). Three sources of salinity affect the Wilcox Group: (1) upward leakage of deep saline waters along faults, (2) incomplete flushing of saline water in muddy areas of the Wilcox Group, and (3) salt-dome dissolution. A high-TDS plume in the Wilcox northeast of Oakwood Dome may represent sodium chloride waters formed by dome dissolution.*

Maximum salinity in sands of the Woodbine Formation was mapped from SP logs according to methods outlined by Keys and MacCary (1971). Maximum salinity values range from 30,000 to 300,000 ppm. Salinities in the Woodbine Formation do not characteristically increase toward salt domes. Sodium chloride in the Woodbine waters probably originated from dissolution of salt stocks, but no evidence of ongoing dissolution exists. The Nacatoch Formation is either missing, very thin, or tightly cemented everywhere except in the northern part of the basin. The thin Nacatoch aquifer poses a negligible threat to the stability of Oakwood and Keechi Domes, which are located in the southern part of the basin.

Salinity of the Wilcox Group was estimated by an empirical relationship between electric log resistivity and total dissolved solids (TDS). A map of percentage thickness of fresh water (TDS less than 1,000 mg/L) in the Wilcox aquifer (fig. 38) indicates three sources of salinity: (1) upward leakage of deep, saline water along faults, (2) incomplete flushing of saline water in muddy areas of the Wilcox Group, and (3) salt-dome dissolution. Faults may allow upward leakage in the Mount Enterprise - Elkhart Graben in southern Anderson and Cherokee and northern Houston Counties, where salinities increase abruptly. High salinities from salt-dome dissolution could be confused with high salinities resulting from upward flow along numerous faults associated with the domes. The lack of high salinities around domes depicted in figure 38, however, suggests that the domes are neither dissolving significantly nor inducing upward leakage.

Incomplete flushing of saline water in muddy areas of the Wilcox Group is suggested on the sand-percentage map (fig. 38) by a close correlation between saline zones and muddy zones in Upshur County, southeast of Mount Sylvan Dome, and east of Whitehouse and Bullard Domes. The saline intervals near the three domes are not caused solely by dome dissolution because salinities decrease and fresh-water thicknesses increase toward the domes. The saline water in the muddy sediments may have been derived from salt-dome dissolution during the geologic past or from seas that submerged the Wilcox aquifer at least twice since deposition 40 Ma ago. The persistence of saline water in muddy facies is possibly enhanced by ground-water flow rates that are probably as low as 0.0015 to 0.9150 m/10<sup>4</sup> yr (0.0049 to 3.0020 ft/10<sup>4</sup> yr). Maximum TDS in the Wilcox was invariably found in muddy sands near the base of the aquifer. In nearly

every aquifer, these concentrations are approximately 5,000 ppm ( $\pm 1,000$  ppm), and in a few isolated areas appear to reach 10,000 ppm.

Of all the domes, only Oakwood is associated with a ground-water plume of anomalously high TDS (fig. 39). Although its salinity has not been verified by water sampling, the plume is assumed to be saline owing to dome dissolution because it flanks the dome and its configuration is consistent with ground-water modeling ("Ground-Water Modeling: Flow Rates and Travel Times," p. 113). Alternatively, the high-TDS water could be channeling up from the deep basin along dome-related faults. Modeling indicates that the northeast orientation of the plume is caused by sand-body distribution and interconnection. Core study of the cap rock ("Cap-Rock - Rock-Salt Interface," p. 97, and "Cap Rock," p. 101) indicates that, where penetrated by the drill, the anhydrite cap rock provides a good hydrologic seal. The possible presence of a saline plume indicates that if the dome is dissolving, dissolution is more likely to be on the sides of the salt stock. According to the TDS concentration in the brackish plume, if salt were dissolved from the entire surface of Oakwood Dome, the dissolution rate (linear with respect to time) would be approximately 10 m/10<sup>4</sup> yr (33 ft/10<sup>4</sup> yr); with localized dissolution over 10<sup>4</sup> m<sup>2</sup> (10<sup>5</sup> ft<sup>2</sup>), the salt would dissolve at a rate of 2,000 m/10<sup>4</sup> yr (6,600 ft/10<sup>4</sup> yr). The relatively muddy Wilcox strata surrounding Oakwood Dome provide a partial barrier that promotes isolation of the dome from the high-permeability, channel-fill sand bodies.

Fogg and Kreitler (1982); Fogg and Kreitler (1981); Fogg (1981b); Fogg (1981a)

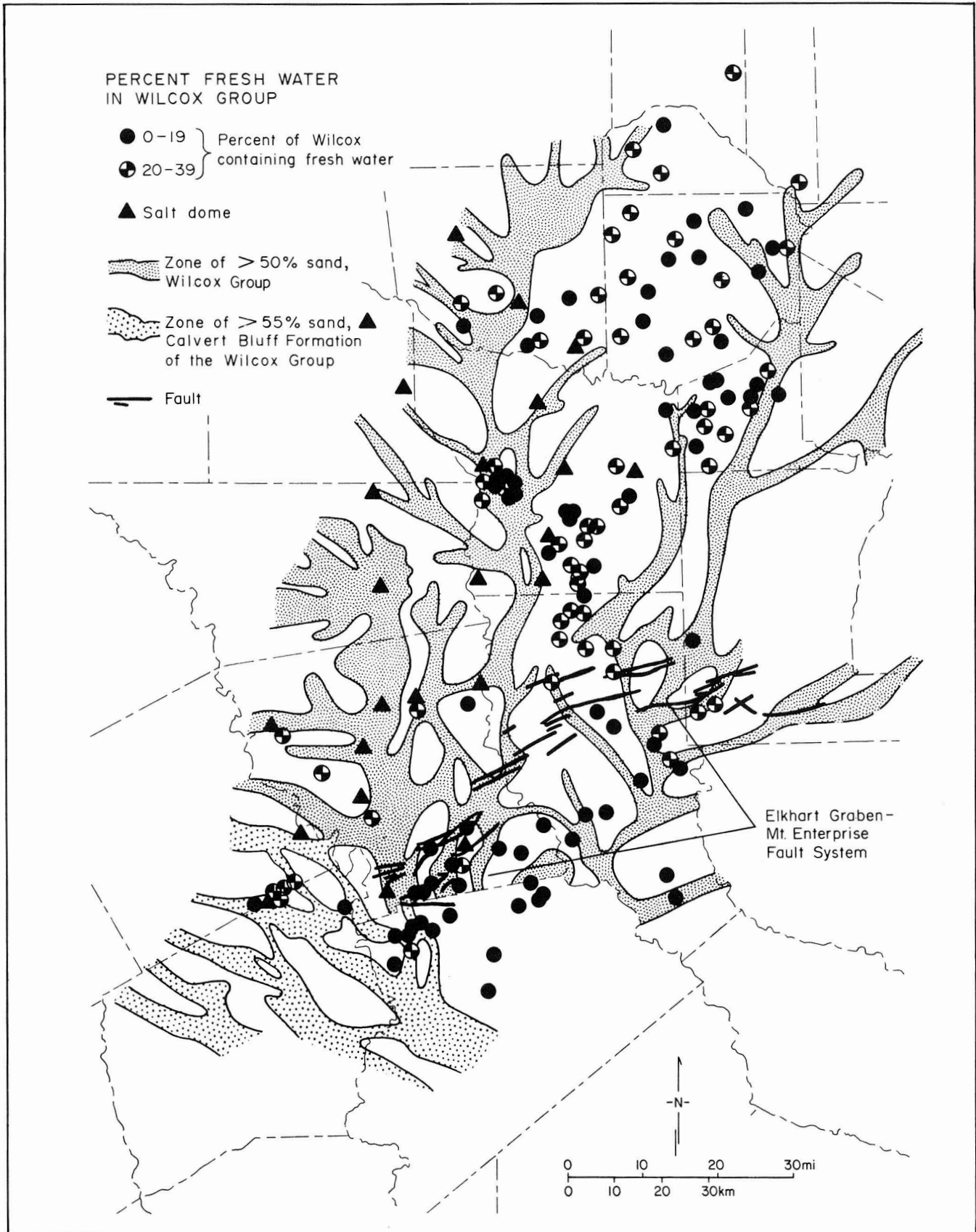


Figure 38. Map showing relationship of percentage thickness of fresh water in Wilcox aquifer to trends of high sand percentage (from Fogg and Kreitler, 1982).



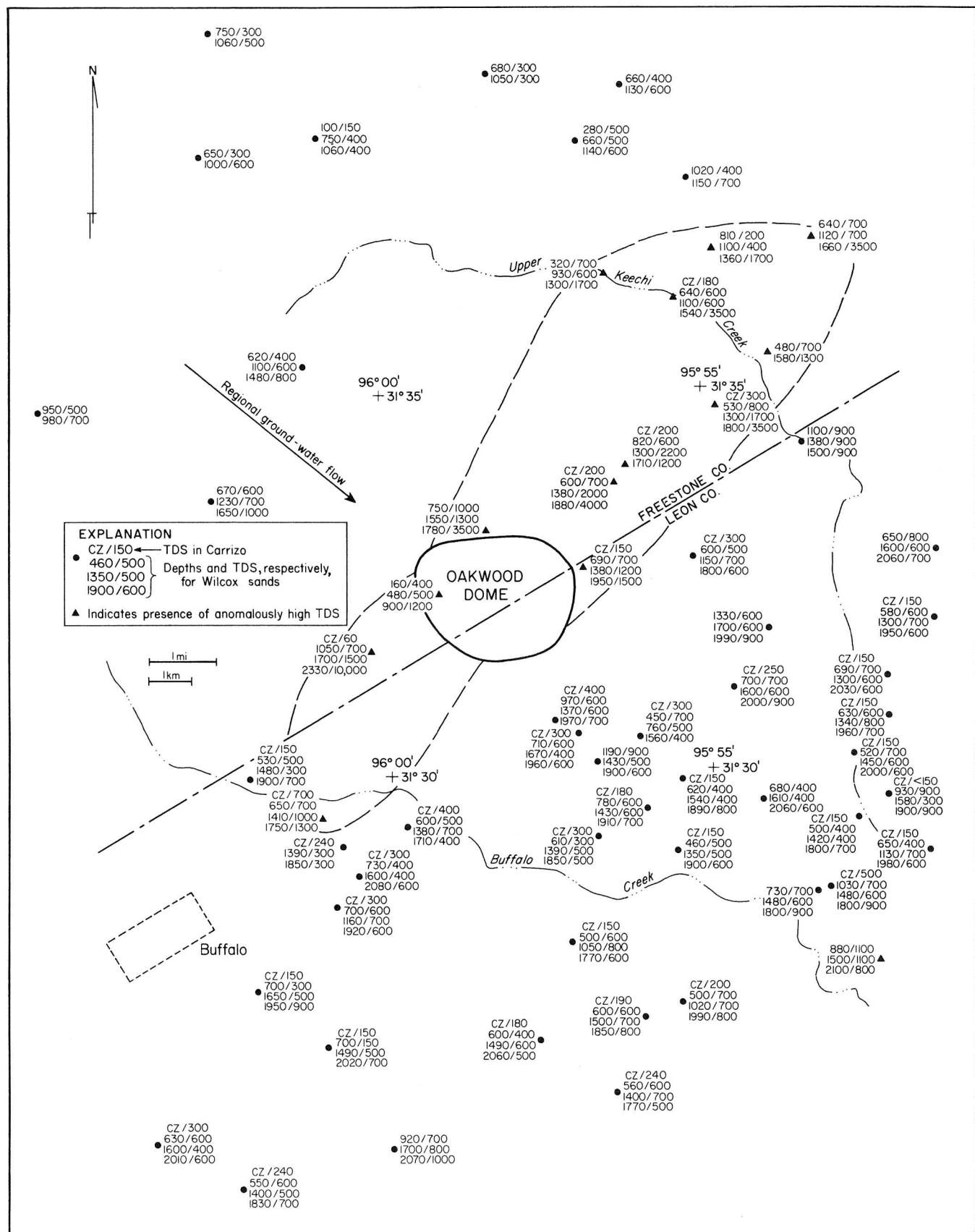


Figure 39. Location of possible saline plume associated with Oakwood Dome (from Fogg and others, 1980).

## Age of Ground Water

*Ground-water  $^{14}\text{C}$  ages (1,000 to 15,000 yr) near Oakwood Dome increase down the hydraulic gradient from the outcrop recharge area toward the Trinity River. Ground-water  $^{14}\text{C}$  ages also increase as the water chemistry evolves. Waters in the shallow Carrizo are younger than waters in the deeper Wilcox aquifer.*

Bicarbonate  $^{14}\text{C}$  ages in ground water at Oakwood Dome help confirm directions and rates of ground-water flow, previously determined by hydraulic head data, and rates for the chemical evolution of the ground water. Ages were corrected for dissolution of carbonates. Ground-water  $\delta^{13}\text{C}$  values and ages in the Wilcox, Carrizo, and Queen City aquifers near Oakwood Dome indicate that ground water flows from outcrop toward the Trinity River, possibly discharging into Upper Keechi Creek, a tributary of the Trinity River (fig. 40). Ground-water ages increase from approximately 1,000 to 4,000 yr in the Carrizo aquifer over Oakwood Dome to 7,000 to 8,000 yr in the deeper Carrizo-Wilcox aquifers to approximately 15,000 yr near Upper Keechi Creek. Thus, the youngest ages are closest to the recharge area over the dome; ages generally increase with depth and distance away from the dome (compare "Ground-Water Modeling: Flow Rates and Travel Times," p. 113).

Evolution of the ground-water chemistry ("Ground-Water Chemistry," p. 69) from a Ca-Mg-Cl-SO<sub>4</sub> water (recharge water) to a Na-HCO<sub>3</sub> water coincides with increased  $^{14}\text{C}$  age of the samples (table 4).

Fogg and Kreitler (1982); Fogg and Kreitler (1981); Fogg and others (1982a); Kreitler and Wuerch (1981)

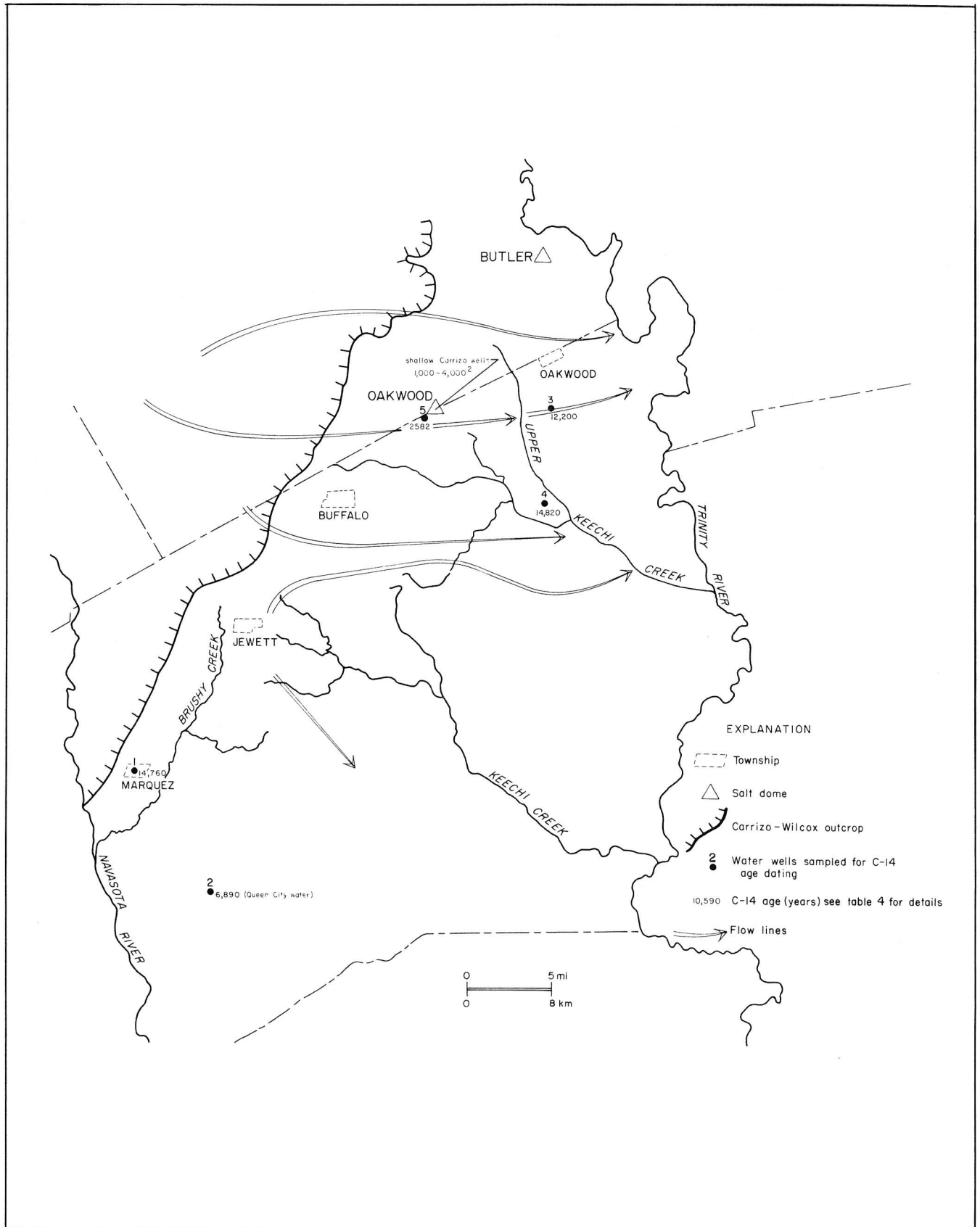


Figure 40. Map of  $^{14}\text{C}$  ages of ground water in Wilcox-Carrizo aquifer near Oakwood Dome (from Kreitler and Wuerch, 1981).

Table 4. Ground-water  $^{14}\text{C}$  ages in Wilcox-Carrizo aquifer near Oakwood Dome (from Kreitler and Wuerch, 1981).\*

	Well Number on Figure 40				
	1	2	3	4	5
<b>Sample no.</b>	3601	3666	3665	3593	3598
<b>Screened intervals [ft]</b>	350-371 601-678	400-482	—	—	340-380
<b>Depth [ft]</b>	691	482	640	190	380
$\delta\text{C}^{13}$	-7.2	-15.5	-6.3	-15.1	-18.6
<b><math>\text{C}^{14}</math> age</b>	22,960 $\pm$ 460	8,920 $\pm$ 220	21,550 $\pm$ 400	18,840 $\pm$ 340	3,160 $\pm$ 90
<b>Corrected <math>\text{C}^{14}</math> age</b>	14,670	6,890	12,200	14,820	2,582
<b>pH</b>	8.8	7.4	8.3	8.6	5.5
<b>Temp. [<math>^{\circ}\text{C}</math>]</b>	26.2	26.7	24.0	28.0	23.0
<b><math>\text{Ca}^{+2}</math></b>	6.1	27.2	5.5	30.8	5.2
<b><math>\text{Na}^{+}</math></b>	297.8	46.5	179.6	72.2	9.7
<b><math>\text{Mg}^{+2}</math></b>	0.53	9.88	1.05	7.83	2.2
<b><math>\text{K}^{+}</math></b>	3.1	7.0	4.0	7.1	4.2
<b><math>\text{Cl}^{-}</math></b>	38.5	34.6	27.0	45.0	12.6
<b><math>\text{SO}_4^{-2}</math></b>	3.0	36.0	5.0	16.5	13.0
<b><math>\text{HCO}_3^{-}</math></b>	640.0	181.0	540.0	236.0	34.0
<b><math>\text{Br}^{-}</math></b>	0.76	1.42	1.27	1.41	<0.1
<b><math>\text{F}^{-}</math></b>	0.68	<0.01	0.21	0.19	<0.1
<b><math>\text{SiO}_2</math></b>	13.6	19.5	13.6	13.0	36.7
<b>Fe</b>	0.01	0.39	0.17	0.03	<0.6
<b>Sr</b>	—	—	—	—	—
<b><math>\text{H}_2\text{S}</math></b>	<0.02	<0.02	<0.02	<0.02	—
<b><math>\text{I}^{-}</math></b>	—	—	—	—	—
<b>Mn</b>	<0.01	0.03	0.01	<0.01	<0.02

\*All chemical analyses measured in mg/L



## Surface Saline Discharge

*Surface saline features occur above all the shallowest salt domes in the East Texas Basin, most of which are located in depressions. Not only are such areas hydrologically unstable, but they also make obvious targets for future salt mining.*

Accidental human intrusion is one major concern in the siting of a nuclear waste repository. One scenario involves accidental breachment during exploration for or exploitation of resources associated with salt domes. Because saline springs indicate the possibility of subterranean salt--an attractive resource--domes associated with surface saline features are less favorable as potential repositories than are other domes.

The five shallowest salt domes in the East Texas Basin have overlying surface saline features (fig. 41). Except possibly at Butler Dome, these features occur within or below well-defined depressions, which suggests dissolution-induced collapse (fig. 42). The shallower domes (1) tend to have been discovered earlier, (2) are the most hydrologically unstable, and (3) are most likely to be breached by future exploration for salt resources. Accordingly, shallow domes (<125 m, <400 ft, depth to salt) are much less favorable as waste repositories than are deeper domes. In the deeper flow systems, the presence of cap rock and muddy facies around a dome and the generally lower flow velocities may be sufficient to reduce dissolution rates to negligible values.

Fogg and others (1982a); Fogg and Kreitler (1980)

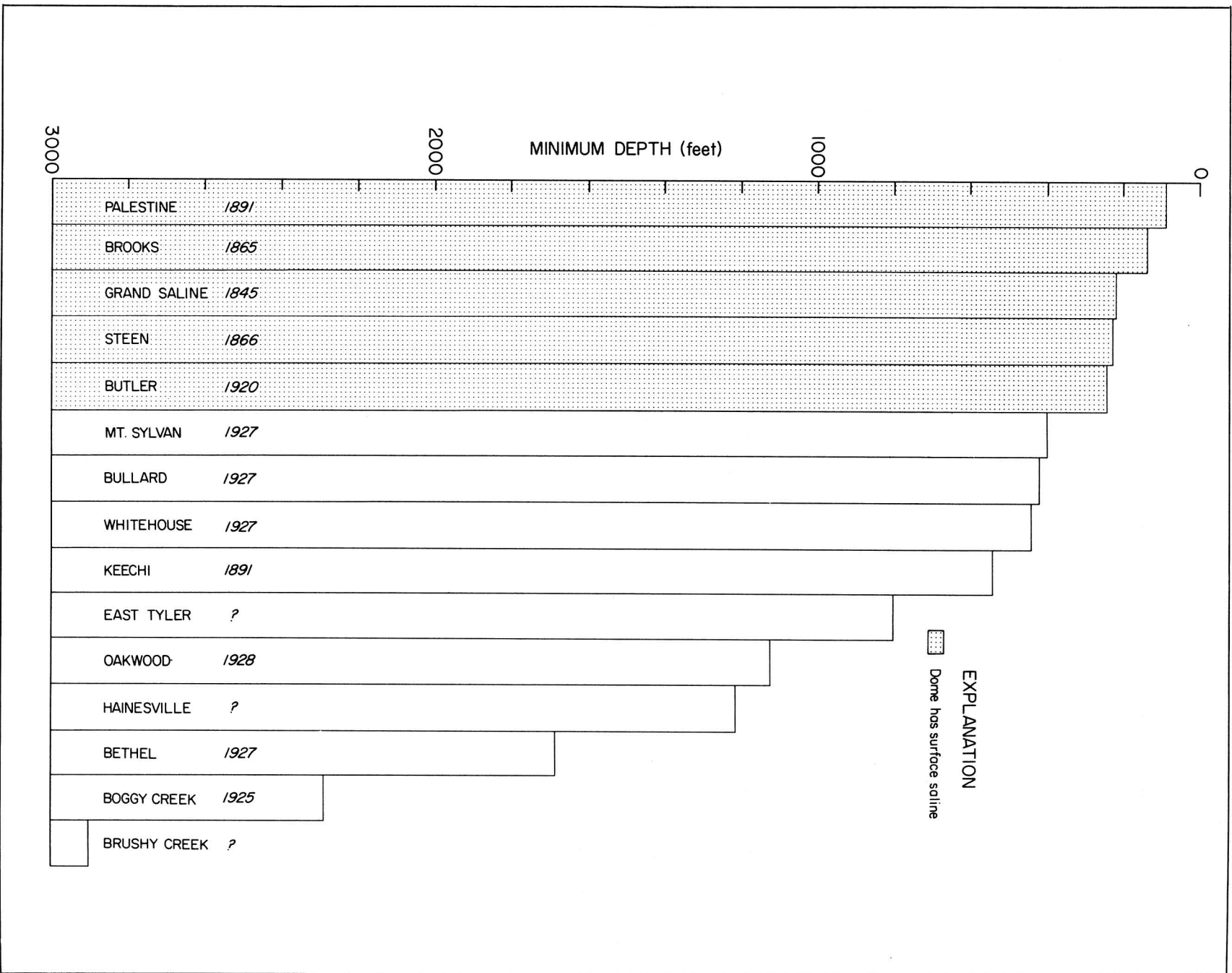


Figure 41. Depths to top of East Texas Basin domes. Five of the shallowest domes have surface salines and were discovered early (from Fogg and others, 1982a).

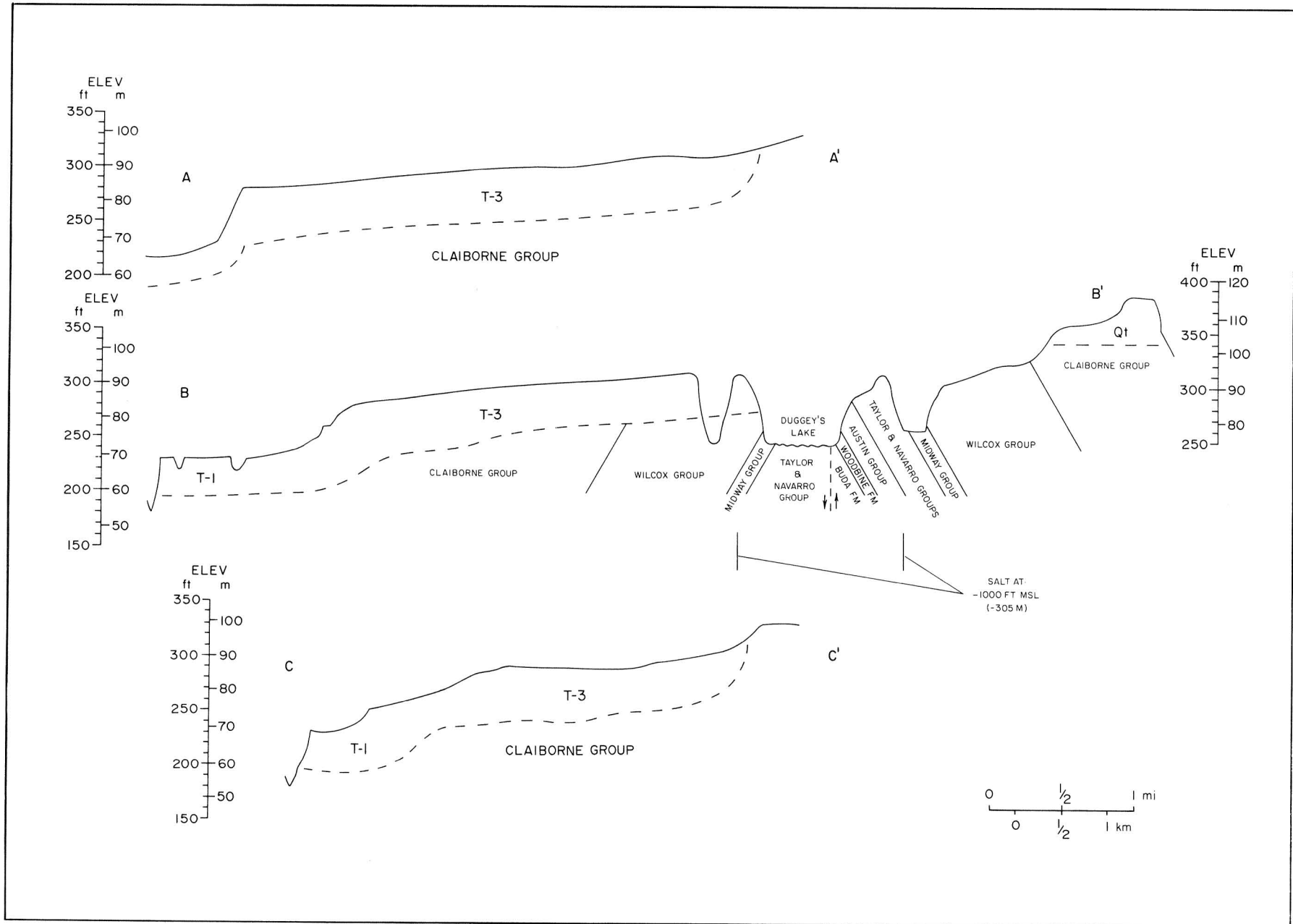


Figure 42. Duggey's Lake overlying possible dissolution-induced collapse over Palestine Dome (from Collins, 1981b).





## Saline Aquifers

*Hydrodynamic and geochemical data reveal two deep, saline aquifer systems: (1) generally normally pressured, slowly circulating, meteoric sodium chloride waters in Upper Cretaceous sands <1,800 m (<6,000 ft) deep and (2) slightly overpressured, slowly circulating, underlying meteoric sodium-calcium-chloride waters. The only known example of mixing between these saline systems and the fresh-water system is at Butler Dome, where pre-Pleistocene false cap rock formed by near-surface discharge of deep-basin brines.*

Given a repository depth of 900 m (3,000 ft), which is below the base of fresh ground water, investigations of deep-basin saline aquifers are necessary to determine potential pathways for radionuclide migration should a release occur.

Pressure data from the deep saline aquifers suggest that two hydrologic systems exist: (1) the generally normally pressured, circulating, Upper Cretaceous aquifers <1,800 m (<6,000 ft) deep and (2) the partly overpressured, slowly circulating, Lower Cretaceous and Upper Jurassic aquifers >1,800 m (>6,000 ft) deep (fig. 43). Basinwide pressures in the extensive, hydrologically continuous Woodbine sands have dropped significantly because of oil production in East Texas since the 1930's. Hydraulic potential is now inadequate to drive fluids from the Woodbine aquifer into overlying meteoric aquifers. Formation pressure may never recover.

Saline waters in the Upper Cretaceous aquifers are predominantly sodium chloride type (fig. 44). The deeper waters are mainly sodium-calcium-chloride type, having much higher total dissolved solids than the shallower sodium chloride waters surrounding a repository. Total dissolved solids are higher in the deeper waters because of clay reactions, albitization, and other chemical reactions in an older, more closed system. On the basis of  $\delta^{2}\text{H}$  and  $\delta^{18}\text{O}$  isotopic composition of the water (fig. 45), both saline systems have been flushed of their original connate waters and recharged by continental meteoric waters. The presence of meteoric water, rather than of connate seawater, implies that both systems are hydrodynamically active rather than stagnant. The sodium and chloride in both systems result from dissolution of salt in pillows and diapirs.

Deep basinal waters have discharged up the flanks of Butler Dome, or a radial fault associated with it, and possibly up the flanks of Palestine Dome. A false cap rock of calcite-cemented Carrizo sandstone has formed at Butler Dome. The  $\delta^{13}\text{C}$  and  $\delta^{18}\text{O}$  values of the calcite suggest that the waters originated from the deep basin. Butler Dome is located where the potentiometric surface is depressed and the Wilcox aquifer is discharging. Lowering of the hydraulic head in the shallow aquifers may have permitted discharge of deep-basin saline waters. In general, salt domes in discharge zones of meteoric aquifers have the greatest potential for migration of deep-basin fluids up the flanks of diapirs and diapir-associated faults.

Fogg and Kreitler (1982); Kreitler and others (1982b)

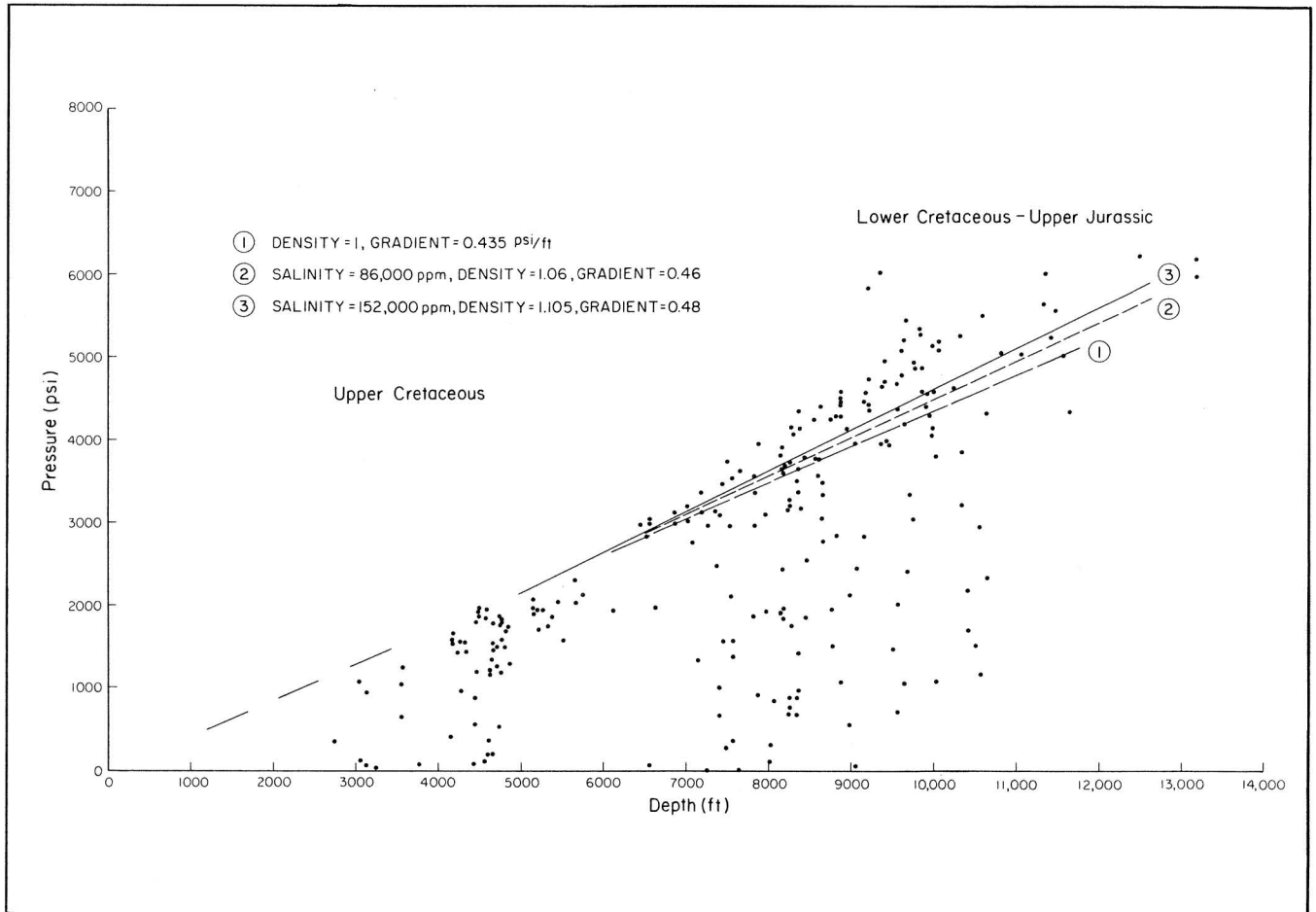


Figure 43. Graph of fluid pressure versus depth for saline aquifers in East Texas Basin (from Kreitler and others, 1982b).

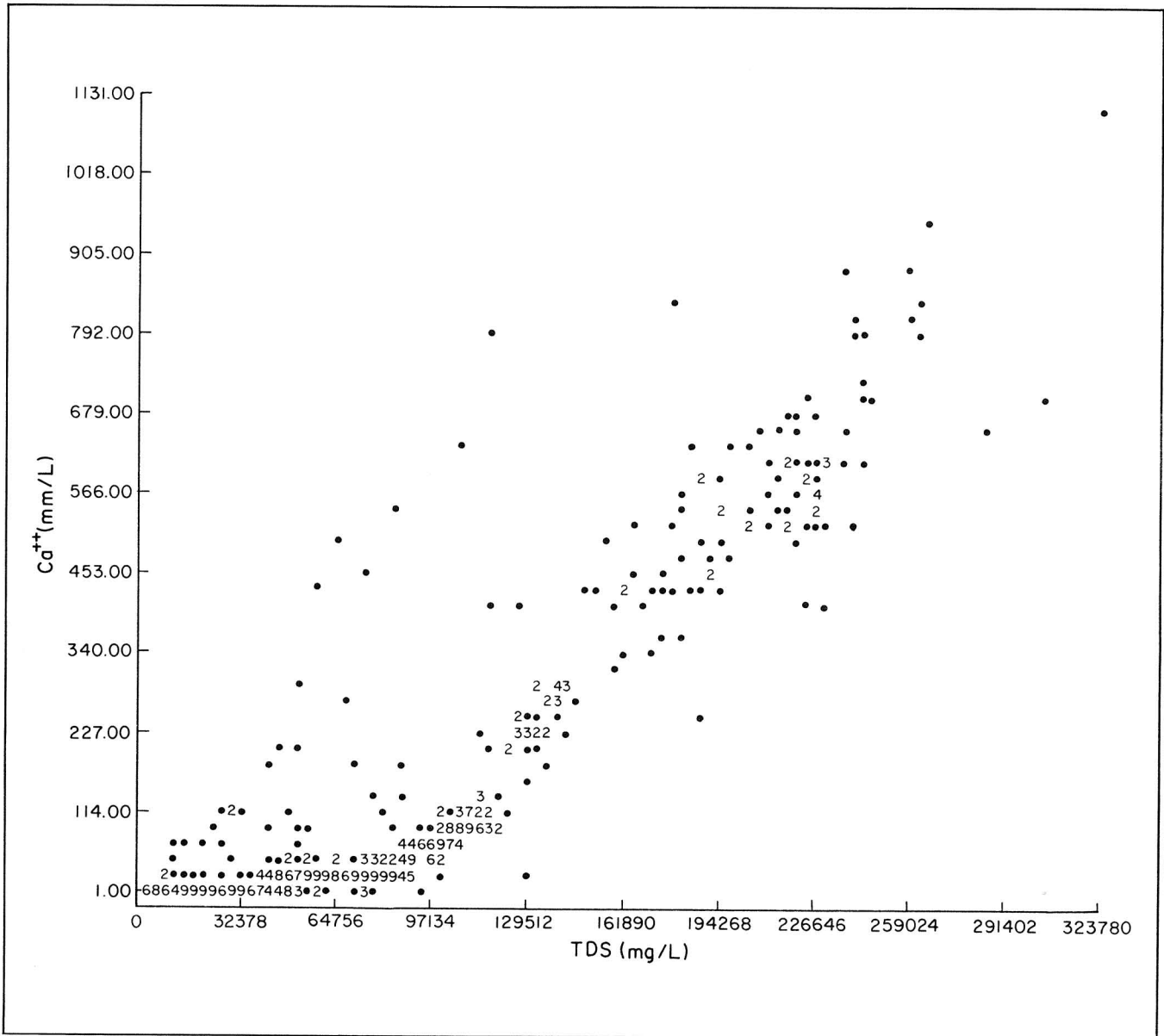


Figure 44. Graph of calcium concentration versus total dissolved solids (TDS) in saline aquifers in East Texas Basin (from Kreitler and others, 1982b).

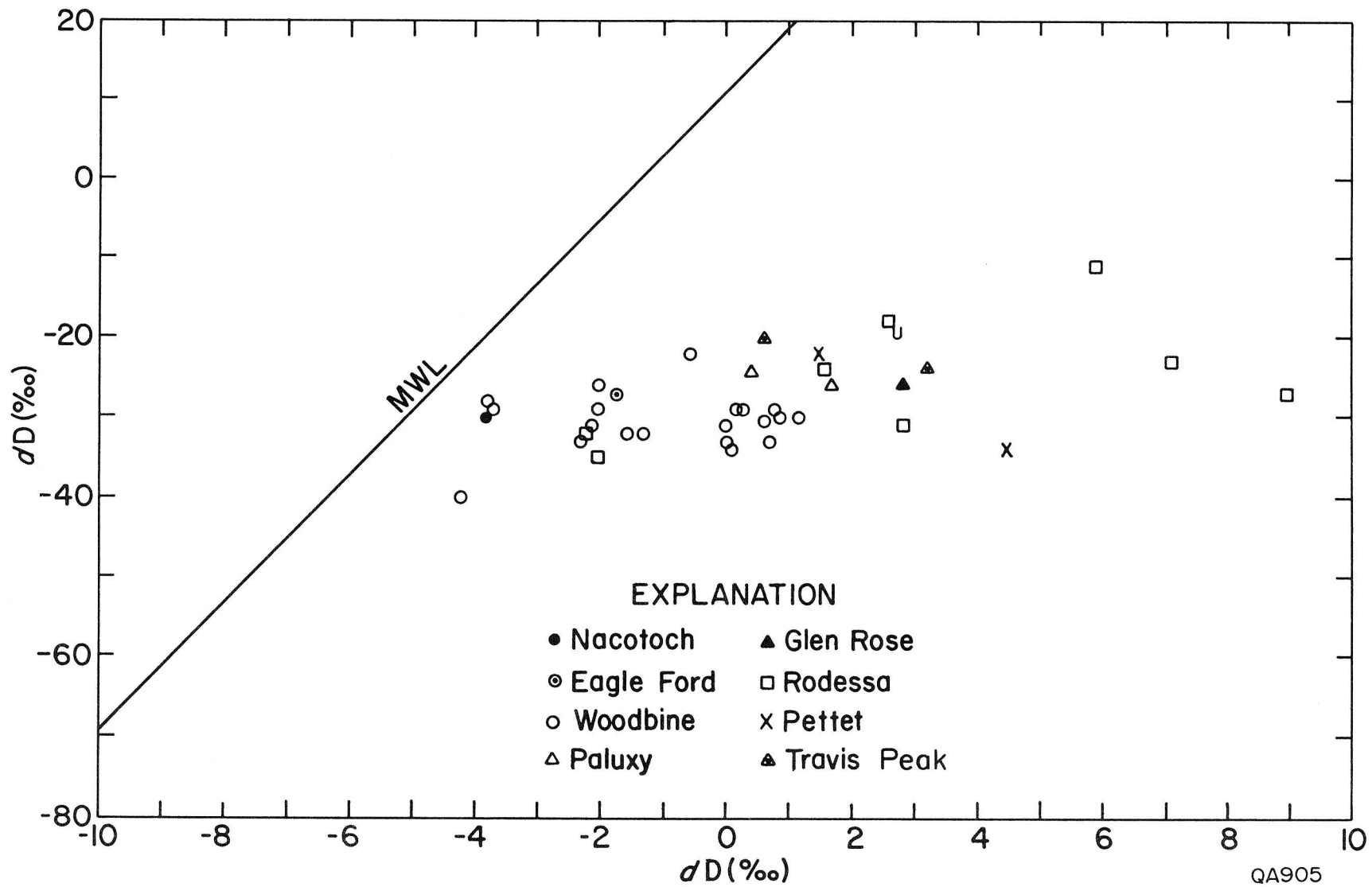


Figure 45. Graph showing  $dD$  (‰) versus  $\delta^{18}O$  in East Texas ground water and meteoric water line (MWL) (from Kreitler and others, 1983).

## CORE STUDIES OF OAKWOOD DOME, EAST TEXAS

### Lithology of Salt

*Salt core from Oakwood Dome is more than 98 percent pure halite and displays evidence of two distinct periods of recrystallization. Deformation and recrystallization during diapir growth produced a penetrative schistosity. Later recrystallization of the upper 2 m (6.6 ft) of salt in the presence of ground water under conditions of low differential stress produced a granoblastic fabric.*

A vertical drill core, LETCO TOG-1, was obtained from just north of the axis of the Oakwood Dome salt stock, Freestone County, East Texas (fig. 46). The borehole intersects rock salt at 354.5 m (1,163 ft) and ends at a depth of 411.8 m (1,351 ft), yielding 57.3 m (188 ft) of rock-salt core (fig. 47). The rock-salt core contains an average of  $1.3 \pm 0.7$  percent anhydrite. If all the cap rock was derived by residual accumulation and subsequent diagenesis of such low concentrations of anhydrite, which seems probable, dissolution of a column of rock salt more than 6 km (20,000 ft) high would be required to produce the cap rock.

The lower 55.4 m (181.5 ft) of rock salt, the R-1 zone, displays a strong schistosity induced by diapiric flow of salt (fig. 47). Recrystallization of previously foliated rock salt produced a granoblastic polygonal texture in the R-2 and R-3 zones of the upper 2 m (6.5 ft) of salt core. Consideration of homologous temperatures, geothermal gradients, and present erosion rates suggests that this recrystallization occurred at least 3 Ma ago at a minimum depth of 760 m (2,493 ft). Microstructure, fluid inclusions, and bromine concentrations in halite suggest that recrystallization of the R-1 and R-2 zones was promoted by downward movement of intercrystalline brine from the lower contact of the anhydrite cap rock. Bromine concentrations in halite suggest that rock salt of the recrystallized R-3 zone has been chemically recycled by limited re-solution to a greater degree than has the remainder of the rock salt. Intracrystalline fluid inclusions are confined to the R-3 zone (fig. 48). Their volume increases upward from 0.0005 percent 60 cm (2 ft) below the cap rock to 0.05 percent at the cap-rock contact.

Dix and Jackson (1982); Dix and Jackson (1981a)

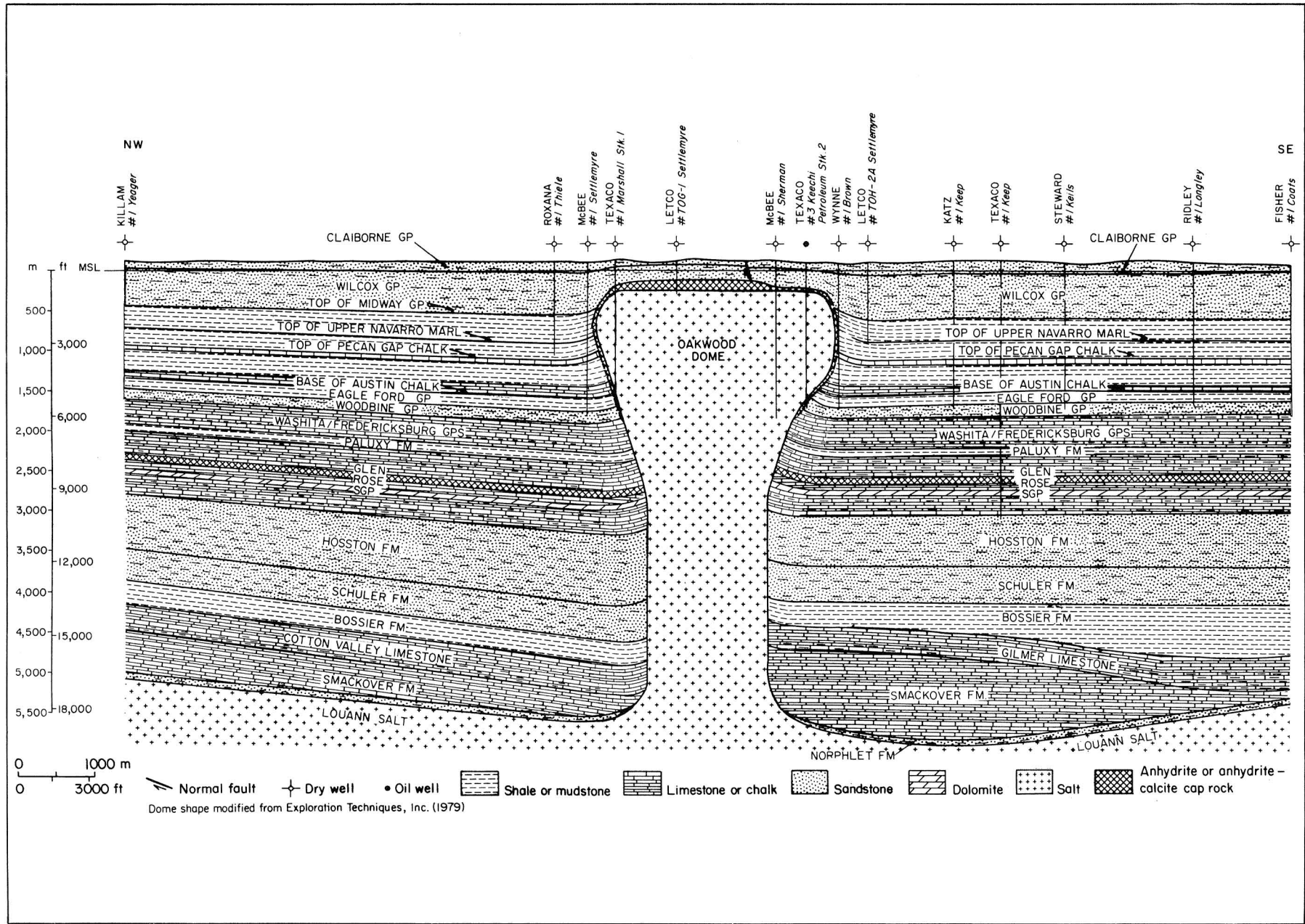


Figure 46. Oakwood Dome cross section showing location of TOG-1 well (modified from Giles and Wood, 1983).

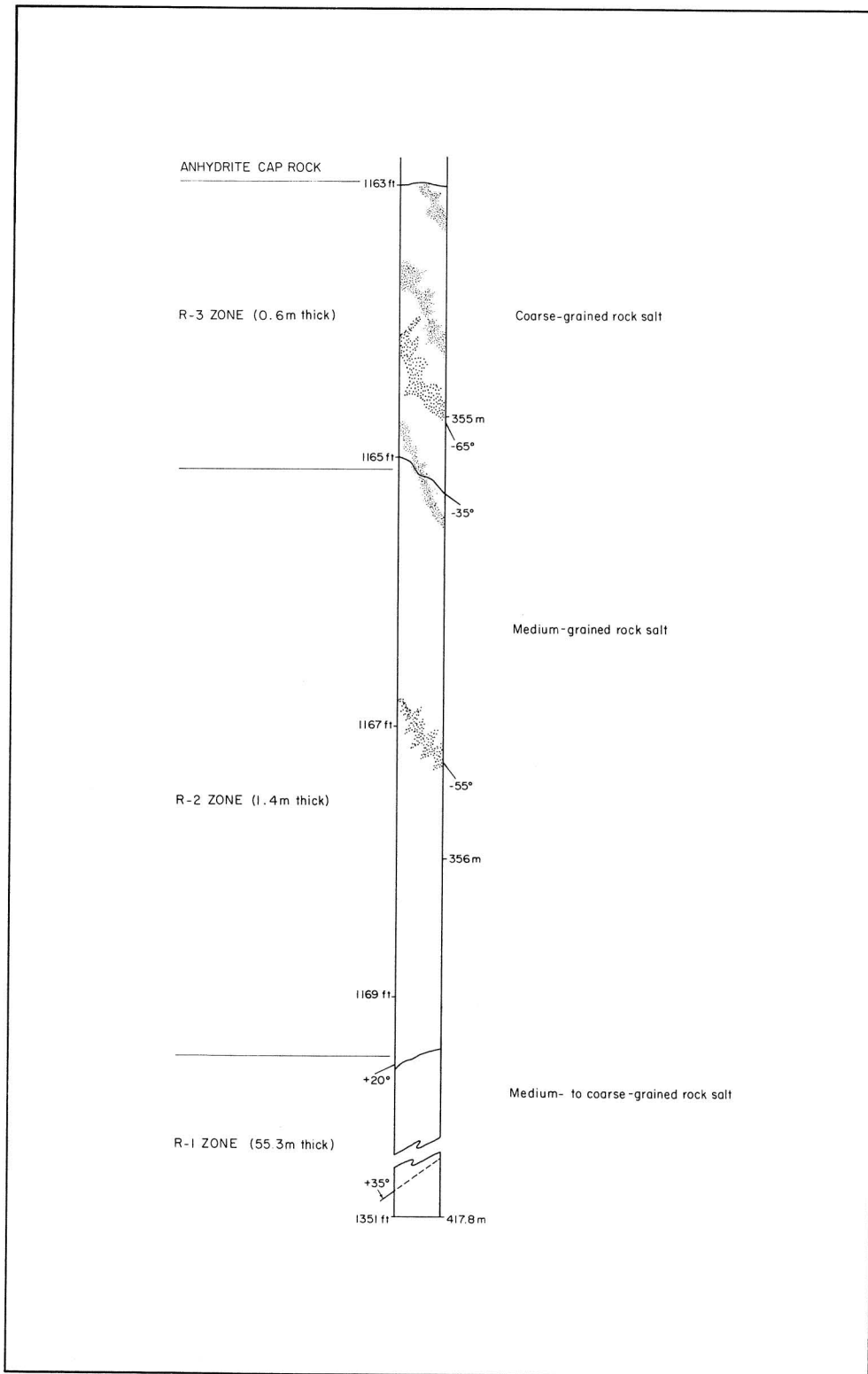
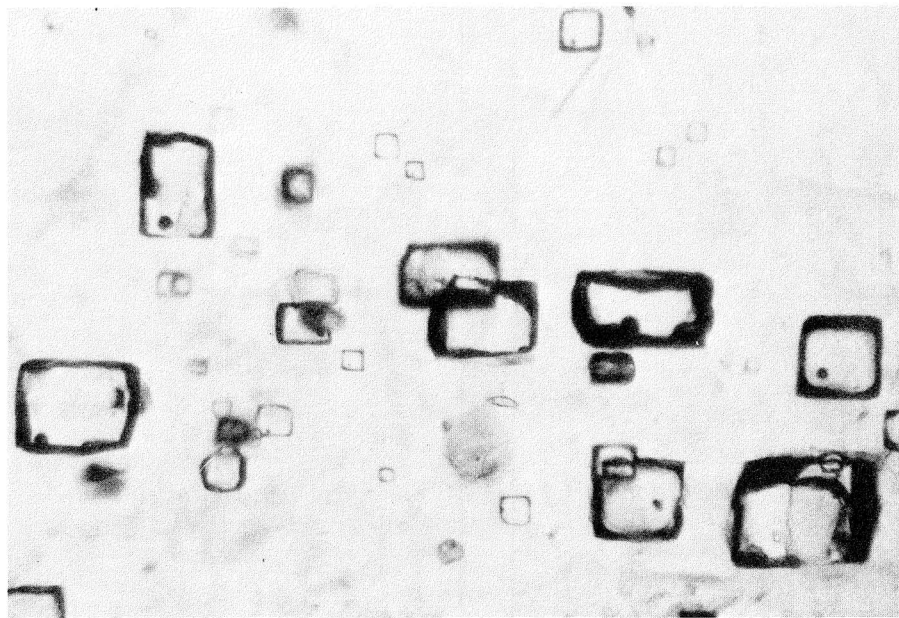


Figure 47. Vertical profile of TOG-1 rock-salt core showing R-1, R-2, and R-3 zones, dip of foliation in R-1 zone (dashed line), and disseminated-anhydrite layers (stippled) (from Dix and Jackson, 1982).





0 | mm

Figure 48. Photomicrograph of brine inclusions within halite in R-3 zone at depth of 354.7 m (1,163.7 ft) (from Dix and Jackson, 1982).

## Structure of Salt

*Geometric analysis of the megascopic structure in the Oakwood salt core suggests that the core has penetrated the hinge zone and the lower part of a large inclined overthrust antiform representing one of the highest and youngest of a series of salt tongues that fed the spreading diapir cap. The fold geometry also suggests that at least tens or hundreds of meters of overlying salt have been truncated from the top of the diapir, most probably by ground-water dissolution. Volumetric calculations based on cap-rock-salt proportions indicate that as much as 6 km (20,000 ft) of salt may have been removed from the diapir crest.*

Geometric synthesis of mesoscopic structures in the Oakwood salt core has determined the form and orientation of the macroscopic structures intersected by the vertical drill core, TOG-1. Nongraded layering, defined by disseminated anhydrite grains in halite, and a tectonite fabric constitute the basic structural elements (fig. 49). The fabric has a weak mineral lineation and a strong schistosity, defined by the preferred orientation of disk-like halite grains.

The structures were extrapolated to zones adjacent to the core by assuming similar-type shear folding. The schistosity is axial planar to a series of younger major folds that jointly define the lower part of a large inclined antiform within the dome. The younger major folds refold older minor isoclines, which are transected by the fabric (fig. 50).

The core has penetrated the hinge zone and lower limb of an inclined, overturned antiform (lobe 5 in figure 51). This is inferred to represent one of several salt tongues that fed the diapir and rose upward and outward, changing in orientation from steeply plunging folds to recumbent, overthrust folds (fig. 51). Fold structures that originally formed deep in the diapir have been bared by ground-water dissolution and are now juxtaposed against the base of the cap rock.

Jackson (1983); Dix and Jackson (1982); Jackson and Dix (1981)

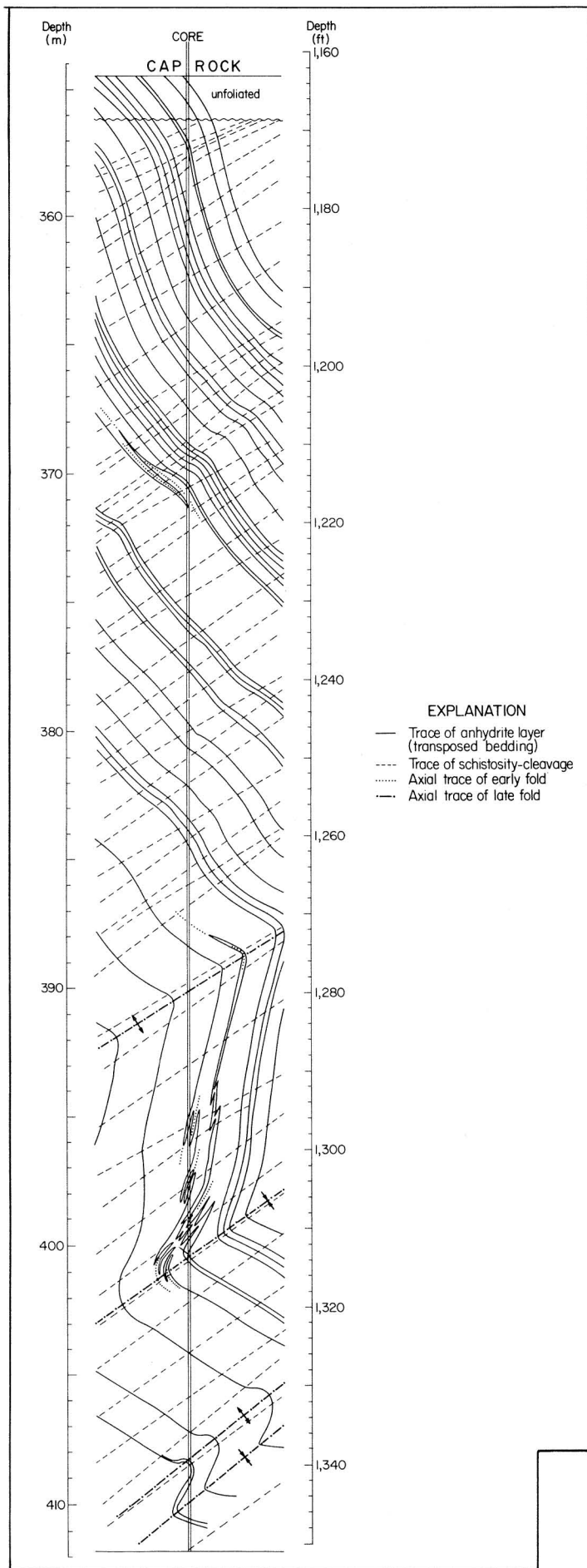


Figure 49. Vertical profile showing schistosity and anhydrite-rich layers in TOG-1 rock-salt core (from Jackson, 1983).

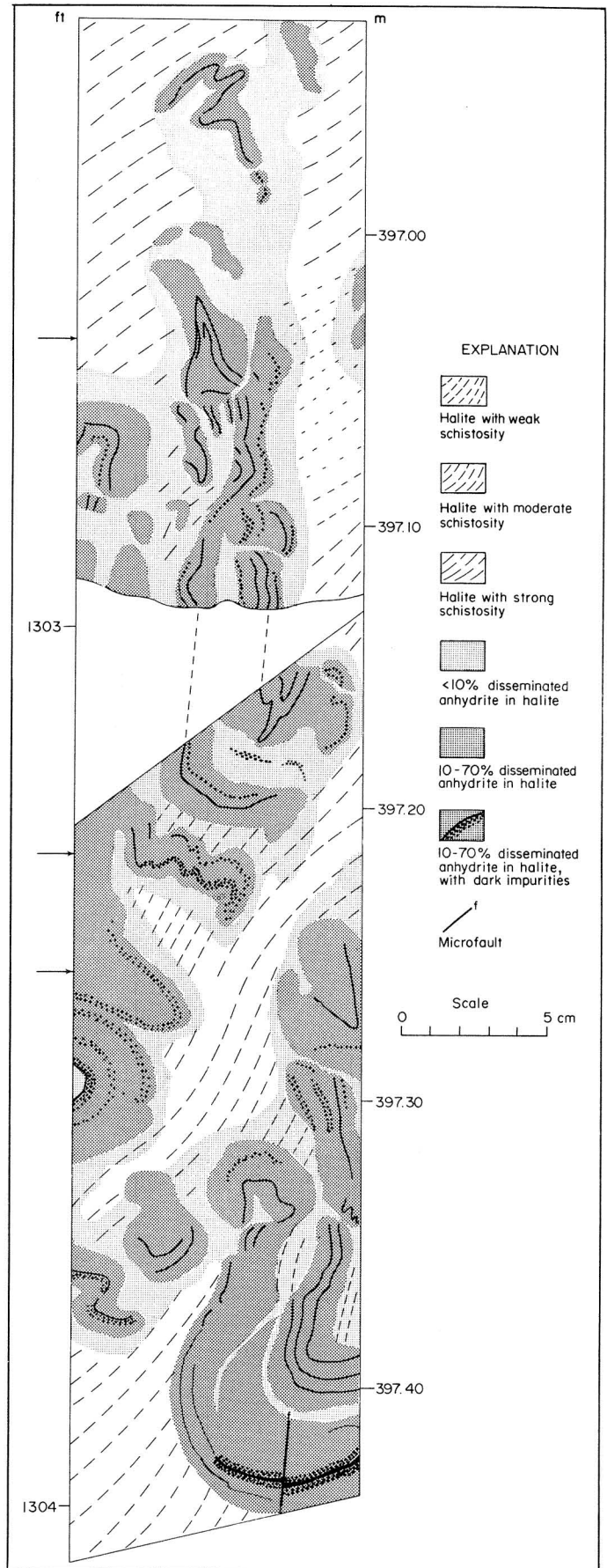


Figure 50. Vertical section along TOG-1 rock-salt core (from Dix and Jackson, 1982).

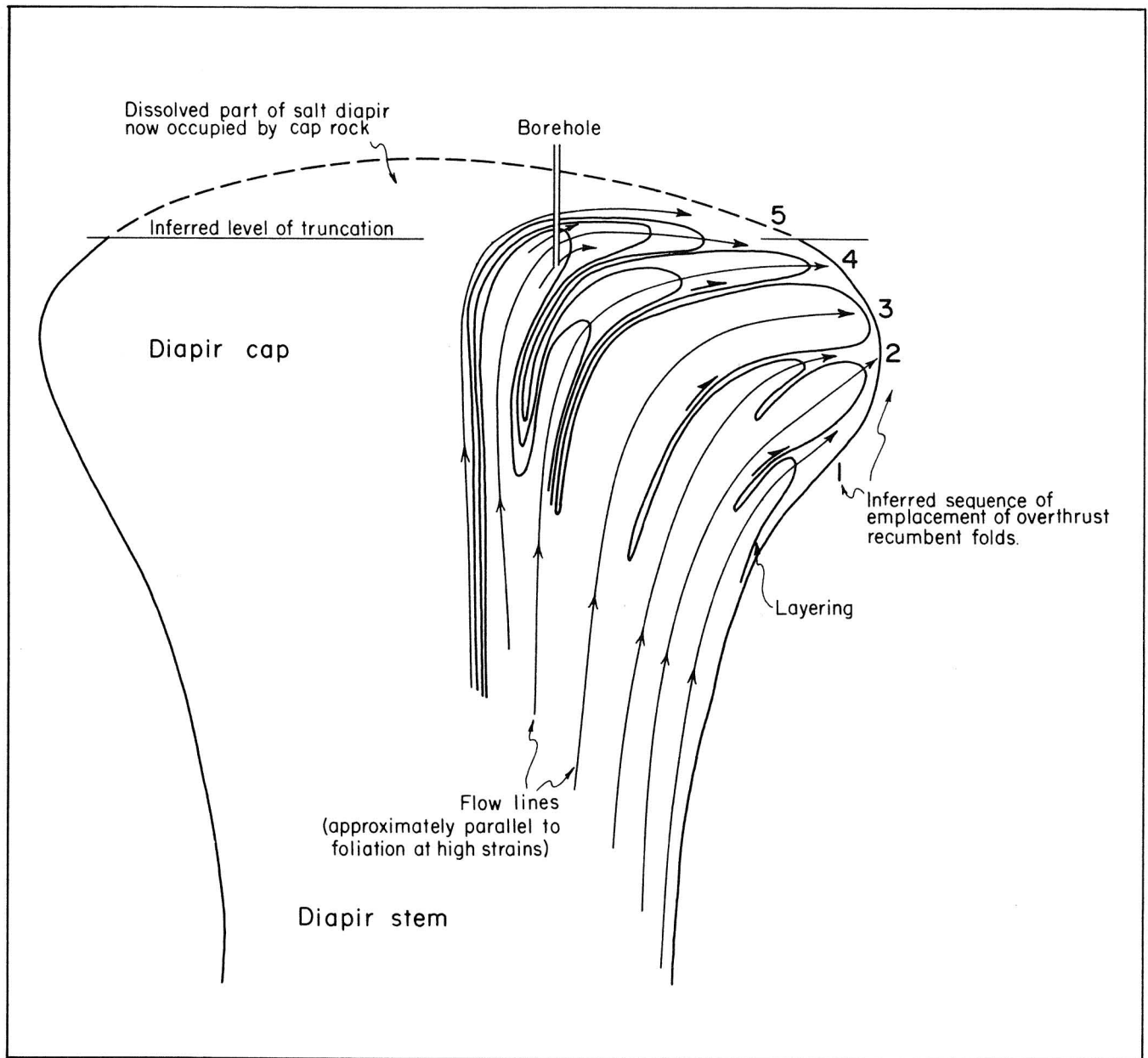


Figure 51. Schematic cross section showing inferred flow patterns within a laterally spreading, rising diapir fed by multiple emplacement of salt tongues as overthrust folds (from Jackson, 1983).

## Strain in Salt

*Strain analysis of 2,400 halite grains in the TOG-1 core indicates that flattening strains predominate; the ratio of flattening to constriction increases upward, whereas strain intensity decreases upward. These results provide further evidence of truncation of the crest of the salt stock in the past.*

Measurement of the orientations and axial ratios of 2,400 halite grains at 8 sample sites along the TOG-1 core has allowed the minimum finite strains to be determined by 3 different methods: the Harmonic Mean method, the Theta Curve method, and the Shape Factor Grid method. All the strains recorded (fig. 52) are of the flattening type ( $0.544 > k > 0.000$ ), and the ratio of flattening to constriction increases upward. The strain intensity decreases upward through the foliated salt from 52 to 37 percent shortening (fig. 53); the unfoliated R-2 salt underwent about 15 percent shortening. This upward decrease in strain intensity may mark the trend toward a "neutral" zone of low strain (present in some model diapirs), which was subsequently removed by dissolution during diapir truncation.

The orientations of maximum extension directions vary widely even though the foliation plane, which contains these directions, dips uniformly. Thus the preferred directions of salt creep or intergranular fluid flow are also likely to vary within the foliation plane.

Jackson (1983); Jackson (1981a)

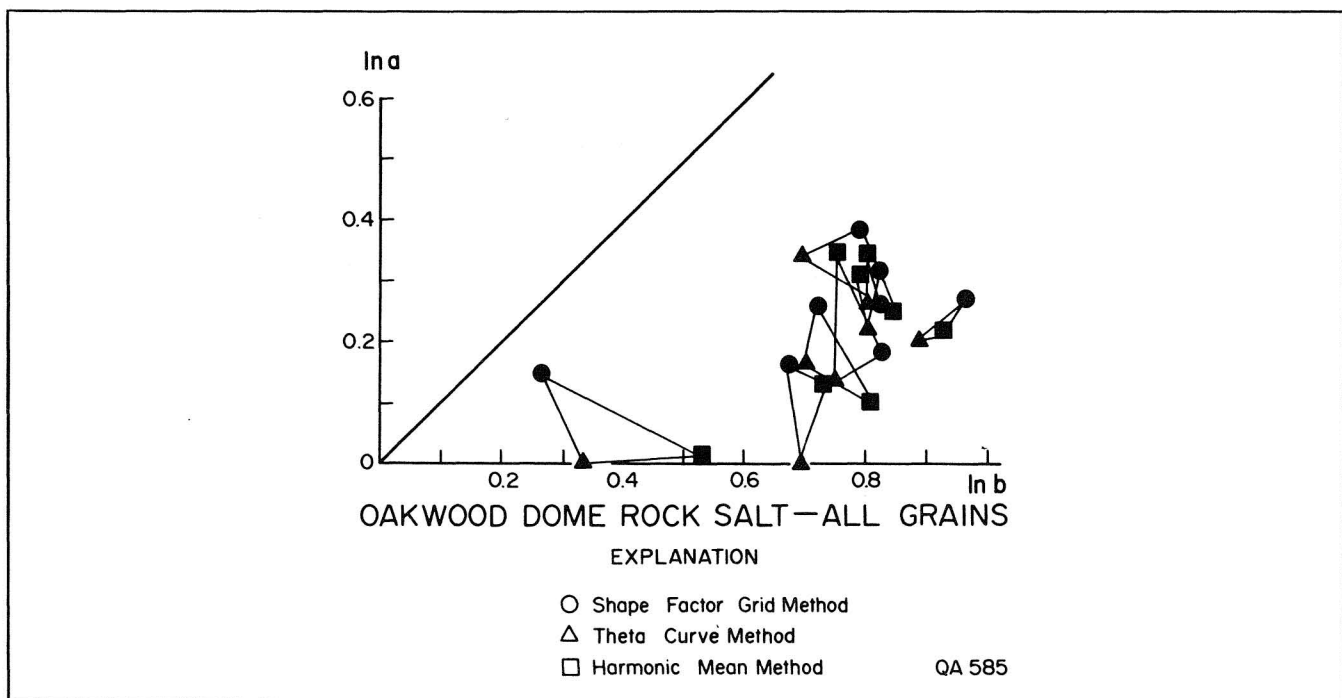


Figure 52. Flinn diagram showing mean strains in Oakwood Dome rock salt.  $\ln a$  = natural log of  $X/Y$ ,  $\ln b$  = natural log of  $Y/Z$ , where  $X > Y > Z$  are the principal strain axes. Numbers refer to depth in feet (from Jackson, 1983).

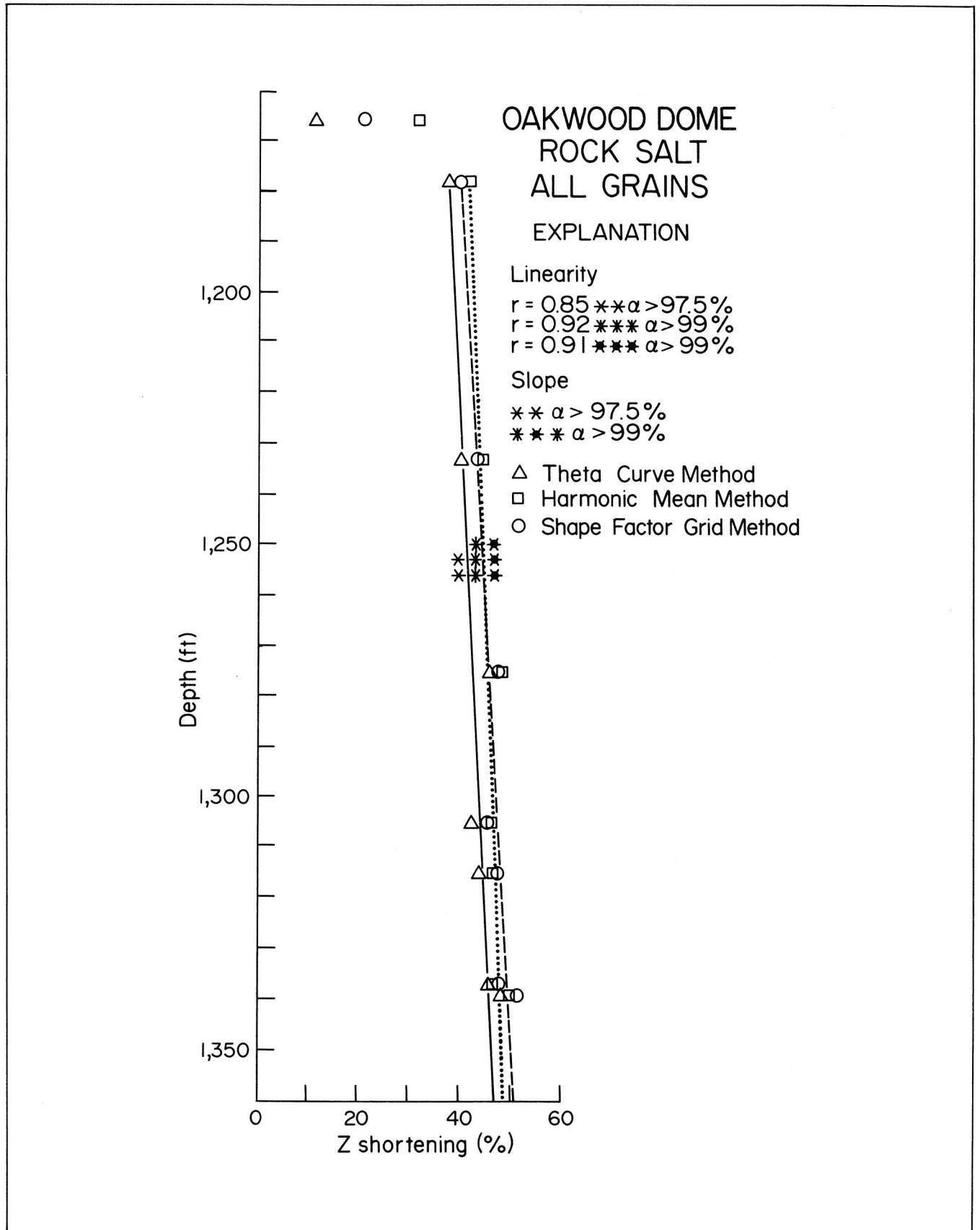


Figure 53. Graph showing statistically significant upward decrease in percentage shortening with decreasing depth (from Jackson, 1983).

## Cap-rock - Rock-salt Interface

*Dissolution of halite at the crest of the salt stock released disseminated anhydrite that accumulated as loose sand on the floor of the dissolution cavity. Renewed rise of the salt tightly closed the cavity and accreted the anhydrite sand against the base of the cap rock.*

Intracrystalline fluid inclusions in the R-3 rock salt are most concentrated directly below the cap-rock contact ("Lithology of Salt," p. 87), a sign that fluids moved down from the base of the cap rock. The absence of a cavity between rock salt and cap rock (fig. 54) demonstrates that the salt stock is not being dissolved where intersected by the borehole.

The presence of an anhydrite-rich lamina across halite-filled extension fractures at the base of the cap rock indicates that anhydrite laminae have accreted against the base of the cap rock as residual sand released by halite dissolution (fig. 55). The microstructure of the anhydrite indicates that anhydrite sand grains formed a compact rock by solid-state recrystallization. Horizontal lamination throughout the anhydrite cap rock is thought to reflect the process of accretion.

Upward force from the rising salt stock probably induced the observed vertical shortening in the cap rock just above the contact. This strain resulted in horizontal, spaced, stylolitic cleavage formed by pressure solution and mass transfer of anhydrite. The stylolitic cleavage, which is marked by a dark, insoluble pyritic residue, transects the older lamination. Further lateral extension and vertical shortening in the base of the cap rock resulted in halite-filled vertical extension fractures and inclined shear fractures (fig. 55).

Ingress of water resulted in dissolution of the salt stock, formation of cap rock, and addition of sodium chloride to the ground water. These processes are both detrimental and favorable to waste isolation (tables 5 and 6). Despite the strong evidence of repeated attrition and uplift of the salt stock, the geologic system of rock salt and cap rock can offset, at least partly, these negative processes by self-sealing and recovery.

Dix and Jackson (1982)





Figure 54. Photograph of tight contact between salt and overlying cap rock (from Dix and Jackson, 1982). Core is 10 cm (4 inches) wide.

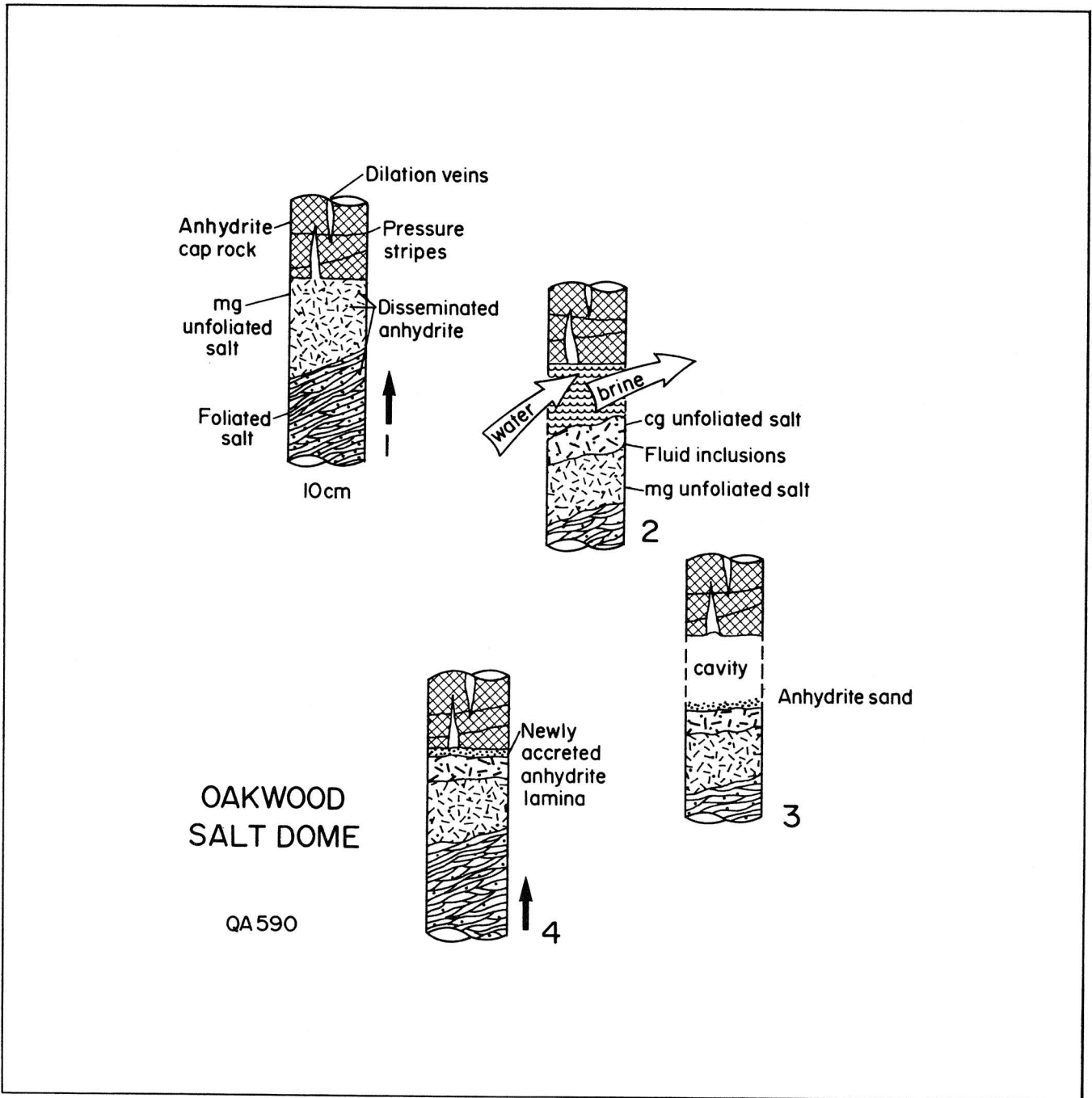


Figure 55. Schematic diagram showing processes at cap-rock - rock-salt interface (from Jackson, 1983).

Table 5. Inferred processes at the cap-rock - rock-salt contact of Oakwood Dome that are favorable for storage of nuclear wastes (from Dix and Jackson, 1982).

OBSERVATION	FAVORABLE SIGNIFICANCE
1. Tight seal between rock salt and anhydrite cap rock. Extension fractures and spaced cleavage in anhydrite cap rock.	Ability of salt flow, driven by diapirism, to close cavities and apply upward pressure on cap rock to keep cavity closed.
2. Halite-filled extension fractures in anhydrite cap rock.	Ability of halite to grow in opening fractures, thereby sealing them.
3. Horizontal, stylolitic, spaced cleavage in anhydrite cap rock.	Ability of anhydrite aggregates to respond to stresses by migrating in solution to nearby pressure shadows and pore spaces, thereby reducing porosity and enhancing sealing properties of the cap rock.

Table 6. Inferred processes at the cap-rock - rock-salt contact of Oakwood Dome that are unfavorable for storage of nuclear wastes (from Dix and Jackson, 1982).

PROCESS OR OBSERVATION	DETRIMENTAL SIGNIFICANCE
1. Structural truncation of diapiric crest.	Considerable diapiric uplift.
2. Water-induced recrystallization of uppermost 2 m of rock salt.	Introduction of water to diapiric crest and destruction of as much as 6 km of rock salt by repeated episodes of dissolution.
Greater abundance of fluid inclusions in rock salt near cap-rock contact.	
Accretion of anhydrite lamina against base of cap rock.	
Similar appearance of lamination throughout anhydrite cap rock.	
3. Tight seal between rock salt and anhydrite cap rock.	Renewed uplift of salt diapir after most recent episode of dissolution.
4. Vertical extension fractures in anhydrite cap rock.	Fracturing and dilation of cap rock because of rise of salt stock, creating further avenues for ground water to enter and wastes to escape.
5. Low bromine content of halite in lens of rock salt in anhydrite cap rock.	Passage of brines through fractures in cap rock, precipitation of halite in cavities, and possible escape of brines from cap rock into surrounding strata.

## Cap Rock

*Cap rock at Oakwood Dome consists of low-permeability anhydrite resting in sharp contact on the underlying rock salt. A more porous calcite section overlies the anhydrite. The cap rock appears to be an effective barrier that inhibits dome dissolution.*

Salt-dome cap rock in general may or may not be an effective low-permeability barrier to future dissolution of salt stocks. Some cap rock, such as that on Gyp Hill Dome, is currently forming by salt dissolution. Other cap rock, such as that on Oakwood Dome, formed in the geologic past and appears to be an effective low-permeability seal. Cap rock on top of Oakwood Dome is 137 m (450 ft) thick in the TOG-1 well. Above a tight contact with salt ("Cap-Rock - Rock-Salt Interface," p. 97), the following zones are present:

(1) Anhydrite zone, 354 to 277 m (1,163 to 908 ft) thick, containing low-porosity, low-permeability granoblastic anhydrite devoid of gypsum (table 7). The rock is horizontally laminated on a millimeter scale by primary variations in organic content and by stylolitic pressure stripes induced by diapiric rise of the underlying salt (fig. 56).

(2) Transitional zone, 277 to 275 m (908 to 902 ft) thick, containing porous, permeable anhydrite partly altered to calcite and gypsum.

(3) Calcite zone, 275 to 217 m (902 to 713 ft) thick, consisting of porous, permeable (table 7) layers of alternating dark-gray, fine-grained calcite and younger, white, coarse-grained calcite that has replaced fractures and occluded porosity.

The anhydrite zone is postulated to have formed by dissolution of 6 km (3.6 mi) of rock salt more than 100 Ma ago in a relatively deep, hot, saline environment. The calcite zone, characterized by extremely depleted  $\delta^{13}\text{C}$  calcite and traces of biodegraded hydrocarbons, formed in a similar environment by reduction of anhydrite cap rock and oxidation of organics, possibly introduced by ground water. In Louisiana, Vacherie Dome cap rock, which was also investigated in this study, has a similar diagenetic history.

In contrast, the anhydrite cap rock of Gyp Hill in South Texas is 52 to 152 percent more porous than that of Oakwood (table 7). According to F and t statistical tests of 25 porosity calculations from the anhydrite zone in Gyp Hill and Oakwood cap rock, excluding the anomalously high porosity value at the base of Gyp Hill cap rock, the absolute mean porosity of the Gyp Hill anhydrite zone exceeds the absolute mean porosity of the Oakwood anhydrite zone by 0.57 to 1.67 percent at the 99-percent confidence level. Textural evidence, chiefly gypsum-cemented anhydrite, indicates that the cap rock formed--and probably still is forming--in a shallower, cooler, and less saline environment, as is the case for Rayburn's Dome, Louisiana.

Kreitler and Dutton (1983); Dutton and others (1982a); Dix and Jackson (1982); Kreitler and others (1981b); Dutton and Kreitler (1981)



0 40 mm

Figure 56. Photograph of black stylolitic laminae, 1 to 2 mm wide, in anhydrite cap rock from TOG-1 (from Dix and Jackson, 1982).

Table 7. Comparison of porosities and permeabilities of cap rock from Oakwood and Gyp Hill salt domes (from Kreitler and Dutton, 1983).

OAKWOOD CAP ROCK

<u>Cap-rock zones</u>	<u>Depth (ft)</u>	<u>Permeability (millidarcys)</u>	<u>Porosity (percent)</u>
Calcite	720	<0.01	1.3
	740	<0.01	2.2
	760	0.04	3.1
	780	0.02	3.8
	800	43.00	9.1
	820	16.00	6.2
	820	0.01	4.0
	840	<0.01	13.0
	880	<0.01	5.1
Transition	904	0.05	5.7
	907	<0.01	2.3
	907	0.29	8.3
Anhydrite	920	<0.01	0.7
	940	<0.01	0.7
	960	<0.01	0.8
	1,040	<0.01	0.9
	1,060	<0.01	0.8
	1,080	<0.01	0.8
	1,100	<0.01	0.9
	1,100	<0.01	1.0
	1,120	<0.01	1.3
	1,138	0.02	3.3
	1,162	<0.01	1.1

(continued)

Table 7. (cont.)

## GYP HILL CAP ROCK

<u>Cap-rock zones</u>	<u>Depth (ft)</u>	<u>Permeability (millidarcys)</u>	<u>Porosity (percent)</u>
Gypsum	50	<0.01	1.6
	123	<0.01	3.0
	152	<0.01	1.4
	171	<0.01	2.0
	230	<0.01	2.5
	272	<0.01	1.2
	284	<0.01	3.4
	Anhydrite	310	<0.01
340		<0.01	1.5
370		<0.01	1.3
400		<0.01	2.6
428		<0.01	1.6
500		<0.01	5.1
600		<0.01	2.6
690		<0.01	3.1
740		<0.01	3.3
794		<0.01	1.6
815		<0.01	2.2
835		<0.01	1.6
855		<0.01	3.6
875		<0.01	4.4
890		45.00	20.0

## HYDROGEOLOGIC STUDIES OF OAKWOOD DOME AND VICINITY

### Hydrogeologic Monitoring and Testing

*Results of pumping tests conducted around Oakwood Dome have been used to calculate transmissivity, hydraulic conductivity, and storativity. Distribution of water levels in wells directly over the dome delineates a recharge area near the Carrizo outcrop and correlates with water-chemistry data from the same wells. Unplugged drillholes through the Oakwood salt overhang could initiate rapid salt dissolution by descending fresh water.*

Data collected from monitor wells help to detect magnitudes and effects of recharging over Oakwood Dome. Water levels in all wells were monitored weekly or biweekly from July 1979 to October 1981.

The water levels of the Carrizo aquifer were measured on May 15, 1980 (fig. 57). Contours clearly indicate a recharge area near the Carrizo and Reklaw outcrops, which is consistent with the water-chemistry data for Oakwood Dome ("Ground-Water Chemistry," p. 69). Faults in the east apparently impede flow, causing the steeper hydraulic gradients. Short-term water-level fluctuations in all the wells reflect barometric pressure changes and artesian conditions.

In 1979 and 1980, pumping tests were conducted in 14 wells around Oakwood salt dome. Most wells were screened in the Carrizo Formation and the Wilcox Group. Each pumping test lasted 8 to 24 hours. Values of transmissivity (T), hydraulic conductivity (K), and storativity obtained from analysis of test data from production wells are shown in table 8. Laboratory-derived K values from depths greater than 305 m (1,000 ft) and field-derived K values are related to electric log resistivity values in the Wilcox Group (fig. 58). The distributions barely overlap, and their median values differ by a factor of about  $10^3$ . All the field-derived K values (except from well TOH-2A) are apparently from thick, channel-fill sand bodies that consistently register high electric log resistivities ( $R_o$ ). The lab-derived values, however, are from thinner interchannel sand bodies that consistently register low resistivities.

Several boreholes through the salt overhang of Oakwood Dome represent a potential hazard. The boreholes may connect the shallow fresh-water aquifer with the deep saline aquifer. Fresh water with greater hydraulic head than that of the saline water could, therefore, descend through these holes and dissolve the salt. Some of these boreholes remain unlocated, which intensifies the problem.

Fogg and Kreitler (1982); Fogg and Kreitler (1981); Fogg (1981b); Fogg and others (1981)



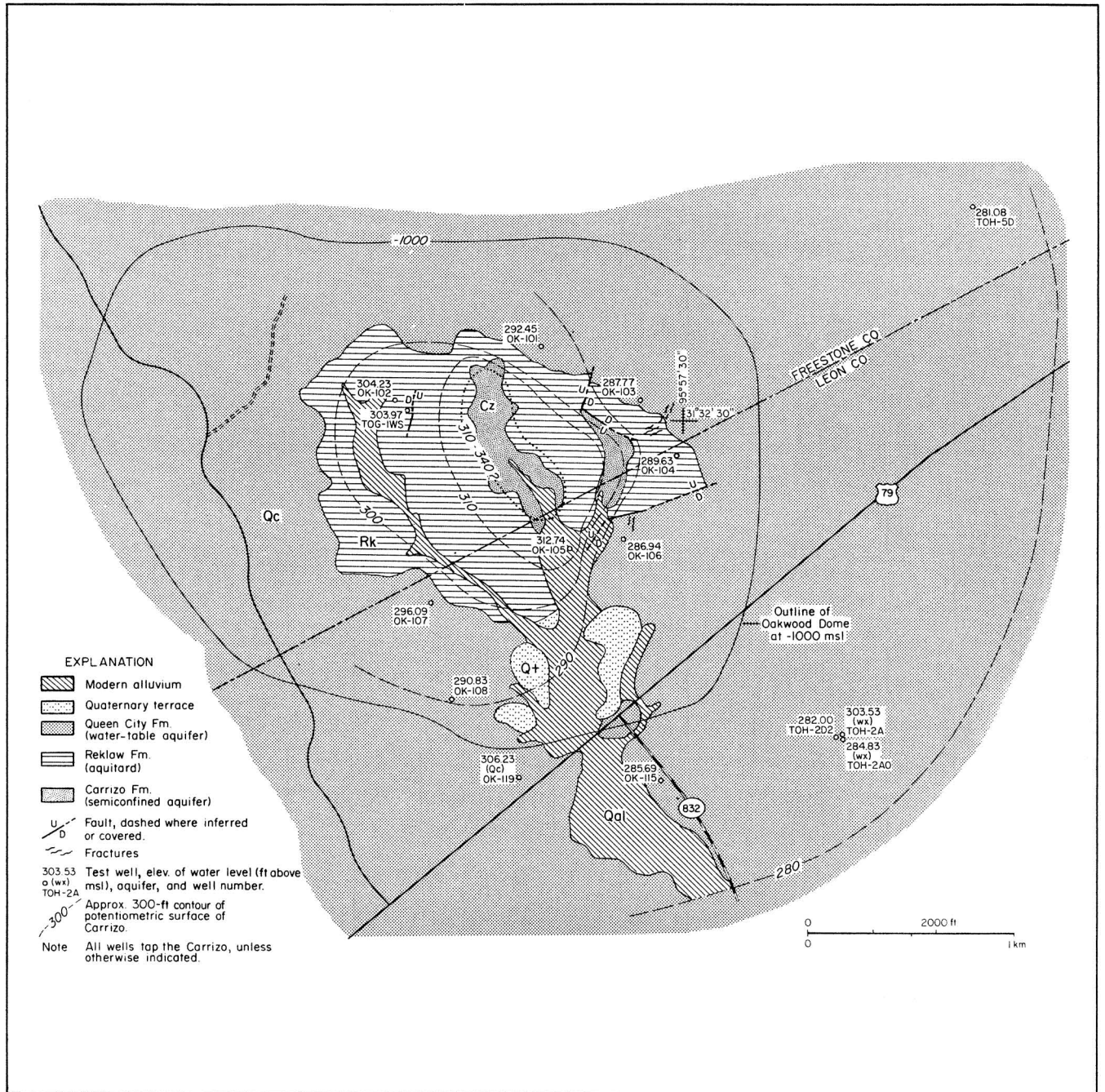


Figure 57. Map showing potentiometric surface of Carrizo aquifer over Oakwood Dome (from Fogg, 1981b). Cz = Carrizo Formation; Rk = Reklaw Formation; Qc = Queen City Formation; Qt = Quaternary terrace; Qal = modern alluvium.

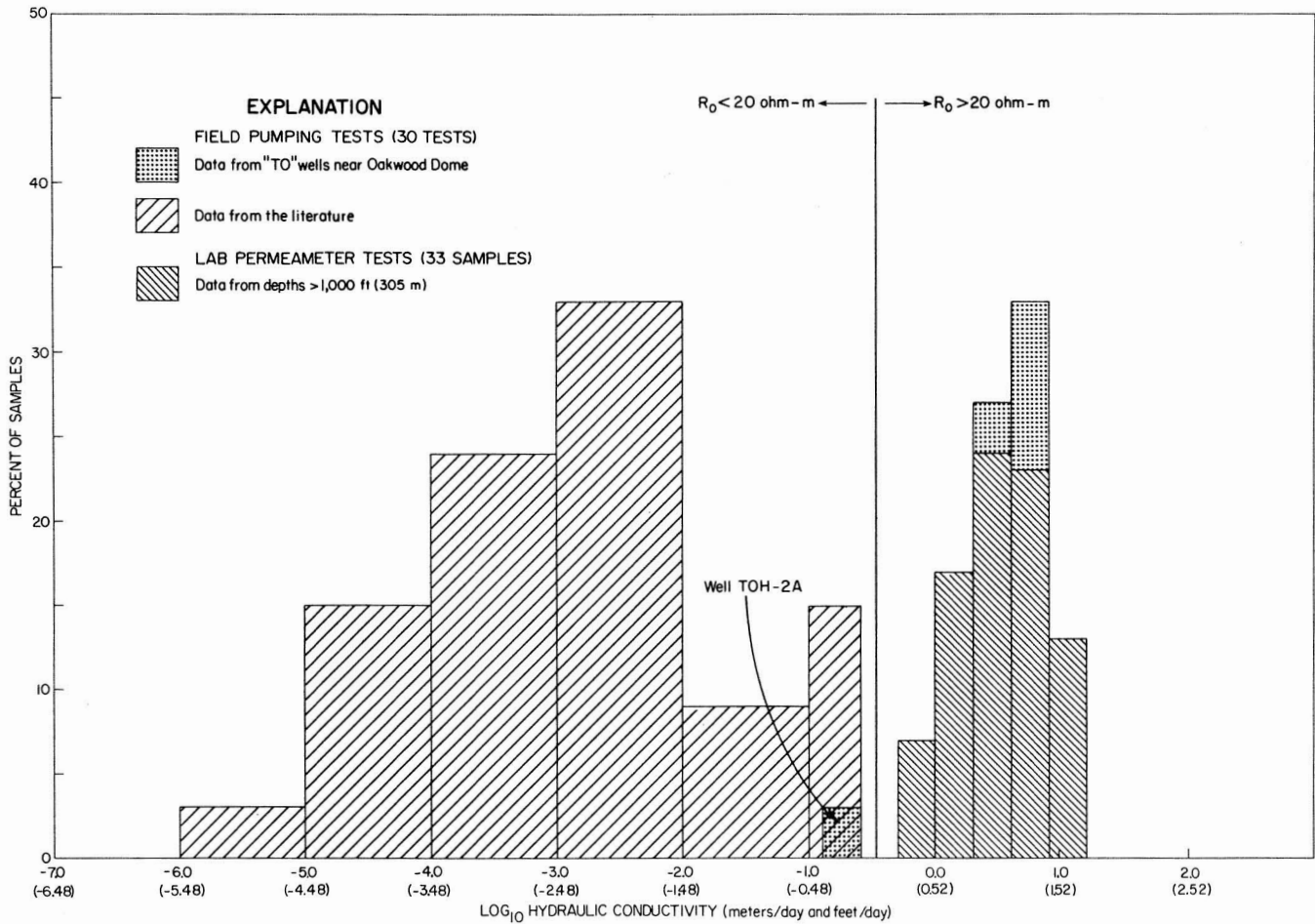


Figure 58. Histogram of electric log resistivity values in the Wilcox Group compared with lab-derived K values (from Fogg and others, 1982b).

Table 8. Test data from monitoring wells around Oakwood Dome (from Fogg, 1981b).

Well	Unit, screened interval (m)	Aquifer interval, thickness (m)	Transmissivity (m <sup>2</sup> /d)		Hydraulic conductivity (m/d)		Storativity		Remarks
			Cooper/Jacob <sup>c</sup> drawdown/ recovery	Theis <sup>d</sup> drawdown/ recovery	Cooper/Jacob <sup>c</sup> drawdown/ recovery	Theis <sup>d</sup> drawdown/ recovery	Cooper/Jacob <sup>c</sup> drawdown/ recovery	Theis <sup>d</sup> drawdown/ recovery	
TOG-1WS	Carrizo	23.8-51.5	76.0	75.	2.7	2.7	--	--	1. Barrier boundary detected. 2. Head in 1WS dropped below bottom of upper aquitard during test.
	30.8-49.4	27.7	80.0	75.	2.9	2.7	--	--	
Obs. well	Carrizo	27.4-48.8	--a	32.?	--a	1.5?	--a	8.2 x 10 <sup>-5</sup> ?	
OK-102	42.1-45.1	21.4	--	--	--	--	--	--	
TOH-5D	Carrizo	142.3-154.5, 157.0-183.5	270.0	220.	7.0	5.7	--	--	1. The observation well re- sults are questionable owing to their great dis- tances from TOH-5D, small drawdown responses, and sparsity of measurements. 2. Observation well data was corrected for barometric effects.
	144.5-150.6, 158.2-182.6	38.7	270.0	240.0	7.0	6.2	--	--	
Obs. well	Carrizo	60.4-79.9	--a	440.?	--a	23.?	--a	1.4 x 10 <sup>-4</sup> ?	
OK-103	70.1-73.2	19.5	--	440.?	--	23.?	--	1.2 x 10 <sup>-4</sup> ?	
Obs. well	Carrizo	39.6-57.9	--a	680.?	--a	37.?	--a	3.3 x 10 <sup>-4</sup> ?	
OK-104	51.8-54.9	18.3	--	--b	--	--b	--	--b	
TOH-2D2	Carrizo	155.8-176.2	170.0	200.0	8.3	9.8	--	--	1. Values of T and K from 2DO are lower because of poor connection to aquifer. 2. During pumping, water lev- els rose 6.7 cm in TOH-2AO and 45.7 cm in TOH-2A.
	157.3-175.9	20.4	160.0	150.0	7.8	7.4	--	--	
Obs. well	Carrizo	155.8-176.2	140.0	140.0	6.5	6.9	1.1 x 10 <sup>-4</sup>	1.3 x 10 <sup>-4</sup>	
TOH-2DO	158.2-176.8	20.4	140.0	140.0	6.9	6.9	2.2 x 10 <sup>-4</sup>	1.7 x 10 <sup>-3</sup>	
TOH-2A	Wilcox	579.0-586.0	1.4	1.4	0.21	0.21	--	--	1. Incomplete recovery.
	579.0-585.0	6.7	1.8	1.6	0.27	0.24	--	--	
TOH-2AO	Wilcox	253.9-285	190.0	170.0	6.1	5.5	--	--	1. Early data used. 2. Barrier boundary detected. 3. During pumping, water level rose 345.0 cm in TOH-2A.
		31.1	195.0	200.0	6.3	6.4	--	--	

<sup>a</sup>Jacob method of analysis inappropriate because u too large.

<sup>b</sup>Recovery measurements were too sparse to use.

<sup>c</sup>From Cooper and Jacob (1946)

<sup>d</sup>From Theis (1935)

## Ground-Water Modeling: Wilcox Multiple-Aquifer System

*A three-dimensional, steady-state ground-water flow model was constructed with an integrated finite-difference mesh for the Oakwood Dome vicinity (fig. 59). The model includes (1) regional ground-water circulation patterns (fig. 60), (2) vertical leakage across the Reklaw aquitard, (3) recharge over Oakwood Dome, and (4) large-scale heterogeneity and anisotropy of the Wilcox-Carrizo aquifer system. Heterogeneity is a volume-averaged distribution of horizontal hydraulic conductivity ( $K_h'$ ). Anisotropy was introduced by lowering the vertical to horizontal ratio ( $K_v'/K_h'$ ) until the model simulated observed pressure-depth trends. Sensitivity of the model to vertical and horizontal and sand-body interconnection was tested by simulating different distributions of  $K_h'$  and  $K_v'/K_h'$ .*

The Wilcox multiple-aquifer system contains channel-fill sand bodies complexly distributed in a less permeable matrix of interchannel sands, silts, and clays. Key uncertainties in the model are heterogeneity, the degree of connection between channel-fill sands, and the hydraulic conductivity ( $K$ ) of interchannel sands. It appears, however, that channel-fill sands are laterally disconnected in low-sand-percentage areas and laterally interconnected in high-sand-percentage areas, resulting in considerable variations in values of  $K_h'$  and ground-water flux. Sand-body vertical interconnection is generally poor, resulting in an anisotropy ratio ( $K_v'/K_h'$ ) of at most  $10^{-4}$  to  $10^{-3}$ . Vertical flow may be locally large where relatively permeable avenues are vertical. Oakwood Dome apparently lies in a transition zone between dominantly horizontal and vertical flow where the hydraulic potential for vertical flow in the Wilcox-Carrizo is relatively small.

The northeast orientation of the brackish plume associated with Oakwood Dome can be modeled by flow resulting from variable sand-body distribution and interconnection. The relatively muddy Wilcox strata surrounding Oakwood Dome provide a partial barrier, in addition to the salt-dome cap rock, that helps to isolate the dome from the high-permeability, channel-fill sand bodies.

Fogg and others (1982b); Fogg and Kreitler (1982); Fogg and Kreitler (1981); Fogg (1981a)



Figure 59. Northwest view of upper surface (top of Wilcox-Carrizo aquifer) of finite-difference model of ground-water flow, Oakwood Dome area (after Fogg, 1981a).

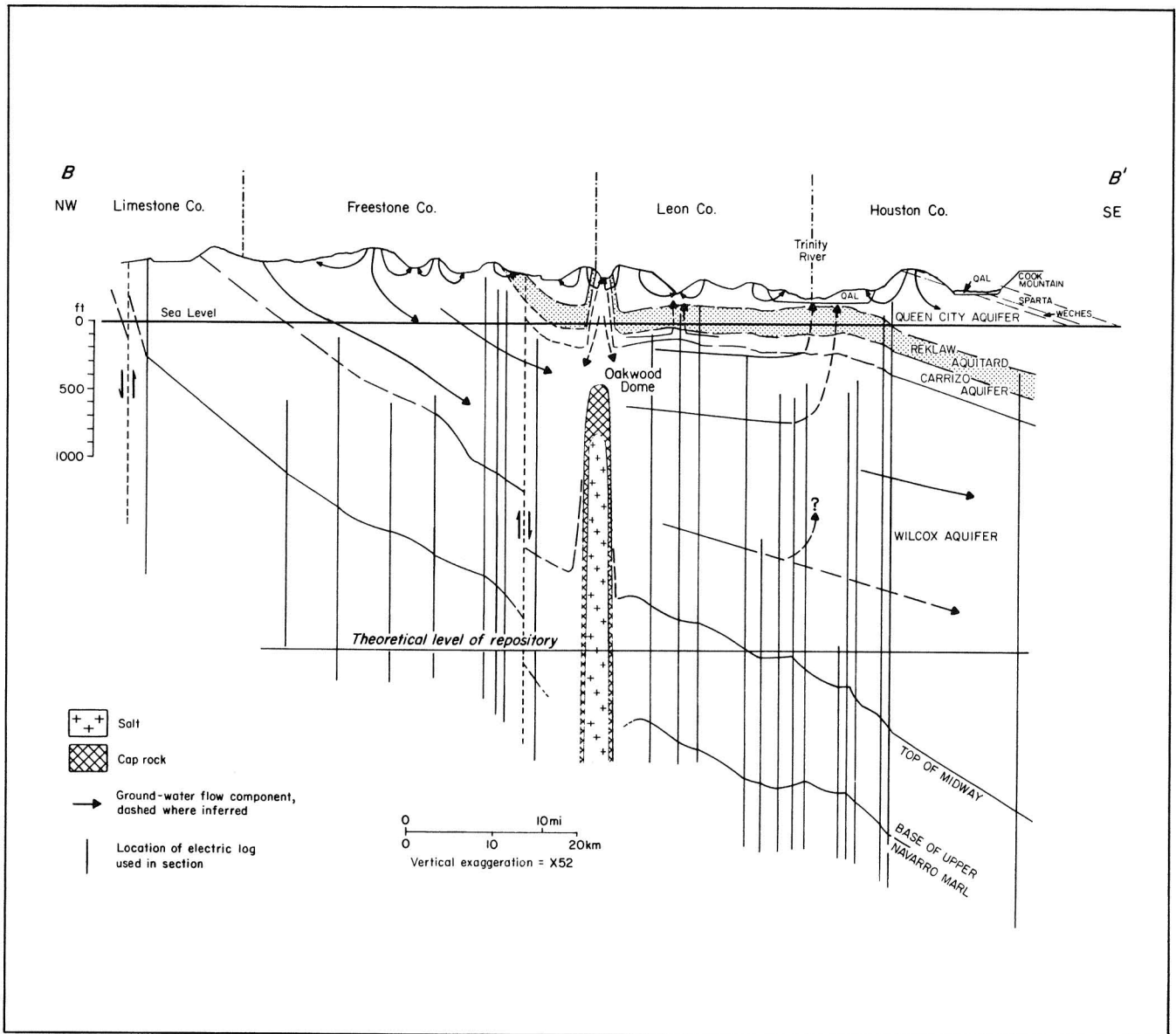


Figure 60. Cross section showing regional ground-water flow lines in Wilcox-Carrizo aquifer near Oakwood Dome (from Fogg, 1981a).



## Ground-water Modeling: Flow Rates and Travel Times

*Computed flow rates are 11 m/10<sup>4</sup> yr (36 ft/10<sup>4</sup> yr) in the fine-grained Wilcox facies enclosing the dome and 1,113 m/10<sup>4</sup> yr (3,652 ft/10<sup>4</sup> yr) in the sandy facies near the dome.*

Model hydraulic-head contours and velocity vectors demonstrate that local fluxes can differ significantly from regional hydraulic gradients. Ground-water flow rates computed from the model are 11 m/10<sup>4</sup> yr (36 ft/10<sup>4</sup> yr) in the fine-grained Wilcox facies around the dome and 1,113 m/10<sup>4</sup> yr (3,652 ft/10<sup>4</sup> yr) in the high-percentage sand facies near Oakwood Dome (fig. 61). These flow rates may decrease by as much as two orders of magnitude from top to bottom of the Wilcox-Carrizo aquifer system. Thus the model predicts a residence time of 10<sup>5</sup> to 10<sup>6</sup> yr in the fine-grained facies and 10<sup>3</sup> to 10<sup>4</sup> yr in the high-percentage sand facies.

Because Oakwood Dome is almost surrounded by interchannel facies as a result of syndepositional dome growth, the dome may be virtually isolated from circulating Wilcox ground water. A possible exception is where channel-fill sandy facies abut against the northeast flank, coinciding with a brackish plume that apparently results from dissolution of salt or cap rock ("Subsurface Salinity Near Salt Domes," p. 71).

Recharge over Oakwood Dome is probably minute and affects only shallow ground-water conditions directly over the dome. Almost all the recharge water is discharged in the outcrop area. Ground-water flow rates in the artesian section are consequently sluggish compared with those in the outcrop section.

Fogg and others (1982b); Fogg and Kreitler (1982); Fogg and Kreitler (1981); Fogg (1981a)



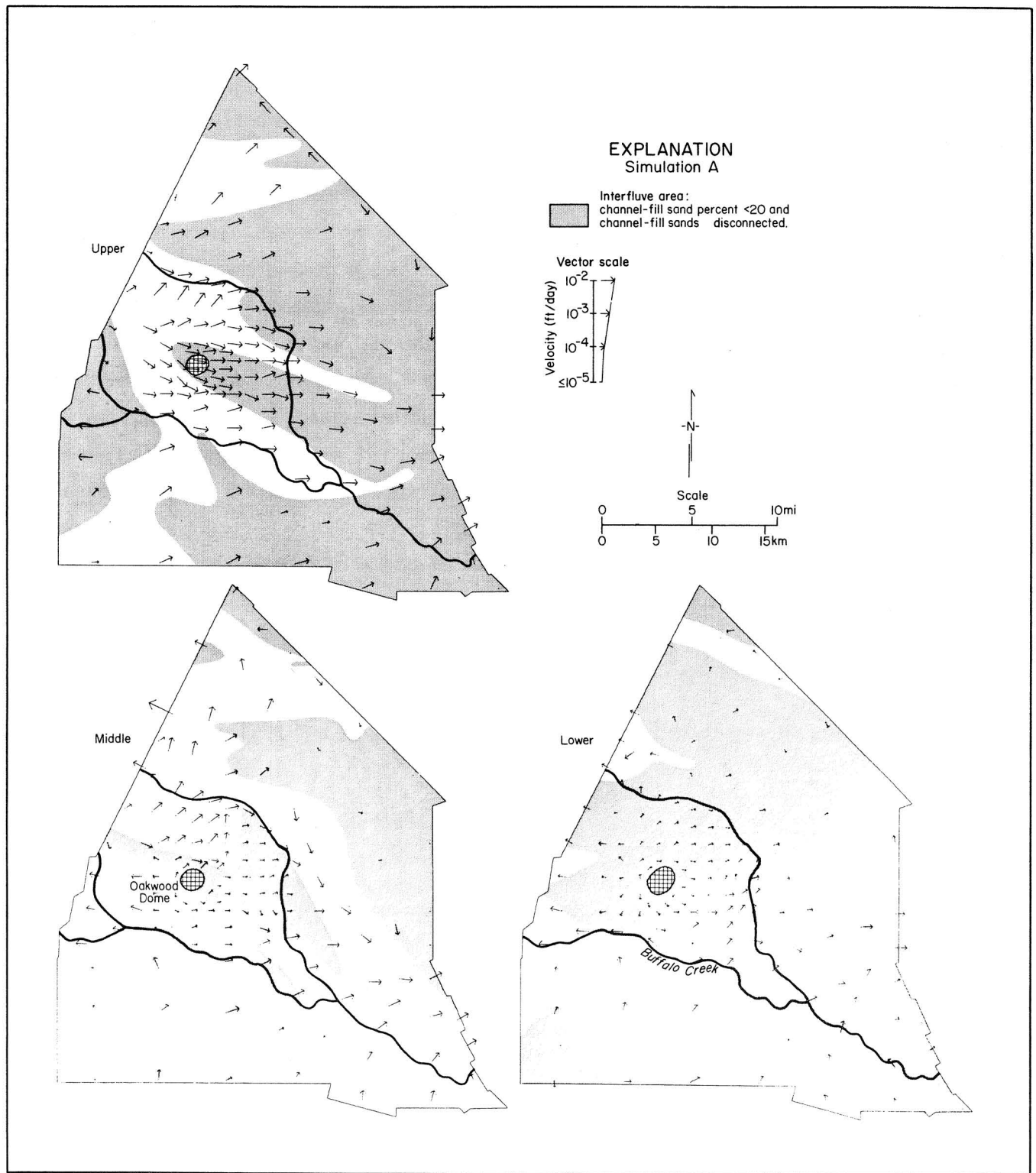


Figure 61. Maps of ground-water velocity vectors computed in model simulation A (from Fogg and others, 1982b).

## ACKNOWLEDGMENTS

We thank all those whose writings we have borrowed freely to produce this summary report. This report was reviewed by G. E. Fogg, C. W. Kreitler, M. Fracasso, W. W. Simpkins, S. D. Hovorka, L. F. Brown, Jr., and A. E. Saucier of the Bureau of Economic Geology and by staff of the U.S. Department of Energy's National Waste Terminal Storage program office. We are particularly grateful to G. E. Fogg and C. W. Kreitler for their constructive suggestions on hydrogeologic aspects of this report.

In addition to M.P.A. Jackson and S. J. Seni, the following geologists coauthored reports summarized in this paper (see bibliography for details): O. K. Agagu, J. M. Basciano, B. Bracken, E. W. Collins, R. D. Conti, E. D. Davidson, Jr., O. R. Dix, G. A. Donaldson, S. P. Dutton, G. E. Fogg, A. B. Giles, E. H. Guevara, D. W. Harris, D. K. Hobday, C. W. Kreitler, C. M. Lopez, M. K. McGowen, W. R. Muehlberger, D. Pass, W. D. Pennington, B. Wilson, D. H. Wood, and H. V. Wuerch. Research assistants who compiled and processed data include F. Boyd, E. Bramson, R. Burks, S. Carlson, C. Chomicky, R. Cobb, S. Cumella, D. Dann, R. Debus, E. Duncan, S. Ghazi, S. Hovorka, J. Hultman, J. Karabaic, D. Legett, E. Lindgren, S. Lovell, J. Lundelius, D. Magouirk, S. Mann, J. McIntyre, G. Meyer, D. Miser, J. O'Neal, L. Orr, E. Pisasale, K. Pollman, D. Prouty, K. Rader, B. Richter, V. Riggert, J. Rogers, L. Ruiz, R. Senger, R. Sherrill, T. Simmons, J. Smith, J. Sugmann, P. Talamas, D. Wiggins, D. Worrell, and D. Young. The project was directed by C. W. Kreitler (1978-1982) and M.P.A. Jackson (1983).

The manuscript was typed by Virginia Zeikus and Jean Wilke. Dorothy C. Johnson word processed the typescript under Lucille Harrell's supervision. Figures were drafted by R. L. Dillon, J. T. Ames, M. T. Bentley, T. M. Byrd, M. R. Day, M. L. Evans, B. M. Hartmann, J. S. Haynes, J. S. Horowitz, J. A. McClelland, R. M. Platt, and D. M. Ridner, under the supervision of Dan Scranton and James Macon. James A. Morgan photographed the text illustrations, and Margaret L. Evans designed this publication. Editing was by R. Marie Jones-Littleton.

This work was supported by the U.S. Department of Energy, under Contract Number DE-AC97-80ET46617 (formerly DE-AC97-79ET44605, formerly EW-78-S-05-5681).

## REFERENCES\*

- Agagu, O. K., Guevara, E. H., and Wood, D. H., 1980a, Stratigraphic framework and depositional sequences of the East Texas Basin, in Kreitler, C. W., and others, Geology and geohydrology of the East Texas Basin, a report on the progress of nuclear waste isolation feasibility studies (1979): The University of Texas at Austin, Bureau of Economic Geology Geological Circular 80-12, p. 4-10.
- Agagu, O. K., McGowen, M. K., Wood, D. H., Basciano, J. M., and Harris, D. W., 1980b, Regional tectonic framework of the East Texas Basin, in Kreitler, C. W., and others, Geology and geohydrology of the East Texas Basin, a report on the progress of nuclear waste isolation feasibility studies (1979): The University of Texas at Austin, Bureau of Economic Geology Geological Circular 80-12, p. 11-19.
- Bailey, T. L., Evans, F. G., and Adkins, W. S., 1945, Revision of stratigraphy of part of Cretaceous in Tyler Basin, northeast Texas: American Association of Petroleum Geologists Bulletin, v. 29, no. 2, p. 170-186.
- Barnes, V. E., 1965, Tyler sheet: University of Texas, Austin, Bureau of Economic Geology, Geologic Atlas of Texas, scale 1:250,000.
- \_\_\_\_\_ 1966, Texarkana sheet: University of Texas, Austin, Bureau of Economic Geology, Geologic Atlas of Texas, scale 1:250,000.
- \_\_\_\_\_ 1967, Sherman sheet: The University of Texas at Austin, Bureau of Economic Geology, Geologic Atlas of Texas, scale 1:250,000.
- \_\_\_\_\_ 1970, Waco sheet: The University of Texas at Austin, Bureau of Economic Geology, Geologic Atlas of Texas, scale 1:250,000.
- \_\_\_\_\_ 1972, Dallas sheet: The University of Texas at Austin, Bureau of Economic Geology, Geologic Atlas of Texas, scale 1:250,000.
- Barrow, T. D., 1953, Mesozoic stratigraphy and structural history of the East Texas Basin: Stanford University, Ph.D. dissertation, 222 p.
- Bushaw, D. J., 1968, Environmental synthesis of the East Texas Lower Cretaceous: Gulf Coast Association of Geological Societies Transactions, v. 18, p. 416-438.
- Caughey, C. A., 1977, Depositional systems in the Paluxy Formation (Lower Cretaceous), northeast Texas--oil, gas, and ground-water resources: The University of Texas at Austin, Bureau of Economic Geology Geological Circular 77-8, 59 p.
- Cloos, E., 1928, Über antithetische Bewegungen: Geologische Rundschau, v. 19, p. 246-251.
- Collins, E. W., 1980, The Reklaw Formation of East Texas, in Middle Eocene coastal plain and nearshore deposits of East Texas: a field guide to the Queen City Formation and related papers: Society of Economic Paleontologists and Mineralogists, Gulf Coast Section, Guidebook, p. 67-70.
- \_\_\_\_\_ 1981a, Morphologic mapping of Oakwood, Palestine, and Keechi salt domes, East Texas, in Kreitler, C. W., and others, Geology and geohydrology of the East Texas Basin, a report on the progress of nuclear waste isolation feasibility studies (1980): The University of Texas at Austin, Bureau of Economic Geology Geological Circular 81-7, p. 102-112.
- \_\_\_\_\_ 1981b, Trinity River terraces near Palestine salt dome, East Texas, in Kreitler, C. W., and others, Geology and geohydrology of the East Texas Basin, a report on the progress of nuclear waste isolation feasibility studies (1980): The University of Texas at Austin, Bureau of Economic Geology Geological Circular 81-7, p. 78-82.

\*Includes uncited reports generated by the East Texas Waste Isolation program.

- \_\_\_\_\_ 1981c, Denudation rates in East Texas, *in* Kreitler, C. W., and others, Geology and geohydrology of the East Texas Basin, a report on the progress of nuclear waste isolation feasibility studies (1980): The University of Texas at Austin, Bureau of Economic Geology Geological Circular 81-7, p. 88-92.
- \_\_\_\_\_ 1982, Surface evidence of tectonic activity and erosion rates, Palestine, Keechi, and Oakwood salt domes, East Texas: The University of Texas at Austin, Bureau of Economic Geology Geological Circular 82-3, 39 p.
- Collins, E. W., Dix, O. R., and Hobday, D. K., 1981, Oakwood salt dome, East Texas: Surface geology and drainage analysis: The University of Texas at Austin, Bureau of Economic Geology Geological Circular 81-6, 23 p.
- Collins, E. W., and Hobday, D. K., 1980, Surface geology and shallow borehole investigations of Oakwood Dome--preliminary studies, *in* Kreitler, C. W., and others, Geology and geohydrology of the East Texas Basin, a report on the progress of nuclear waste isolation feasibility studies (1979): The University of Texas at Austin, Bureau of Economic Geology Geological Circular 80-12, p. 88-92.
- Collins, E. W., Hobday, D. K., and Kreitler, C. W., 1980, Quaternary faulting in East Texas: The University of Texas at Austin, Bureau of Economic Geology Geological Circular 80-1, 20 p.
- Collins, S. E., 1980, Jurassic Cotton Valley and Smackover reservoir trends, East Texas, north Louisiana and south Arkansas: American Association of Petroleum Geologists Bulletin, v. 64, no. 7, p. 1004-1013.
- Dix, O. R., 1980, Analysis of selected stream drainage systems in the East Texas Basin, *in* Kreitler, C. W., and others, Geology and geohydrology of the East Texas Basin, a report on the progress of nuclear waste isolation feasibility studies (1979): The University of Texas at Austin, Bureau of Economic Geology Geological Circular 80-12, p. 93-100.
- Dix, O. R., and Jackson, M.P.A., 1981a, Lithology of the Oakwood salt core, *in* Kreitler, C. W., and others, Geology and geohydrology of the East Texas Basin, a report on the progress of nuclear waste isolation feasibility studies (1980): The University of Texas at Austin, Bureau of Economic Geology Geological Circular 81-7, p. 172-178.
- \_\_\_\_\_ 1981b, Statistical analysis of lineaments and their relation to fracturing, faulting, and halokinesis in the East Texas Basin: The University of Texas at Austin, Bureau of Economic Geology Report of Investigations No. 110, 30 p.
- \_\_\_\_\_ 1981c, Statistical analysis of lineaments on aerial photographs and Landsat imagery of the East Texas Basin and their relation to regional structure, *in* Kreitler, C. W., and others, Geology and geohydrology of the East Texas Basin, a report on the progress of nuclear waste isolation feasibility studies (1981): The University of Texas at Austin, Bureau of Economic Geology, report prepared for the U.S. Department of Energy under Contract No. DE-AC97-80ET46617, p. 83-87.
- \_\_\_\_\_ 1982, Lithology, microstructures, fluid inclusions, and geochemistry of rock salt and of the cap-rock contact in Oakwood Dome, East Texas: significance for nuclear waste storage: The University of Texas at Austin, Bureau of Economic Geology Report of Investigations No. 120, 59 p.
- Dutton, S. P., and Kreitler, C. W., 1980, Caprock formation and diagenesis, Gyp Hill salt dome, South Texas: Gulf Coast Association of Geological Societies Transactions, v. 30, p. 333-339.
- \_\_\_\_\_ 1981, Cap-rock studies of Oakwood Dome, *in* Kreitler, C. W., and others, Geology and geohydrology of the East Texas Basin, a report on the progress of nuclear waste isolation feasibility studies (1980): The University of Texas at Austin, Bureau of Economic Geology Geological Circular 81-7, p. 162-166.

- Dutton, S. P., Kreitler, C. W., and Bracken, B., 1982a, Cap rock, in Kreitler, C. W., and others, Geology and geohydrology of the East Texas Basin, a report on the progress of nuclear waste isolation feasibility studies (1980): The University of Texas at Austin, Bureau of Economic Geology, report prepared for the U.S. Department of Energy under Contract No. DE-AC97-80ET46617, p. 35-40.
- \_\_\_\_\_ 1982b, Formation and diagenesis of salt-dome cap rock, Texas Gulf Coast: Society of Economic Paleontologists and Mineralogists Core Workshop No. 3, p. 100-129.
- Eaton, R. W., 1956, Resumé of subsurface geology of northeast Texas with emphasis on salt structures: Gulf Coast Association of Geological Societies Transactions, v. 6, p. 79-84.
- \_\_\_\_\_ 1961, Developments and future possibilities of the Jurassic in northeast Texas: East Texas Geological Society, 15 p.
- Eaton, R. W., and Reynolds, E. J., 1951, Notes on Washita-Fredericksburg contact in the East Texas Basin: Gulf Coast Association of Geological Societies Transactions, v. 1, p. 213-238.
- Ellisor, A. C., and Teagle, J., 1934, Correlation of Pecan Gap Chalk in Texas: American Association of Petroleum Geologists Bulletin, v. 18, no. 11, p. 1506-1536.
- Finley, R. J., Wermund, E. G., and Ledbetter, J. O., 1981, The feasibility of locating a Texas salt test facility: The University of Texas at Austin, Bureau of Economic Geology, U.S. Department of Energy Milestone Report, 171 p.
- Fisher, W. L., and McGowen, J. H., 1967, Depositional systems in the Wilcox Group of Texas and their relationship to occurrence of oil and gas: The University of Texas at Austin, Bureau of Economic Geology Geological Circular 67-4, p. 105-125.
- Fogg, G. E., 1980a, Regional aquifer hydraulics, East Texas Basin, in Kreitler, C. W., and others, Geology and geohydrology of the East Texas Basin, a report on the progress of nuclear waste isolation feasibility studies (1979): The University of Texas at Austin, Bureau of Economic Geology Geological Circular 80-12, p. 55-67.
- \_\_\_\_\_ 1980b, Salinity of formation waters, in Kreitler, C. W., and others, Geology and geohydrology of the East Texas Basin, a report on the progress of nuclear waste isolation feasibility studies (1979): The University of Texas at Austin, Bureau of Economic Geology Geological Circular 80-12, p. 68-72.
- \_\_\_\_\_ 1981a, Aquifer modeling of the Oakwood salt dome area, in Kreitler, C. W., and others, Geology and geohydrology of the East Texas Basin, a report on the progress of nuclear waste isolation feasibility studies (1980): The University of Texas at Austin, Bureau of Economic Geology Geological Circular 81-7, p. 139-149.
- \_\_\_\_\_ 1981b, Aquifer testing and monitoring around Oakwood salt dome, East Texas, in Kreitler, C. W., and others, Geology and geohydrology of the East Texas Basin, a report on the progress of nuclear waste isolation feasibility studies (1980): The University of Texas at Austin, Bureau of Economic Geology Geological Circular 81-7, p. 126-135.
- \_\_\_\_\_ 1981c, Fluid-pressure versus depth relationships in the Wilcox-Carrizo aquifer system, East Texas, in Kreitler, C. W., and others, Geology and geohydrology of the East Texas Basin, a report on the progress of nuclear waste isolation feasibility studies (1980): The University of Texas at Austin, Bureau of Economic Geology Geological Circular 81-7, p. 115-122.
- Fogg, G. E., and Kreitler, C. W., 1980, Impacts of salt-brining on Palestine salt dome, in Kreitler, C. W., and others, Geology and geohydrology of the East Texas Basin, a report on the progress of nuclear waste isolation feasibility studies (1979): The University of Texas at Austin, Bureau of Economic Geology Geological Circular 80-12, p. 46-54.

- \_\_\_\_\_ 1981, Ground-water hydrology around salt domes in the East Texas Basin: a practical approach to the contaminant transport problem: Bulletin of the Association of Engineering Geologists, v. 18, no. 4, p. 387-411.
- \_\_\_\_\_ 1982, Ground-water hydraulics and hydrochemical facies of Eocene aquifers in the East Texas Basin: The University of Texas, Bureau of Economic Geology Report of Investigations No. 127, 75 p.
- Fogg, G. E., Kreitler, C. W., and Dutton, S. P., 1980, Hydrologic stability of Oakwood Dome, in Kreitler, C. W., and others, Geology and geohydrology of the East Texas Basin, a report on the progress of nuclear waste isolation feasibility studies (1979): The University of Texas at Austin, Bureau of Economic Geology Geological Circular 80-12, p. 30-32.
- Fogg, G. E., Kreitler, C. W., and Wuerch, H. V., 1982a, Meteoric hydrology, in Kreitler, C. W., and others, Geology and geohydrology of the East Texas Basin, a report on the progress of nuclear waste isolation feasibility studies (1981): The University of Texas at Austin, Bureau of Economic Geology, report prepared for the U.S. Department of Energy under Contract No. DE-AC97-80ET46617, p. 12-27.
- Fogg, G. E., Seni, S. J., and Dutton, S. P., 1981, Core analysis of hydrologic parameters, Eocene Wilcox aquifer, East Texas, in Kreitler, C. W., and others, Geology and geohydrology of the East Texas Basin, a report on the progress of nuclear waste isolation feasibility studies (1980): The University of Texas at Austin, Bureau of Economic Geology Geological Circular 81-7, p. 136-138.
- Fogg, G. E., Seni, S. J., and Kreitler, C. W., 1982b, Three-dimensional modeling of ground-water flow through depositional systems in the Oakwood salt dome vicinity, East Texas: The University of Texas at Austin, Bureau of Economic Geology, report prepared for the U.S. Department of Energy under Contract No. DE-AC97-80ET46617, 56 p.
- Forgotson, J. M., Jr., 1954a, Regional stratigraphic analysis of Cotton Valley Group of the upper Gulf Coastal Plain: American Association of Petroleum Geologists Bulletin, v. 38, no. 12, p. 2476-2499.
- \_\_\_\_\_ 1954b, Regional stratigraphic analysis of the Cotton Valley Group of the upper Gulf Coastal Plain: Gulf Coast Association of Geological Societies Transactions, v. 4, p. 143-154.
- \_\_\_\_\_ 1956, A correlation and regional stratigraphic analysis of the formations of the Trinity Group of the Comanchean Cretaceous of the Gulf Coastal Plain; and the genesis and petrography of the Ferry Lake Anhydrite: Gulf Coast Association of Geological Societies Transactions, v. 6, p. 91-108.
- \_\_\_\_\_ 1957, Stratigraphy of Comanchean Cretaceous Trinity Group: American Association of Petroleum Geologists Bulletin, v. 41, no. 10, p. 2328-2363.
- \_\_\_\_\_ 1958, The basal sediments of the Austin Group and the stratigraphic position of the Tuscaloosa Formation of central Louisiana: Gulf Coast Association of Geological Societies Transactions, v. 8, p. 117-125.
- Forgotson, J. M., Sr., and Forgotson, J. M., Jr., 1976, Definition of Gilmer Limestone, Upper Jurassic formation, northeastern Texas: American Association of Petroleum Geologists Bulletin, v. 60, no. 7, p. 1119-1123.
- Giles, A. B., 1980, Evaluation of East Texas salt domes, in Kreitler, C. W., and others, Geology and geohydrology of the East Texas Basin, a report on the progress of nuclear waste isolation feasibility studies (1979): The University of Texas at Austin, Bureau of Economic Geology Geological Circular 80-12, p. 20-29.
- \_\_\_\_\_ 1981, Growth history of Oakwood salt dome, East Texas, in Kreitler, C. W., and others, Geology and geohydrology of the East Texas Basin, a report on the progress of nuclear waste isolation feasibility studies (1980): The University of Texas at Austin, Bureau of Economic Geology Geological Circular 81-7, p. 39-42.

- Giles, A. B., and Wood, D. H., 1983, Oakwood salt dome, East Texas: geologic framework, growth history, and hydrocarbon production: The University of Texas at Austin, Bureau of Economic Geology Geological Circular 83-1, 55 p.
- Granata, W. H., Jr., 1963, Cretaceous stratigraphy and structural development of the Sabine Uplift area, Texas and Louisiana, in Report on selected north Louisiana and south Arkansas oil and gas fields and regional geology: Shreveport Geological Society, Reference Volume V, p. 50-95.
- Guevara, E. H., and Garcia, R., 1972, Depositional systems and oil-gas reservoirs in the Queen City Formation (Eocene), Texas: The University of Texas at Austin, Bureau of Economic Geology Geological Circular 72-4, 22 p.
- Guevara, E. H., and Giles, A. B., 1979, Upper Cretaceous - Lower Eocene strata, Hainesville, Keechi, and Oakwood salt domes, East Texas: Gulf Coast Association of Geological Societies Transactions, v. 29, p. 112-120.
- Hobday, D. K., 1980, Geology of the Queen City Formation and associated units, in Middle Eocene coastal plain and nearshore deposits of East Texas, a field guide to the Queen City Formation and related papers: Society of Economic Paleontologists and Mineralogists, Gulf Coast Section, Guidebook, p. 1-45.
- Hobday, D. K., Morton, R. A., and Collins, E. W., 1979, The Queen City Formation in the East Texas Embayment: a depositional record of riverine, tide, and wave interaction: Gulf Coast Association of Geological Societies Transactions, v. 29, p. 136-146. Reprinted in 1980 as The University of Texas at Austin, Bureau of Economic Geology Geological Circular 80-4, 11 p.
- Hobday, D. K., and Perkins, B. F., 1980, Sedimentary facies and trace fossils of a large aggrading delta margin embayment: upper Woodbine Formation of northeast Texas: Gulf Coast Association of Geological Societies Transactions, v. 30, p. 131-142.
- Imlay, R. W., 1943, Jurassic formations of Gulf region: American Association of Petroleum Geologists Bulletin, v. 27, no. 11, p. 1407-1533.
- Jackson, M.P.A., 1981a, Strain analysis of halite in the Oakwood core, in Kreitler, C. W., and others, Geology and geohydrology of the East Texas Basin, a report on the progress of nuclear waste isolation feasibility studies (1980): The University of Texas at Austin, Bureau of Economic Geology Geological Circular 81-7, p. 183-187.
- \_\_\_\_\_ 1981b, Tectonic environment during early infilling of the East Texas Basin, in Kreitler, C. W., and others, Geology and geohydrology of the East Texas Basin, a report on the progress of nuclear waste isolation feasibility studies (1980): The University of Texas at Austin, Bureau of Economic Geology Geological Circular 81-7, p. 7-11.
- \_\_\_\_\_ 1982, Fault tectonics of the East Texas Basin: The University of Texas at Austin, Bureau of Economic Geology Geological Circular 82-4, 31 p.
- \_\_\_\_\_ 1983, Natural strain in glacial and diapiric rock salt, with emphasis on Oakwood Dome, East Texas: The University of Texas at Austin, Bureau of Economic Geology, report prepared for the U.S. Department of Energy under Contract No. DE-AC97-80ET46617, 121 p.
- Jackson, M.P.A., and Dix, O. R., 1981, Geometric analysis of macroscopic structures in Oakwood salt core, in Kreitler, C. W., and others, Geology and geohydrology of the East Texas Basin, a report on the progress of nuclear waste isolation feasibility studies (1980): The University of Texas at Austin, Bureau of Economic Geology Geological Circular 81-7, p. 177-182.
- Jackson, M.P.A., and Harris, D. W., 1981, Seismic stratigraphy and salt mobilization along the northwestern margin of the East Texas Basin, in Kreitler, C. W., and others, Geology and geohydrology of the East Texas Basin, a report on the progress of nuclear waste isolation

- feasibility studies (1980): The University of Texas at Austin, Bureau of Economic Geology Geological Circular 81-7, p. 28-32.
- Jackson, M.P.A., and Seni, S. J., 1983, Geometry and evolution of salt structures in a marginal rift basin of the Gulf of Mexico, East Texas: *Geology*, v. 11, no. 3, p. 131-135.
- \_\_\_\_\_ in press, Atlas of salt domes in the East Texas Basin: The University of Texas at Austin, Bureau of Economic Geology.
- Jackson, M.P.A., Wilson, B., and Pennington, W. D., 1982, Basin tectonics, in Kreitler, C. W., and others, *Geology and geohydrology of the East Texas Basin, a report on the progress of nuclear waste isolation feasibility studies (1981)*: The University of Texas at Austin, Bureau of Economic Geology, report prepared for the U.S. Department of Energy under Contract No. DE-AC97-80ET46617, p. 54-59.
- Jaritz, W., 1980, Einige Aspekte der Entwicklungsgeschichte der nordwestdeutschen Salzstocke: *Zeitschrift Deutsch Geologische Gesellschaft*, v. 131, p. 387-408.
- Jones, W. V., 1945, Bacon Limestone, East Texas: *American Association of Petroleum Geologists Bulletin*, v. 29, no. 6, p. 839-845.
- Kaiser, W. R., 1978, Depositional systems in the Wilcox Group (Eocene) of east-central Texas and the occurrence of lignite, in Kaiser, W. R., ed., *Proceedings, Gulf Coast Lignite Conference: geology, utilization, and environmental aspects*: The University of Texas at Austin, Bureau of Economic Geology Report of Investigations No. 90, p. 33-53.
- Keys, W. C., and MacCary, L. M., 1971, Application of borehole geophysics to water-resource investigations, in *Techniques of water-resources investigations*, chapter E1, book 2: Washington, D. C., U.S. Government Printing Office, 124 p.
- Kreitler, C. W., 1979, Evaluating the potential of East Texas salt domes for isolation of nuclear waste: The University of Texas at Austin, Bureau of Economic Geology, report prepared for the U.S. Department of Energy under Contract No. EW-78-S-05-5681, 29 p.
- \_\_\_\_\_ 1980, Studies of the suitability of salt domes in East Texas Basin for geologic isolation of nuclear wastes: The University of Texas at Austin, Bureau of Economic Geology Geological Circular 80-5, 7 p.
- Kreitler, C. W., Agagu, O. K., Basciano, J. M., Collins, E. W., Dix, O., Dutton, S. P., Fogg, G. E., Giles, A. B., Guevara, E. H., Harris, D. W., Hobday, D. K., McGowen, M. K., Pass, D., and Wood, D. H., 1980, *Geology and geohydrology of the East Texas Basin, a report on the progress of nuclear waste isolation feasibility studies (1979)*: The University of Texas at Austin, Bureau of Economic Geology Geological Circular 80-12, 112 p.
- Kreitler, C. W., Bracken, B., Collins, E. W., Conti, R., Dutton, S. P., Fogg, G. E., Jackson, M.P.A., McGowen, M. K., Pennington, W. C., Seni, S. J., Wilson, B., Wood, D. H., and Wuerch, H. V., 1982a, *Geology and geohydrology of the East Texas Basin, a report on the progress of nuclear waste isolation feasibility studies (1981)*: The University of Texas at Austin, Bureau of Economic Geology, report prepared for the U.S. Department of Energy under Contract No. DE-AC97-80ET46617, 62 p.
- Kreitler, C. W., Collins, E. W., Davidson, E. D., Jr., Dix, O. R., Donaldson, G. W., Dutton, S. P., Fogg, G. E., Giles, A. B., Harris, D. W., Jackson, M.P.A., Lopez, C. M., McGowen, M. K., Muehlberger, W. R., Pennington, W. D., Seni, S. J., Wood, D. H., and Wuerch, H. V., 1981a, *Geology and geohydrology of the East Texas Basin, a report on the progress of nuclear waste isolation feasibility studies (1980)*: The University of Texas at Austin, Bureau of Economic Geology Geological Circular 81-7, 207 p.
- Kreitler, C. W., Collins, E. W., Fogg, G. E., Jackson, M.P.A., and Seni, S. J., 1983, Hydrogeologic characterization of the saline aquifers, East Texas Basin, implications to nuclear waste storage in East Texas salt domes: The University of Texas at Austin, Bureau of Economic Geology, report prepared for the U. S. Department of Energy under Contract No. DE-AC97-80ET46617, 55 p.



- Kreitler, C. W., and Dutton, S. P., 1983, Origin and diagenesis of cap rock, Gyp Hill and Oakwood salt domes, Texas: The University of Texas at Austin, Bureau of Economic Geology Report of Investigations No. 131, 58 p.
- Kreitler, C. W., Dutton, S. P., and Fogg, G. E., 1981b, Geochemistry of ground water and cap rock from Gyp Hill salt dome, South Texas, in Kreitler, C. W., and others, Geology and geohydrology of the East Texas Basin, a report on the progress of nuclear waste isolation feasibility studies (1980): The University of Texas at Austin, Bureau of Economic Geology Geological Circular 81-7, p. 167-171.
- Kreitler, C. W., and Fogg, G. E., 1980, Geochemistry of ground water in the Wilcox aquifer, in Kreitler, C. W., and others, Geology and geohydrology of the East Texas Basin, a report on the progress of nuclear waste isolation feasibility studies (1979): The University of Texas at Austin, Bureau of Economic Geology Geological Circular 80-12, p. 73-78.
- Kreitler, C. W., Fogg, G. E., and Collins, E. W., 1982b, Deep-basin hydrology, in Kreitler, C. W., and others, Geology and geohydrology of the East Texas Basin, a report on the progress of nuclear waste isolation feasibility studies (1981): The University of Texas at Austin, Bureau of Economic Geology, report prepared for the U.S. Department of Energy under Contract No. DE-AC97-80ET46617, p. 28-34.
- Kreitler, C. W., and Wuerch, H. V., 1981, Carbon-14 dating of ground water near Oakwood Dome, East Texas, in Kreitler, C. W., and others, Geology and geohydrology of the East Texas Basin, a report on the progress of nuclear waste isolation feasibility studies (1980): The University of Texas at Austin, Bureau of Economic Geology Geological Circular 81-7, p. 156-161.
- Kumar, M. B., 1977, Growth rates of salt domes of the North Louisiana Salt Basin, in Martinez, J. D., and others, An investigation of the utility of Gulf Coast salt domes for the storage or disposal of radioactive wastes: Institute for Environmental Studies, Louisiana State University, Baton Rouge, Louisiana, p. 225-229.
- Loocke, J. E., 1978, Growth history of the Hainesville salt dome, Wood County, Texas: The University of Texas at Austin, Master's thesis, 95 p.
- Martin, R. G., 1978, Northern and eastern Gulf of Mexico continental margin stratigraphic and structural framework, in Bouma, A. H., and others, Framework, facies, and oil-trapping characteristics of the upper continental margin: American Association of Petroleum Geologists Studies in Geology No. 7, p. 21-42.
- McGowen, M. K., and Lopez, C. M., 1983, Depositional systems in the Nacatoch Formation (Upper Cretaceous), East Texas and southwest Arkansas: The University of Texas at Austin, Bureau of Economic Geology Report of Investigations No. 137, 59 p.
- McGowen, M. K., and Harris, D. W., 1981, Preliminary study of the Upper Jurassic (Cotton Valley) and Lower Cretaceous (Hosston/Travis Peak) Formations of the East Texas Basin, in Kreitler, C. W., and others, Geology and geohydrology of the East Texas Basin, a report on the progress of nuclear waste isolation feasibility studies (1980): The University of Texas at Austin, Bureau of Economic Geology Geological Circular 81-7, p. 43-47.
- \_\_\_\_\_ in press, Cotton Valley (Upper Jurassic) and Hosston (Lower Cretaceous) depositional systems and their influence on salt tectonics in the East Texas Basin: The University of Texas at Austin, Bureau of Economic Geology Geological Circular.
- Mosteller, M. A., 1970, Subsurface stratigraphy of the Comanchean Series in east-central Texas: Baylor Geological Studies Bulletin 19, 34 p.
- Netherland, Sewell and Associates, 1976, Geological study of the interior salt domes of northeast Texas salt dome basin to investigate their suitability for possible storage of radioactive waste material as of May 1976: Report prepared for the Office of Waste Isolation, Energy Research and Development Administration, Union Carbide Corp., Nuclear Division, 57 p.

- Nichols, P. H., 1964, The remaining frontiers for exploration in northeast Texas: Gulf Coast Association of Geological Societies Transactions, v. 14, p. 7-22.
- Nichols, P. H., Peterson, G. E., and Wuestner, C. E., 1968, Summary of subsurface geology of northeast Texas, *in* Beebe, W. B., and Curtis, B. F., eds., Natural gases of North America--Part 2, natural gases in rocks of Mesozoic age: American Association of Petroleum Geologists Memoir 9, v. 1, p. 982-1004.
- Office of Nuclear Waste Isolation, 1981, Evaluation of area studies of the U.S. Gulf Coast salt dome basins: Battelle Memorial Institute Technical Report ONWI-109, 168 p.
- Oliver, W. B., 1971, Depositional systems in the Woodbine Formation (Upper Cretaceous), northeast Texas: The University of Texas at Austin, Bureau of Economic Geology Report of Investigations No. 73, 26 p.
- Pennington, W. D., and Carlson, S. M., 1983, Summary of observations from the East Texas seismic network: The University of Texas at Austin, Bureau of Economic Geology, report prepared for the U.S. Department of Energy under Contract No. DE-AC97-80ET46617, 62 p.
- Scott, R. W., Fee, D., Magee, R., and Laali, Hooman, 1978, Epeiric depositional models for the Lower Cretaceous Washita Group, North-Central Texas: The University of Texas at Austin, Bureau of Economic Geology Report of Investigations No. 94, 23 p.
- Sellards, E. H., Adkins, W. S., and Plummer, F. B., 1932, The geology of Texas, Volume I, stratigraphy: University of Texas, Austin, Bureau of Economic Geology Bulletin 3232, 1007 p.
- Seni, S. J., 1981, The effect of salt tectonics on deposition of the Lower Cretaceous Paluxy Formation, East Texas, *in* Kreitler, C. W., and others, Geology and geohydrology of the East Texas Basin, a report on the progress of nuclear waste isolation feasibility studies (1980): The University of Texas at Austin, Bureau of Economic Geology Geological Circular 81-7, p. 53-59.
- Seni, S. J., and Fogg, G. E., 1982, Wilcox Group facies and syndepositional dome growth, southern East Texas Basin: The University of Texas at Austin, Bureau of Economic Geology, report prepared for the U.S. Department of Energy under Contract No. DE-AC97-80ET46617, 33 p.
- Seni, S. J., and Jackson, M.P.A., 1983a, Evolution of salt structures, East Texas diapir province, Part I: sedimentary record of halokinesis: American Association of Petroleum Geologists Bulletin, v. 67, no. 8, p. 1219-1244.
- \_\_\_\_\_ 1983b, Evolution of salt structures, East Texas diapir province, Part II: patterns and rates of halokinesis: American Association of Petroleum Geologists Bulletin, v. 67, no. 8, p. 1245-1274.
- \_\_\_\_\_ 1984, Sedimentary record of Cretaceous and Tertiary salt movement, East Texas Basin: times, rates, and volumes of salt flow and their implications for nuclear waste isolation and petroleum exploration: The University of Texas at Austin, Bureau of Economic Geology Report of Investigations No. 139, 89 p.
- Seni, S. J., and Kreitler, C. W., 1981, Evolution of the East Texas Basin, *in* Kreitler, C. W., and others, Geology and geohydrology of the East Texas Basin, a report on the progress of nuclear waste isolation feasibility studies (1980): The University of Texas at Austin, Bureau of Economic Geology Geological Circular 81-7, p. 12-20.
- Shreve, R. L., 1967, Infinite topologically random channel networks: Journal of Geology, v. 75, p. 178-186.
- Stehli, F. G., Creath, W. B., Upshaw, C. F., and Forgotson, J. M., Jr., 1972, Depositional history of Gulfian Cretaceous of East Texas Embayment: American Association of Petroleum Geologists Bulletin, v. 56, no. 1, p. 38-67.

- Stephenson, L. W., 1937, Stratigraphic relations of the Austin, Taylor, and equivalent formations in Texas: U.S. Geological Survey Professional Paper 186-G, p. 133-146.
- Swain, F. M., 1944, Stratigraphy of Cotton Valley beds of northern Gulf Coast Plain: American Association of Petroleum Geologists Bulletin, v. 28, no. 5, p. 577-614.
- \_\_\_\_\_ 1949, Upper Jurassic of northeastern Texas: American Association of Petroleum Geologists Bulletin, v. 33, no. 7, p. 1206-1250.
- Thompson, L. B., Percival, S. F., and Patricelli, J. A., 1978, Stratigraphic relationships of the Annona Chalk and Gober Chalk (upper Campanian) type localities in northeast Texas and southwest Arkansas: Gulf Coast Association of Geological Societies Transactions, v. 28, p. 665-679.
- Todd, R. G., and Mitchum, R. M., Jr., 1977, Seismic stratigraphy and global changes of sea level, Part 8, identification of Upper Triassic, Jurassic, and Lower Cretaceous seismic sequences in Gulf of Mexico and offshore West Africa, in Payton, C. E., ed., Seismic stratigraphy--applications to hydrocarbon exploration: American Association of Petroleum Geologists Memoir 26, p. 145-164.
- Trusheim, F., 1960, Mechanism of salt migration in northern Germany: American Association of Petroleum Geologists Bulletin, v. 44, no. 9, p. 1519-1540.
- Waters, J. A., McFarland, P. W., and Lea, J. W., 1955, Geologic framework of Gulf Coastal Plain of Texas: American Association of Petroleum Geologists Bulletin, v. 39, no. 9, p. 1821-1850.
- Wood, D. H., 1981, Structural effects of salt movement in the East Texas Basin, in Kreitler, C. W., and others, Geology and geohydrology of the East Texas Basin, a report on the progress of nuclear waste isolation feasibility studies (1980): The University of Texas at Austin, Bureau of Economic Geology Geological Circular 81-7, p. 21-27.
- Wood, D. H., and Giles, A. B., 1982, Hydrocarbon accumulation patterns in the East Texas salt dome province: The University of Texas at Austin, Bureau of Economic Geology Geological Circular 82-6, 36 p.
- Wood, D. H., and Guevara, E. H., 1981, Regional structural cross sections and general stratigraphy, East Texas Basin: The University of Texas at Austin, Bureau of Economic Geology Cross Sections, 21 p.
- Woodbury, H. O., Murray, I. B., Jr., and Osborne, R. E., 1980, Diapirs and their relation to hydrocarbon accumulation, in Miall, A. D., ed., Facts and principles of world petroleum occurrence: Calgary, Canadian Society of Petroleum Geologists, p. 119-142.

## APPENDIX

### Lithologic descriptions, correlation notes, and selected references: East Texas Basin (from Wood and Guevara, 1981).

STRATIGRAPHIC UNITS		LITHOLOGY, FACIES RELATIONSHIPS,* AND STRATIGRAPHIC NOTES		SELECTED REFERENCES†	
SYSTEM	GROUP	FORMATION	*Lithic composition is from Sellards and others (1932), Bailey and others (1945), Barrow (1953), Waters and others (1955), Nichols and others (1968), and Forgotson and Forgotson (1976).  †The following references describe the entire stratigraphic column in the East Texas Basin: Sellards and others (1932), Waters and others (1955), Eaton (1956), Nichols and others (1968), Agagu and others (1980a). Other references listed below discuss the specific units and refer specifically to basin strata. See text for further references on adjacent areas.		
	SERIES				
TERTIARY	EOCENE	CLAIBORNE Shallow-marine to nonmarine clastic strata. Weches, Queen City, and Reklaw sometimes have been combined to form Mount Selman Formation. Contacts between formations are typically difficult to delineate by electric logs.	Yegua Fm.	Barnes (1965, 1966, 1967, 1970), Guevara and Garcia (1972), Hobday and others (1980).	
		Cook Mountain Fm.	Clay and shale that are brown, glauconitic, fossiliferous; contains some sandy shale, some limestone. Formerly known as "Crockett Member" of Cook Mountain Formation.		
		Sparta Fm.	Gray to buff sand with erratic sandy shale or clays; contains some glauconitic sand, limonite, and lignite. Formerly member of Cook Mountain Formation.		
		Weches Fm.	Glauconite that is sand sized, dark green to black, fossiliferous, bedded; contains significant glauconitic clay and glauconitic sand.		
		Queen City Fm.	Sand and sandy clay that are thin bedded, white and red.		
		Reklaw Fm.	Green to black, glauconitic clay; locally sandy or gypsiferous.		
		Carrizo Fm.	Medium-grained sand to sandy clay; locally ferruginous. Formerly considered part of underlying Wilcox Group.		
	WILCOX	Undifferentiated	Nonmarine clastic strata. Poorly consolidated silt to coarse-grained sandstone; interbedded with medium-brown-gray, very carbonaceous, micaceous, pyritic, soft and flaky shale; contains lignite, siderite, clay ironstone, and bentonite stringers. Wilcox locally is very calcareous. In outcrop Wilcox divides into Calvert Bluff, Simsboro, and Hooper Formations. Wilcox in outcrop was formerly called "Rockdale Formation." Some workers place Wilcox entirely within the Eocene; others (including this paper) contend that it includes upper Paleocene strata.	Barnes (1965, 1966, 1967, 1970, 1972), Fisher and McGowen (1967), Kaiser (1978).	
	PALEOCENE	MIDWAY	Undifferentiated	Marine shale that is medium gray to brown gray, micaceous, calcareous to noncalcareous; contains thin beds of fine-grained sandstone and siderite near top, thin beds of glauconitic quartz sandstone toward base, black phosphatic nodules at base. Upper contact with Wilcox Group is gradational; this report places top of Midway at base of last sand greater than 10 ft thick. In outcrop Midway subdivides into Wills Point and Kincaid Formations.	Barnes (1965, 1966, 1967b, 1970, 1972).
	CRETACEOUS	GULFIAN	NAVARRO Upper contact is an unconformity that is difficult to delineate in subsurface without paleontological data. Locally, black phosphatic nodules at base of Midway Group have been used as contact.	Upper Navarro Clay	Barrow (1953), Granata (1963), Barnes (1966, 1967, 1972), Stehli and others (1972), McGowen and Lopez (1983).
Upper Navarro Marl			Marl; occurs throughout basin.		
Nacatoch Sand			Sandstone that is fine grained, well sorted, somewhat calcareous. Thins and pinches out to the south.		
Lower Navarro Fm.			Shale that is microfossiliferous, micaceous, and flaky. Has been called "Neylandville Marl."		
TAYLOR Upper contact with Navarro Group is difficult to determine without paleontological data.		Upper Taylor Fm.	Marl and shale. Marl is gray, microfossiliferous. Shale is brown gray, flaky, slightly calcareous. A limy shale, the Saratoga, occurs at base of unit at eastern edge of basin.	Ellisor and Teagle (1934), Stephenson (1937), Barrow (1953), Granata (1963), Stehli and others (1972), Thompson and others (1978).	
Pecan Gap Chalk		Light-gray, microfossiliferous chalk throughout most of basin. Thickens and is transitional to east with Annona Chalk.			
Wolfe City Sand		Sandstone that is very fine grained, thinly bedded, argillaceous, and glauconitic. In the western part of the basin, locally porous and thick.			
Lower Taylor Fm.		Shale that is medium gray, fissile, micaceous, glauconitic, and calcareous to noncalcareous. Transitional to east with Annona Chalk and Ozan Chalk.			

STRATIGRAPHIC UNITS		LITHOLOGY, FACIES RELATIONSHIPS, AND STRATIGRAPHIC NOTES		SELECTED REFERENCES			
SYSTEM	SERIES	GROUP	FORMATION				
CRETACEOUS	GULFIAN	AUSTIN No definitive stratigraphic study of group has been accomplished for basin. Thus, major differences are cited in the literature for stratigraphic and facies relationships, as well as nomenclature.	Gober Chalk	Chalk that occurs throughout most of basin, but may be discontinuous. "Gober" has been applied to any chalk in this stratigraphic position. Top of Gober conventionally has been called "top of Austin Group," but lithologic unit appears to grade into Ozan Chalk (Taylor Group) to east.	Barrow (1953), Forgotson (1958), Granata (1963), Nichols (1964), Stehli and others (1972), Thompson and others (1978).		
			Brownstown Fm.	Clay or shale. Where underlying Blossom Sand is absent, Brownstown is indistinguishable on electric logs from Bonham Clay.			
			Blossom Sand	Sand, discontinuous. Most sands in this stratigraphic position have been called "Blossom."			
			Bonham Clay	Clay or shale.			
			Austin Chalk	Limestone that is light gray, argillaceous, fossiliferous, and chalky; interbedded with thin shale beds. Top is marked by "glauconitic chalk stringer" across much of basin. Discontinuous sand below glauconitic chalk stringer is sometimes known as "Second Blossom." At base of Austin Chalk there is a distinctive member, Ector Chalk, which is white to dark gray and brown, and massive. Austin Group becomes sandier to east and grades into Tokio Formation. Due to uplift and erosion of Sabine Uplift, base of Austin Chalk is marked by unconformity that truncates Eagle Ford, Woodbine, and part of Washita along eastern margin of study area.			
		EAGLE FORD	Undifferentiated	Shale with sand members. Shale is very fine grained, medium gray, platy, and micaceous; becomes sandy, particularly to north. Sand members, Subclarksville, Coker, and Harris Sands, are fine grained, glauconitic, micaceous, and locally porous. "Subclarksville Sand" has come to mean youngest sand beneath unconformity at base of Austin Chalk and commonly has been applied to sands that correlate with other sand members. Notations such as "first," "second," and "third" Subclarksville Sand are also common. Harris Sand may consist of reworked Woodbine sands. Eagle Ford is missing in eastern part of basin because of overlying unconformity.	Barrow (1953), Forgotson (1958), Granata (1963), Nichols (1964), Stehli and others (1972).		
		WOODBINE	Undifferentiated	Sand that is very fine to medium grained, well sorted, friable, calcareous to noncalcareous; interbedded with multicolored and waxy shales; conglomeratic; containing abundant bentonitic volcanic ash. There are two members: Lewisville is shelf-strandplain facies and underlying Dexter is fluvial facies. Woodbine is overlain by Austin Chalk along eastern part of basin where Eagle Ford has been removed. Farther east, Woodbine is also truncated by unconformity. Some workers indicate a significant pre-Woodbine unconformity in basin; this report shows an unconformity below Woodbine only where Maness Shale is missing.	Bailey and others (1945), Barrow (1953), Forgotson (1958), Granata (1963), Nichols (1964), Oliver (1971), Stehli and others (1972).		
	COMANCHEAN	WASHITA	Maness Shale	Shale that is dark gray, faintly laminated; distinguished by copper or bronze color, and conchoidal fractures. Transitional between Washita Group and Woodbine Group and sometimes has been included in Woodbine Group.	Bailey and others (1945), Eaton and Reynolds (1951), Barrow (1953), Granata (1963), Nichols (1964), Mosteller (1970), Scott and others (1978).		
				Buda Limestone		Limestone that is white, dense; marly near top, slightly porous to southwest.	
				Grayson-Del Rio Fm.		Gray, calcareous shale; contains interbedded limestone that is brown gray, microcrystalline, dense, slightly argillaceous.	
				GEORGETOWN SUBGROUP		Mainstreet Limestone	Limestone that is gray or white, fossiliferous; marly to south.
						Weno-Paw Paw Limestone	Gray limestone; interbedded with shales. Paw Paw is sandy and shaly facies in outcrop and in extreme northwest part of basin.
						Denton Shale	Gray shale and marl in northwest part of basin. Thins and includes limestone beds in southeast.
Fort Worth Limestone						Limestone that is white to light gray, hard, dense; containing some marly streaks; becomes shaly to north. Nonporous in north and west; porous elsewhere.	
Duck Creek Shale						Dark-gray marl; interbedded with gray, fossiliferous, nodular limestone.	
Duck Creek Limestone	Gray limestone; contains some marl. Commonly combined with overlying shale and named Duck Creek Formation.						

STRATIGRAPHIC UNITS			LITHOLOGY, FACIES RELATIONSHIPS, AND STRATIGRAPHIC NOTES	SELECTED REFERENCES		
SYSTEM	SERIES	GROUP	FORMATION			
CRETACEOUS COMANCHEAN		Fredericksburg	Kiamichi Shale	Black, laminated shale; contains thin beds of fossiliferous limestone; becomes porous to southeast. Interfingers with limestones of overlying Washita Group; in this report upper boundary is base of last Washita limestone.	Bailey and others (1945), Eaton and Reynolds (1951), Barrow (1953), Granata (1963), Nichols (1964), Mosteller (1970), Scott and others (1978).	
			Goodland Limestone	Limestone that is white to light grayish-brown, dense; contains calcite veins. Grades into porous Edwards Limestone at southeastern extremity of basin.		
		TRINITY	GLEN ROSE SUBGROUP	Paluxy Fm.	Very fine to medium-grained sandstone; interbedded with varicolored, waxy shale, and with mudstone; contains thin carbonaceous laminae, and thin lenses of conglomerate. Grades southward into shale that is dark gray, pyritic, sideritic, fissile, and interbedded limestone. Shale and limestone facies in southern third of the basin is Walnut Formation and is difficult to distinguish from overlying Goodland Limestone. Paluxy grades into Antlers Sandstone in northern extremities of basin. Walnut is considered to be of Fredericksburg age, but Paluxy is normally grouped with Trinity Group because it is difficult to distinguish from clastic facies of underlying Upper Glen Rose in northern part of basin. In Louisiana, "Paluxy" has come to include clastic facies of underlying Upper Glen Rose. In this report, Walnut is undistinguished from Paluxy.	Bailey and others (1945), Barrow (1953), Granata (1963), Nichols (1964), Mosteller (1970), Caughey (1977).
				Upper Glen Rose Fm.	Limestone that is light to medium brown-gray, dense, locally porous; interbedded with medium- to dark-gray, fissile shale. Anhydrite zones in lower part of formation are called "stray," "first," "second," and "third" anhydrite stringers and can be correlated over large areas. Toward northeast uppermost Glen Rose becomes Paluxy-like clastic facies, and limestone occurs only at base of formation. Upper Glen Rose in Texas is equivalent to Rusk Formation in Louisiana, where term "Glen Rose" excludes Paluxy-like clastic facies mentioned above.	Barrow (1953), Forgotson (1956, 1957), Nichols (1964).
				Massive Anhydrite	White, saccharoidal anhydrite; interbedded with red to gray shale, light- to medium-gray, dense, pelletal limestone, and some dolomite. Anhydrite has mottled, chicken-wire texture. Ferry Lake Anhydrite of Louisiana is equivalent to Massive Anhydrite of Texas. "Mooringport Formation" has been used for interval from top of anhydrite stringer in the Upper Glen Rose to base of Massive Anhydrite. Bacon Lime is local limestone, porous, pelletal, oolitic, at base of Massive Anhydrite. Top of Massive Anhydrite is difficult to correlate but base is good marker.	Jones (1945), Barrow (1953), Forgotson (1956, 1957), Granata (1963), Nichols (1964), Bushaw (1968).
				Lower Glen Rose Fm.	Composed of the Rodessa Member (interbedded shale, anhydrite, limestone, and sandstone), James Limestone Member (limestone is gray, dense, nonporous, locally oolitic and coquinoidal; contains shale), Pine Island Shale Member (dark shale with some interbedded limestone and sandstone), and Pettet (Sligo) Member (medium- to dark-brown-gray, dense limestone, interbedded with dark-gray shale). Pettet is fossiliferous, pelletal, and oolitic to north and west; it is transitional with underlying Travis Peak (Hosston) and is commonly considered a member of Travis Peak. This report includes Pettet with Lower Glen Rose primarily because of lithology; sands of Travis Peak are easily identified, but top of Pettet is difficult to identify in northern part of basin. All members of Lower Glen Rose become more terrigenous in northern part of basin; James Limestone becomes indistinguishable, and a sandy unit called "Pittsburg" appears near base. Rodessa includes local porous, productive zones such as Hill, Neugent, and Henderson sandy zones, and Gloyd, Dees, and Young limestones. Shale between Rodessa and James is normally called "Bexar Shale"; in this report it is included with Rodessa. "Pettet" is commonly used in East Texas; however, in Louisiana and South Texas, same unit is called "Sligo." In Louisiana, "Pettet" refers only to porous limestone facies of Sligo.	Barrow (1953), Forgotson (1956, 1957), Granata (1963), Nichols (1964), Bushaw (1968).

STRATIGRAPHIC UNITS			LITHOLOGY, FACIES RELATIONSHIPS, AND STRATIGRAPHIC NOTES	SELECTED REFERENCES	
SYSTEM	SERIES	GROUP	FORMATION		
CRETACEOUS	COMANCHEAN	TRINITY (con.)	Travis Peak Fm.	Predominantly fine- to medium-grained sandstone and interbedded dull-red and gray-green, arenaceous shale. Pale-green, carbonaceous siltstone found in upper part of unit; lenticular chert and quartz pebble conglomerate beds found throughout. "Hosston," commonly used in Louisiana and Arkansas, is generally favored over "Travis Peak"; however, "Travis Peak" has been retained within East Texas Basin by common usage. Confusion persists because subsurface unit is not equivalent to Travis Peak in outcrop in Central Texas; Travis Peak at outcrop is equivalent to part of Lower Glen Rose. Base of unit is unconformable except in southern part of basin, but it is rarely distinguishable on electric logs due to similar composition of Travis Peak and underlying Schuler.	Barrow (1953), Forgotson (1957), Granata (1963), Bushaw (1968).
			COTTON VALLEY	Schuler Fm. Bossier Fm.	Fine- to medium-grained sandstone interbedded with varicolored, waxy shale. Locally conglomeratic. Fossiliferous limestones occur in the lower portion. Shale that is gray, micaceous, and noncalcareous; interbedded with microcrystalline limestone.
JURASSIC	UPPER	LOUARK	Gilmer Limestone	Limestone that is gray to brown, dense, micritic; sometimes oolitic and pseudo-oolitic, or sometimes argillaceous; interbedded with thin beds of dark-gray shale. Unit occurs over most of study area and becomes increasingly shaly to southeast. Gilmer previously has been informally known as "Cotton Valley Limestone," "Lower Cotton Valley Lime," or "Haynesville." However, unit is not part of Cotton Valley Group, and it is lithically different from, but does grade laterally into, terrigenous Haynesville Formation of Louisiana.	Forgotson (1954a, b), Forgotson and Forgotson (1976), Todd and Mitchum (1977), Collins, S. E. (1980).
			Buckner Fm.	Pink to white anhydrite and halite, red shale, and pink dolomite. Evaporites occur primarily in northeast. Buckner grades into Smackover Formation to southeast.	Imlay (1943), Swain (1949), Barrow (1953), Forgotson (1954a, b), Todd and Mitchum (1977).
		Smackover Fm.	Limestone that is brownish gray, dense, microcrystalline. At north and west parts of basin are some moderately fossiliferous oolitic limestones and some tan, porous to nonporous dolomite.	Eaton (1961), Collins, S. E. (1980).	
		LOUANN	Norphlet Fm.	Red beds consisting of very fine grained, well-sorted, slightly calcareous sandstone; interbedded with siltstone and small amounts of red to maroon, plastic shale; some halite at base; some thin dolomites, anhydrites, and conglomerates throughout. Unit becomes more fine grained to south.	Barrow (1953), Eaton (1961), Nichols (1964), Todd and Mitchum (1977).
			Louann Salt	Halite that is white to pale gray or pale blue. Gradational with overlying Norphlet and underlying Werner Formations.	
	LOWER	Werner Fm.	Anhydrite containing local sandstone and conglomerate at base.		
TRIASSIC	UPPER	Eagle Mills Fm.	Red shale, some fine-grained red to pink sandstone, and red to brown, dense limestone. May not extend into center of basin.		
PALEOZOIC		PRE-EAGLE MILLS	Pennsylvanian and older, partially metamorphosed shales.	Swain (1949), Nichols (1964).	





